T.C.

İSTANBUL KÜLTÜR UNIVERSITY

INSTITUTE OF GRADUATE STUDIES

GLOBAL RESPONSE OF 2D REINFORCED CONCRETE STRUCTURES UNDER BLAST LOADS AND PROGRESSIVE COLLAPSE

Masters of Applied Science Thesis

MOHAMED ABDULLAHI ADAN MAHAD

1800004369

Department: Civil Engineering

Program: Structural Engineering

Supervisor: Prof. Dr. HÜSEYİN FARUK KARADOĞAN

JUNE 2021

T.C.

İSTANBUL KÜLTÜR UNIVERSITY

INSTITUTE OF GRADUATE STUDIES

GLOBAL RESPONSE OF 2D REINFORCED CONCRETE STRUCTURES UNDER BLAST LOADS AND PROGRESSIVE COLLAPSE

Masters of Applied Science Thesis

MOHAMED ABDULLAHI ADAN MAHAD

1800004369

Department: Civil Engineering

Program: Structural Engineering

Supervisor: Prof. Dr. HÜSEYİN FARUK KARADOĞAN

Thesis jury members:

Dr. Üyesi Erdal Coşkun

Dr. Üyesi Gökhan Yazıcı

June 2021

ACNOWLEDEMENT

In the name of ALLA, the most gracious and the most merciful

First and foremost, I thank Allah for his countless blessings, and then I am extremely grateful to my supervisor, Prof. Dr. Faruk Karadogan for his invaluable advices, continuous supports, and patience during my M.Sc study. His immense knowledge and plentiful experience have encouraged me in all the time of my academic research and daily life.

I would also like to thank İstanbul Kultur University (IKU) for giving me the opportunity to be one of their students. Special thanks to my department of Civil Engineering.

I am very thankful for my parents, who I cannot fulfill their rights whatever I do, I dedicate this book to them, my wife and son.

ABSTRACT

Explosion gained the interest of structural engineers in the last decades due to the increase of the terrorist attacks done by terrorism groups around the universe; an example of such attacks is the bombing attack at the World Trade Center in 1993. The progressive collapse follows such events and leads the structures to total collapse. In this book, the global response of a 2D reinforced concrete structure under the blast and progressive collapse was focused. The aim of this study is to investigate the effect of the strain-rates on the overall response of RC structures, assess and compare the resistance capacity of two identical structures; one is designed with low strength concrete (Frame B) while the other is designed with relatively high strength concrete (Frame A) to blast loads and progressive collapse. The strain-rate effect on the response of structures is examined by performing second-order pushover analysis under different strain-rates then the pushover curves were compared. To assess the blast resistance capacity of the structures, the structures were subjected to two surface-burst scenarios (100 and 300kg) both at 10m away from the structures, the blast pressure-time history of each joint is calculated as per UFC_3_340_02, and three loading patterns were compared. The progressive collapse resistance capacities of the two structures were compared in various column removal locations as per GSA guidelines. The blast and progressive collapse analyses were done by nonlinear dynamic analysis by step-by-step integration using Newmark's average method. Mass and stiffness proportional Rayleigh damping was taken into account in the analyses. From the results it was observed that the structural strength increases with the increase of the strain-rate, also from the blast analysis, it was noticed that the simplified methods of blast load modeling with considering the incident angles give acceptable accuracy. Frame B failed in all cases of the progressive collapse while Frame A failed in the case of two internal columns removal.

Keywords: Strain-rate, Dynamic increasing factor, Blast, Standoff distance, Angle of incidence, Reflected pressure, Positive phase, Negative phase.

Özet

Patlama, evrendeki terör grupları tarafından yapılan terör saldırılarının artması nedeniyle son yıllarda yapı mühendislerinin ilgisini çekti; Bu tür saldırılara bir örnek, 1993 yılında Dünya Ticaret Merkezi'ne yapılan bombalı saldırıdır. Aşamalı çöküş, bu tür olayları takip eder ve yapıların tamamen çökmesine neden olur. Bu kitapta, 2B betonarme bir yapının patlama ve aşamalı çökme altındaki küresel tepkisi üzerinde durulmuştur. Bu çalışmanın amacı, gerinim oranlarının RC yapılarının genel tepkisi üzerindeki etkisini araştırmak, iki özdeş yapının direnç kapasitesini değerlendirmek ve karşılaştırmak; biri düşük dayanımlı beton (Çerçeve B) ile tasarlanırken, diğeri yükleri patlatmak ve kademeli olarak çökmek için nispeten yüksek dayanımlı beton (Çerçeve A) ile tasarlanmıştır. Farklı gerinim hızları altında ikinci mertebeden itme analizi yapılarak, yapıların tepkisi üzerindeki gerinim hızı etkisi incelenmiş, ardından itme eğrileri karşılaştırılmıştır. Yapıların patlama direnci kapasitesini değerlendirmek için yapılar, her ikisi de yapılardan 10 m uzaklıkta iki yüzey patlaması senaryosuna (100 ve 300 kg) tabi tutuldu, her bir eklemin patlama basıncı-zaman geçmişi UFC_3_340_02'ye göre hesaplandı ve üç yükleme kalıpları karşılaştırılmıştır. İki yapının aşamalı çökme direnci kapasiteleri, GSA yönergelerine göre çeşitli kolon kaldırma konumlarında karşılaştırıldı. Patlama ve aşamalı çökme analizleri, Newmark'ın ortalama yöntemi kullanılarak adım adım entegrasyonla doğrusal olmayan dinamik analizle yapıldı. Analizlerde kütle ve sertlik orantılı Rayleigh sönümü dikkate alınmıştır. Sonuçlardan, gerinim hızının artmasıyla yapısal mukavemetin arttığı gözlemlenmiş, ayrıca patlatma analizinden, olay açıları dikkate alınarak basitleştirilmiş patlama yükü modelleme yöntemlerinin kabul edilebilir doğruluk sağladığı fark edilmiştir. B Çerçevesi, aşamalı çöküşün tüm durumlarında başarısız olurken, iki dahili sütunun çıkarılması durumunda Çerçeve A başarısız oldu.

Anahtar Kelimeler: Gerinim oranı, Dinamik artan faktör, Patlama, Uzaklık mesafesi, Gelme açısı, Yansıyan basınç, Pozitif faz, Negatif faz.

LIST OF FIGURES

LIST OF TABLES

TABLE OF CONTENTS

LIST OF SYMBOLS AND ABBREVIATIONS

ASCE: American Society of Civil Engineers.

GSA: General Service Administration.

UFC: Unified Facilities Criteria.

DIF: Dynamic Increasing Factor.

TNT: Trinitrotoluene.

2D: Two Dimension.

DOD: Department Of Defense.

DL: Dead Load.

LL: Live Load.

Z: Scaled distance.

R: Standoff distance.

P_o**:** Ambient pressure.

t_A**:** Arrival Time.

P_{so}**:** Positive peak overpressure.

P_{so}^-**:** Negative peak overpressure.

t_A**:** Arrival Time.

t_o **:** Positive phase duration time.

t_{o^-} : Negative phase duration time.

t_c **:** Clearing Time.

P_r **:** Reflected pressure.

$\acute{\varepsilon}$: Strain-rate.

$\acute{\varepsilon}_s$: Static strain-rate

CHAPTER 1

1.1 INTRODUCTION

Blast load is considered one of the most dangerous and destructive loads that a structure can experience throughout its existence span. Blast loads may be caused by terrorism attacks, unintended explosions, and other explosions used for excavation, mining, and the controlled demolition. Although the chance of occurrence of this event in the period of the existence of a normal structure may be very small, the very intense consequences of this hazard call for designers to do not underestimate or forget it in the analysis and design of structures which are considered to be critical or have a high probability of being exposed to blast loading. Examples of such structures are high-profile governmental structures and monuments. Therefore, it is very important to develop analytical strategies and processes that expect the response of the systems to blast loads with reasonable accuracy.

Over the last few decades, the world has experienced terrorism attacks that targeted civilian buildings and other governmental structures which created considerable attention to the structural engineers to study the behavior of engineering structures under blast loading. These days explosives became modern and very powerful, but smaller compared to a few decades ago, and this made easier the transportation and hiding processes of the explosives.

Many research projects have been carried out or are underway to improve methods to reduce the hazard of such attacks. The resistance of the structures for blast loading has been under study for decades and has been well advanced in military communities. That is why most of the information is not accessible to the public, except some documents for the prediction of the effects of the explosions available for structural engineers. The most trusted resources and references are from the USA military such as The Army Technical Manual 5-1300[1], which gives detailed approaches for designing structures against the effects of explosions.

Explosions are unpredictable similar to the earthquake, the magnitude of the pressure depends on the weight of the charge and its distance from the structure. It is an instantaneous hazard that only exists parts of seconds. The pressure goes from zero to very high grades immediately.

The most famous examples of Explosion attacks are the bomb attack on the Alfred P. Murrah Federal Building in Oklahoma City in 1995, the world trade center in 1993, the British Embassy, and the HSBC Bank bomb attack in Turkey in October 2004 which was approximately three tons of TNT.

Also, the 14th October 2017 events in Mogadishu, which caused the death of 587 people and more than 316 injuries, the explosives were in two trucks with explosive weight assessed as 2.2 Tons of TNT in each. These recent events express the importance of blast-resistant design issues.

(a) (b) (c)

Figure 1.1: Explosion effects on Murrah federal building (a) before (b) during and (c) after the event.

Structural engineers aim to save lives and properties as much as possible. One of the methods used to achieve that aim is the mitigation of what is called Progressive collapse. Progressive collapse is a phenomenon named when the failure of one or more vertical load-carrying members leads to partial or complete failure to the structure or when the local failure spreads to cause global failure. And it gained the attention of the structural engineers after the famous event at Ronan point apartment in London in 1968. The building was a 22 storey structure from precast concrete. A

gas explosion on the 18th floor led to the failure of a load-bearing wall which caused in its turn the failure of the upper part because of lack of support and failure of the lower part because of the excessive weight.

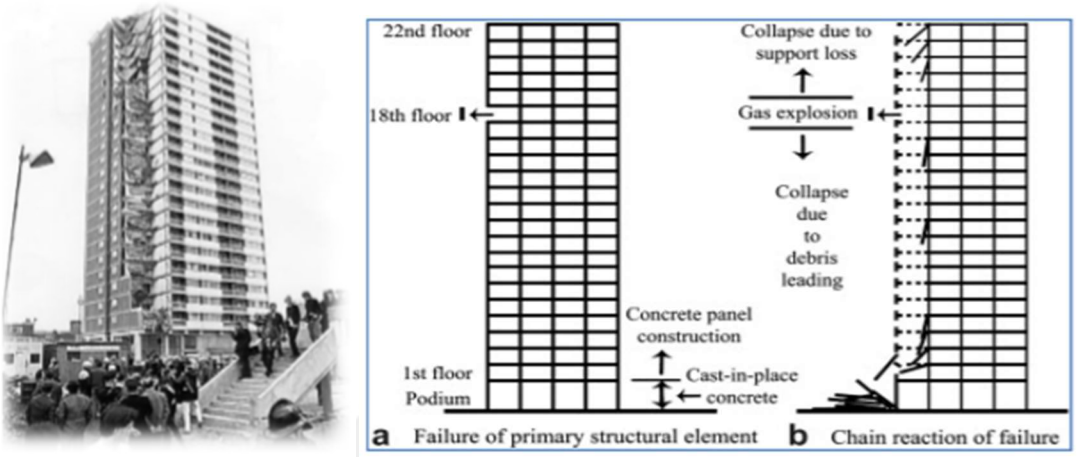

Figure 1.2: progressive collapse at Ronan point apartment building 1968.

After the Ronan point apartment, the United Kingdom started developing standards to prevent the progressive collapse. The British standards BS 6399 was the first standards found for that purpose around the world, Then the Eurocodes against accidental loading conditions. The first American codes were The American Society of Civil Engineers (ASCE) and the US General Service Administration (GSA). The ASCE focused on the reduction methods of the progressive collapse without providing definite requirements while the GSA guideline concentrated on the design approaches.[2].

1.1.1 DEFINITIONS AND TERMINOLOGIES

Explosion: a very fast chemical reaction involving a solid, dust, or gas, during which a rapid release of hot gasses and energy takes place**.**

Trinitrotoluene (TNT): a high explosive, a chemical compound in the formula of $CH_3C_6H_2(NO_2)_3$, that can change quickly from solid to hot expanding gasses.

Scaled distance: The idea behind it is that during the explosion of two charges of similar explosive that has the same geometry but different weight and are placed at the similar scaled distance from a target surface, identical blast waves are propagated at the point of interest as long as they are under the same environmental conditions.

Arrival time (TA): the time between the detonation time and when the blast wave reaches the target point.

Reflected pressure: the pressure reflected from the front wall which is always bigger than the incident pressure.

The angle of incidence (α): the angle between an imaginary horizontal line of the detonation point and the point of interest on the front side.

Strain-rate: the rate of changing the strain of material per time or the speed at which deformation of an object from its original shape occurs.

Dynamic Increasing Factor (DIF): is a factor multiplied by the static properties of a material to get its dynamic properties.

1.1.2 SCOPE AND OBJECTIVES

This thesis focuses on the Global response of two structures of five-story 2D frames (Frame A and Frame B) under two different Surface burst scenarios of 100 and 300 kilograms of Trinitrotoluene (TNT) explosives at 10 meters from the structure. For each scenario, three different loading patterns were examined. The two frames have similar properties and dimensioning except the compressive strength of the concrete, in Frame A concrete Grade C30 is used while in Frame B is used Grade C10 to represent both low and relatively high levels of concrete compressive strengths. The effect of strain-rates on the resistance of the two frames was examined by carrying out pushover analysis for the frames at different strain-rates taking into account the P-Delta effects, the dynamic increasing factors (DIF) of each material

property was calculated as the result of the strain-rate values using the formulas given in CEB-FIP-1990 code.

The structures were analyzed using nonlinear dynamic analysis as per UNIFIED FACILITIES CRITERIA (UFC 3-340-02) as there were no neighboring structures and the openings like doors and windows were neglected. The fragmentation effects of the explosion on the façade of the structure were not considered. The incident angle was considered in the calculation of the blast pressure also both positive and negative phases were taken into account as well as the strain-rate effects. The two structures were investigated for their resistance capacity for progressive collapse as per GENERAL SERVICES ADMINISTRATION (GSA 2003) under three cases of column removal which are all on the ground floor:

- Corner column failure
- Internal column failure
- Failure of two consecutive internal columns

SAP2000 is used as the primary structural analysis software to model the buildings of interest. The analysis is limited to 2D structural models. Both analyses were done by a nonlinear dynamic analysis which is considered the most accurate and the dynamic analysis was carried out by step-by-step integration using Newmark's average method. The mass and stiffness proportional Rayleigh damping was taken into account in the analysis.

The objectives of this study are:

1. To expand the knowledge about the explosion phenomenon and blast wave characteristics, also the concept of the progressive collapse.
2. To clarify the effect of strain-rates on the performance of reinforced concrete structures.
3. To monitor the effects of some simplifications made in the blast load modeling to the response of the structures.

4. To compare the performance of the structures designed with low and relatively high strength concrete (Frame A and Frame B) for blast loads.
5. To find out the progressive collapse resistance capacity of structures designed with low and relatively high strength concrete.

1.2 LITERATURE REVIEW

T. Ngo et al. (2007), gave detailed explanations on blast phenomenon, different estimation methods of blast loads, and also the responses of the structures, they summarized also the dynamic behavior of materials at high strain-rates. In their point of view the load capacity, standoff distance and the angle of incidence influences the type of the structural response of the structure to the blast load. They carried out a parametric study on the effect of high strain-rates on the ductility of the reinforced concrete members, from that study they found out that the high strain-rates increase the yield strength of the steel and the compressive strength of the concrete, therefore, increase in the ductility of the reinforced members. By using the LS-DYNA they took the material and geometric nonlinearities into consideration and analyzed a 52 storey structure for explosion at the ground level and found out failed members of columns, beams, and slabs. They removed the failed members and checked the remaining part for progressive collapse and the results illustrated that the surrounding beams and slabs became critical due to the failed columns.[3]

Danesh Nourzadeh et al. **(2015)**, Studied the global response of moderate height reinforced concrete structure to an explosion at the ground surface, they determined the structural response with nonlinear dynamic analysis using OPENSEES software, they also made an assessment for the effect of some of the simplifications or assumptions we make in modeling the blast pressure on the structure and Dynamic increase factors of 1.25 and 1.23 were applied to the compressive strength for concrete and yield strength steel reinforcing bars13, respectively. In the first analysis, the angle of incidence is taken into consideration and the building is loaded from all directions while in the other one the angle of incidence is taken into account and only the front face of the structure is loaded, to consider the large deformations in the building the

effect of the P-Delta considered, their results showed that the two load patterns mentioned above give very close results. They also compared the response of the same structure modeled in three dimensions once and two dimensions in the other model; the 3D model was loaded from every direction while the 2D model was loaded from the front face, roof, and the rear side. Their global response results came out almost the same.[4]

S. Vladimir et al. **(2015)**, their study aimed to be familiar with the blast load because of the overgrowing terrorism attacks in the world. They gave explanations in detail about types of explosions and how to calculate the blast load. They used Unified Facilities Criteria (UFC 3-340-02) code for the calculations of the blast pressure-time history functions and also the dynamic increasing factors. They modeled the structure in three dimensions by SAP2000 V14. They assumed the structure to have neighboring buildings from three directions therefore it is loaded only in the front face. They considered the material nonlinearity by using the Mander model for the concrete and the Simple model for the reinforcing bars. Different charge weights were examined (1kg, 10 kg, and 100 kg) of TNT at a standoff distance of 1.2m from the structure; their results showed no collapse though the explosives were very close to the structure, however, the 100kg charge caused the failure of the middle columns. They carried out a progressive collapse check to the damaged structure after removing the failed members and the results illustrated that the structure redistributed the loads to the adjoining members and there was no progressive collapse.[5]

Danesh Nourzadeh et al. **(2017),** compared the response of structures for two of the most destructive events that can take place during the structure's lifetime which are explosions and earthquakes. To monitor the intensity of deformations from both events they investigated the global behavior of 10 storey building to ten different earthquake scenarios. They applied the blast loads at the nodes depending on the standoff distance, angle of incidence, weight of the charge, and the tributary area. They used OPENSEES software for the nonlinear dynamic analysis, 5% of Rayleigh damping was used for both analysis and the second-order effects was taken into consideration. For the blast analysis, they modeled the structure in both 2D and 3D

models and they got their results very close and the lateral storey drifts from the blast load appeared to be much larger than those of the seismic drifts.[6]

David Stephen et al. **(2019),** studied and compared some numerical approaches to imitate the sudden column removal and the influence of rising time on the response of the structure. In their study, they took up the GSA guideline recommendations on the column removal time to be less than one-tenth of the structural period in the vertical vibration mode. They used the commercial finite element software SAP2000 to build their model of a ten-storey steel moment-resisting structure designed based on the EUROCODE 3 (2005). They compared four modeling techniques based on the displacement and rotational response criteria. They also studied the effect of the column removal time in the range of 0.001 – 5 seconds and recorded the maximum displacement and rotational responses of the structure and finally they observed that within the range of 0.001 to 0.02 occurs the critical response of the structure and the stability of the structural columns occurs when the column removal time tends to zero. They also observed the rotational response of the structure in the internal column removal scenario was small compared to the responses of the corner and edge column removal scenarios.[7]

Kwangbo Kwon et al. **(2014),** Estimated the progressive collapse resistance capacity for real construction projects based on the alternative path method as per General Services Administration's guidelines they used two models for their study the first model was a 22-storey reinforced concrete moment resisting frames with core-wall and the second one was a 44-storey interior concrete core and external steel diagrid structure. The progressive collapse potentials for these models were assessed using the linear static, nonlinear static, and nonlinear dynamic analyses. They also gave useful information about each procedure, demand capacity ratio, and also the gravity load coefficient for the linear static procedure. By using the GSA guidelines the results showed similar in both models, in the linear static procedure the progressive collapse takes place in the two models when an interior column was removed however the models were safe in the nonlinear static and nonlinear dynamic analyses and eventually the concluded their study that the linear static method is more

conservative for estimating the progressive collapse potentials compared to the other methods.[2]

CHAPTER 2

2.1 EXPLOSIONS AND BLAST PHENOMENON

During the explosions hot gases are produced, these hot gases expand to occupy the available space, causing wave-type propagation through space that is transmitted spherically through an unbounded surrounding medium. Along with the produced gases, the air around the blast also expands, and its particles pile-up, causing what is known as a blast wave and shock front. The blast wave contains a large amount of the energy that was released during the detonation and spreads at a speed faster than the speed of the sound.

Figure 2.1 illustrates the typical profile of the pressure-time function for a point in the front wall, at a certain distance from the explosive. The pressure around the element is at first equal to the ambient pressure Po, at the arrival time t_A the shock front reaches that point then the pressure increases instantaneously to a peak pressure Pso also known as side-on overpressure or peak overpressure. The time in which the pressure gets its maximum value is very small and normally neglected. After the pressure reaches the peak pressure, it drops down with an exponential rate until it becomes equal to the ambient pressure at t_A+t_o which is the positive phase (pushing pressure) duration.

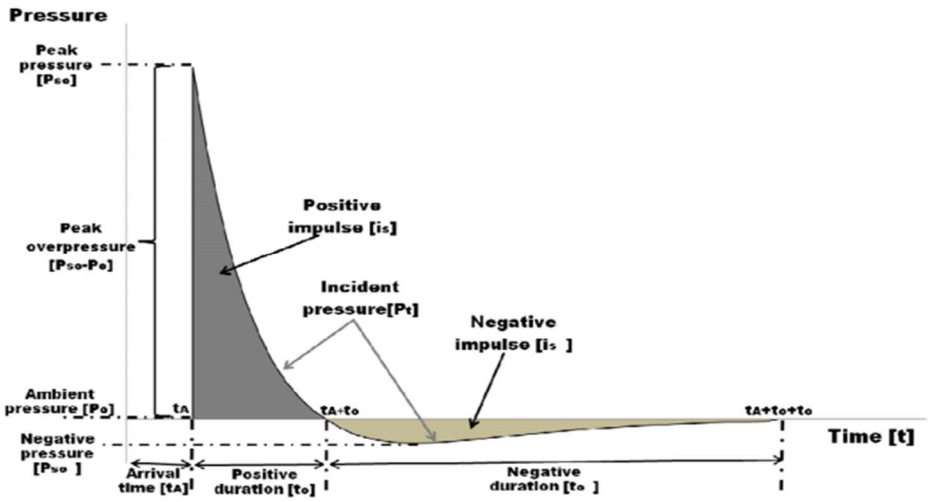

Figure 2.1: typical blast pressure-time history.[8]

Then the pressure decreases below the ambient pressure to start the negative phase (suction pressure), then reaches its minimum value denoted as P_{so}^{-}. The total duration of the negative is t_o^{-}. The negative phase always continues longer than the positive phase but its magnitude is smaller. Because of the negative phase, we see the glass and timber fragments outside of the structures close to the explosions after the event.

Since the magnitude of the negative phase is too small compared to the positive one it is sometimes neglected in design purposes as it has been proved that the major structural damages are connected to the positive phase. The negative phase should be considered if the total structural performance of a structure during the blast is estimated not the structural integrity.[8]

2.1.1 BLAST WAVE SCALING LAWS

One of the most important steps in blast load calculation is to find out the distance between the detonation point and the structure of interest. The value of the blast wave pressure and its velocity drops down quickly as well as the duration of the positive phase when the distance between the explosive and the target point increases as shown in the Figure below.

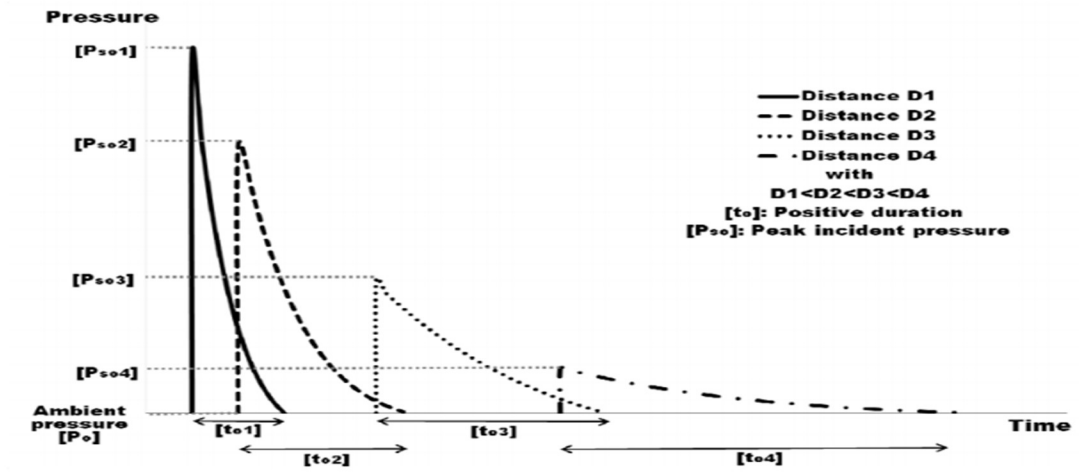

Figure 2.2: Effect of the explosive standoff distance to the positive phase pressure.[8]

There are various scaling laws, but the most commonly used formula is that found by Hopkinson-Cranz. The idea behind the scaling laws is that during the explosion of two charges of the same type of explosive that have different weight and are located at the same scaled distance from a target surface, the same blast waves are produced at the point of interest since they are under the same atmospheric conditions.[9]
Hopkinson-Cranz introduced this equation for the scaling law:

$$Z = \frac{R}{\sqrt[3]{W}} \quad (1)$$

R is the distance from the explosive to the point of interest.

W is the weight of the explosive.

2.1.2 EXPLOSIVE TYPES

Explosions produce very destructive pressure and can cause the collapse of surrounding buildings as well as human life losses. The foremost step to protect structures and save human lives is to design the structures to withstand blast loading. Nowadays the explosives became more modern; they became smaller in size but very powerful and more destructive.

There are various differentiations for the explosives, but the most commonly known and most used in terrorist attacks are solid explosives. And since there are various types of solid explosives it would be difficult to create diagrams for each, TNT (trinitrotoluene) is normally used for the calculation of the blast wave parameters because its blast properties are almost similar to the most solid explosives.

The weight of the exact explosive charge is changed to equivalent TNT weight depending on the heat of detonation of each explosive type using Equation (2).

$$W_{TNT} = W_{exp} \frac{H_{exp}}{H_{TNT}} \quad (2)$$

Where W_{TNT} is the equivalent TNT weight in kilograms,

W_{exp} is the weight of any other solid explosive in kilograms,

H_{exp} is the heat of detonation of any other explosive rather than TNT in (MJ/Kg)

H_{TNT} is the heat of detonation of the TNT in (MJ/kg)

Table 2.1 below gives the heat of detonation of some of the most common known solid explosives.

Table 2.1: Heat of detonation of commonly known explosives.[8]

Name of the explosive	Heat of detonation (MJ/kg)
TNT	4.10-4.55
C4	5.86
RDX	5.13-6.19
PETN	6.69
PENTOLITE 50/50	5.86
NITROGLYCERIN	6.3
NITROMETHANE	6.4
NITROCELLULOSE	10.6
AMON./NIT. (AN)	1.59

The weight of the explosive is unpredictable but it can be estimated from the data saved from the relevant previous events or the type of cars that can be used for transportation, in the design process the estimated weight is increased 20% for safety. Table 2.2 gives the maximum weight that can be transported by each car.

Table 2.2: Transportable weight of explosives for different car types.[8]

Transporter	Explosive Weight (Kg)
Suitcase	10
Medium-size car	200
Large-size car	300
Pick-up truck	1400
Van	3000
Truck	5000
Truck with trailer	10000

2.1.3 TYPES OF EXPLOSIONS AND BLAST LOADING

Explosions are classified according to the location it takes place into confined (internal) and unconfined (external) explosions and due to the multi reflection process, the computation and analysis of the confined explosion are much more complex than the unconfined explosions.

The external explosions are also categorized according to the relative location of the detonation point and the structure of interest into three types and with these types the computation process changes, figure 2.3 illustrates these three types:

a) **Free airburst**: the explosion occurs in the air at the top of the structure and the horizontal distance between them is small compared to the vertical distance so the blast wave expands spherically and hits the structure before it is reflected from the ground.

b) **Airburst**: the explosion occurs also in the air but this time the horizontal distance between the detonation point and the structure is larger than the vertical distance between them and the blast wave also expands spherically and hits the structure after pre-interacting with the ground.

c) **Surface burst**: the explosion occurs at the ground or close to it, the blast wave spreads instantly and hits the ground, and from that hemispherical wave initiates and hits the structure.

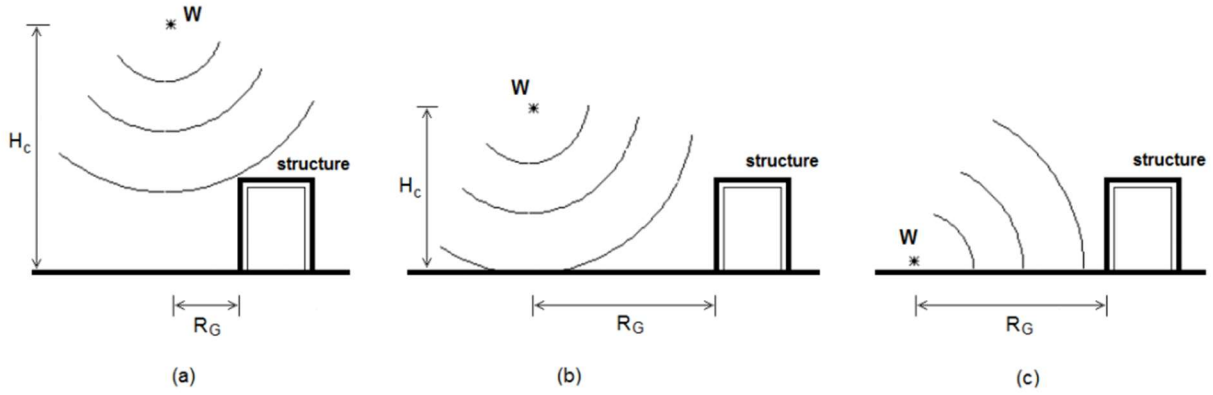

Figure 2.3: External explosion types; (a) Free air burst, (b) Airburst, (c) Surface burst.[8]

2.1.4 BLAST WAVE REFLECTION

The blast wave changes its characteristics when it contacts with an object, creating new wave properties different from the properties of the original wave shown in Figure 2.1, the contact of the blast wave with a stiff object generates reflected pressure that is greater than the side-on- overpressure P_{so} as illustrated in Figure 2.4.

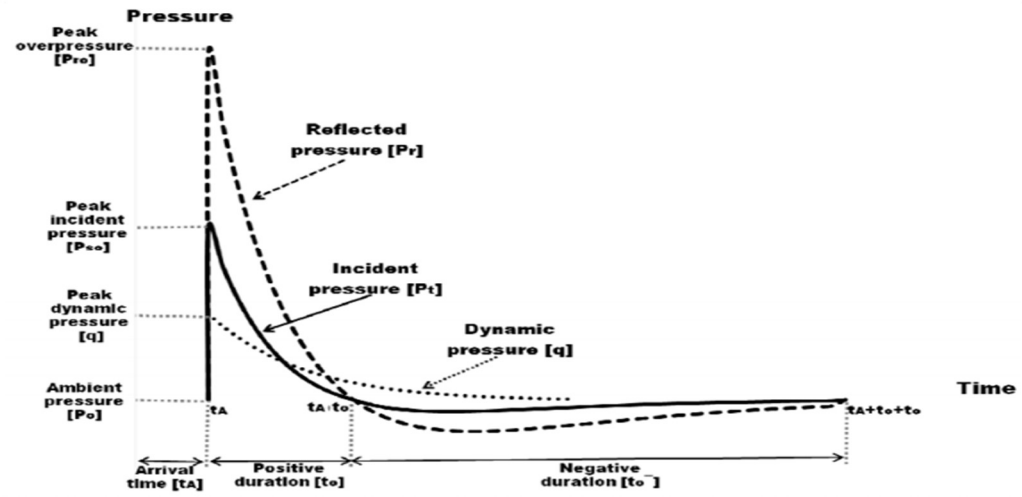

Figure 2.4: Incident and reflected pressure-time history.[8]

The reflected pressure can be significantly greater than the incident pressure depending on the obstacles located between the explosive and the structure, the angle of incidence, the weight of the explosive, the standoff distance, and also the geometry of the structure relative to the explosion direction as shown in Figure 2.5.

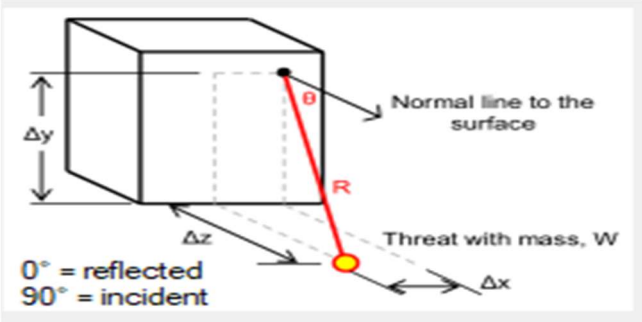

Figure 2.5: Parameters affect the reflected pressure. [27]

The front side or the side opposite to the direction of the detonation experience reflected pressure while the other parts experience side-overpressure as in Figure 2.6.

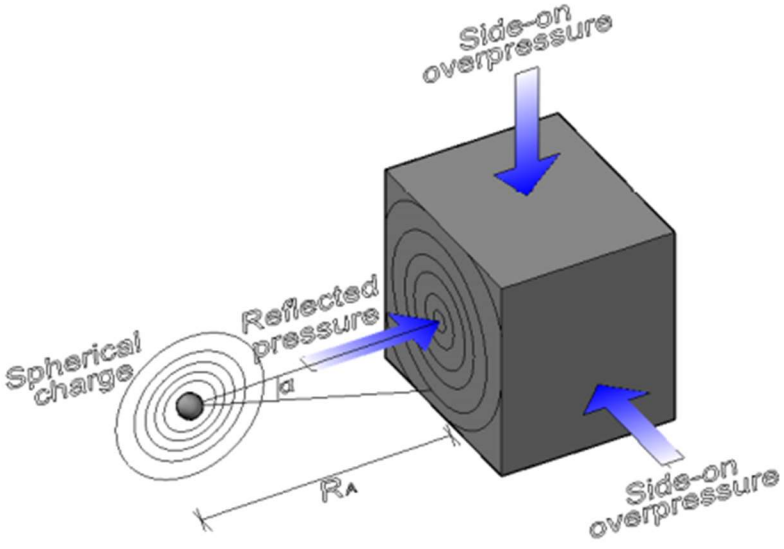

Figure 2.6: Reflected pressure for each side of the structure.[8]

2.1.5 BLAST PRESSURE ESTIMATION

Several studies have been carried out on high explosive materials in the mid of 20th century after the second world war by several scientists in the world to find out formulas for the calculation of the blast pressure. Few equations were proposed and most of these use the scaled distance, such as:

In 1995 Brode proposed formulas for the prediction of the peak overpressure for the spherical blast.[18]

$$P_{so} = \frac{6.7}{Z^3} + 1 \qquad P_{so} > 10 \text{ bars} \tag{3}$$

$$P_{so} = \frac{0.975}{Z} + \frac{1.455}{Z^2} + \frac{5.85}{Z^3} - 0.019 \qquad 0.1 < P_{so} < 10 \text{ bars} \tag{4}$$

Where Z is in m/$kg^{1/3}$

For Peak pressures over 10 bars (1Mpa), it is a near-field explosion therefore equation (3) is used and for peak pressures less than 10bars it is medium or far-field and equation (4) is used.

In 1961 Newmark proposed a formula for the calculation of the peak overpressure for hemispherical ground explosions.[19]

$$P_{so} = 6784 \frac{W}{R^3} + 93 \sqrt{\frac{W}{R^3}} \tag{5}$$

Where Pso is in bars
W is TNT explosive charge weight in tons
R is the standoff distance in meters

In 1987 another equation for the peak overpressure in kpa is proposed by Mills.[20]

$$P_{so} = \frac{1772}{Z^3} + \frac{114}{Z^2} + \frac{108}{z} \quad (6)$$

Where Z is in m/$kg^{1/3}$

The reflected pressure which is generated when the blast wave contacts with an obstacle when the angle of incidence is zero is calculated by:

$$P_r = \left\{ \frac{4Pso+7Po}{P_{so}+ 7P_o} \right\} \quad (7)$$

2.1.6 BLAST PRESSURE FUNCTION CALCULATION AND SIMPLIFICATIONS

It is very difficult to model the blast pressure function in its real shape if solid work software that automatically calculates the blast pressure function is not used since it contains curves that are difficult to estimate manually.

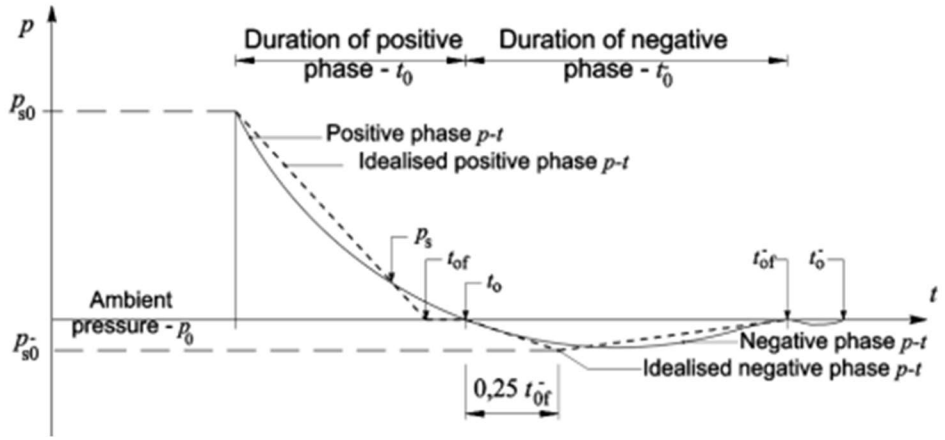

Figure 2.7: Actual pressure time-history shape.[5]

Instead of that triangular function is used which easier in the modeling process. The blast pressure parameters can be obtained from diagrams in the UFC_3_340_02 guideline using the scaled distance.

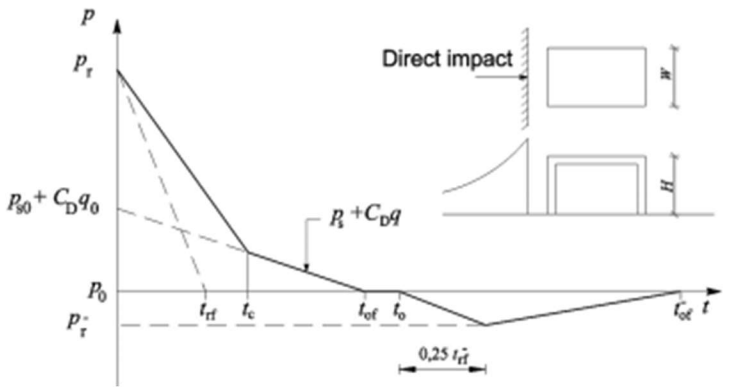

Figure 2.8: Triangular pressure-time history for the front face of the structure.[5]

The dashed line is used if $t_{rf} < t_c$, so the positive phase duration is equal to the fictitious length of the refracted front wave (t_{rf}).

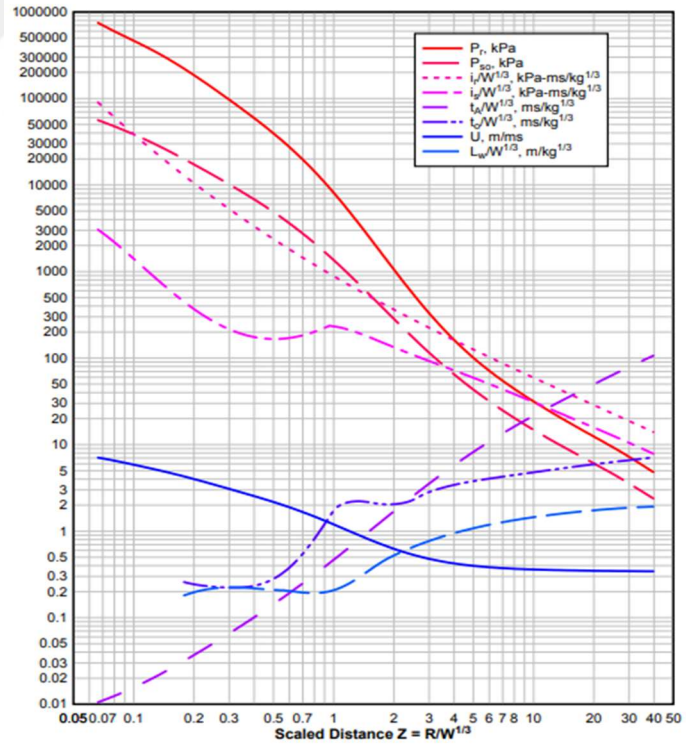

Figure 2.9: Positive phase parameters for a hemispherical wave of TNT charge.[8]

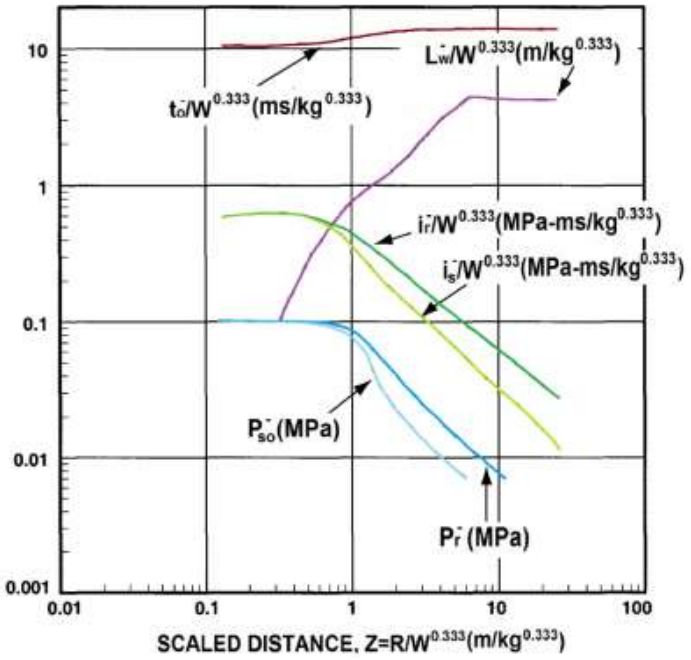

Figure 2.10: Negative phase parameters for a hemispherical wave of TNT charge.[8]

The clearing time (t_c), which is the time that the reflected pressure becomes equal to the initial pressure can be computed by:

$$t_c = \frac{4S}{(1+R).Cr} \tag{8}$$

Where:

S: is the smallest value among the height of the structure (H) and half of its width.

R: is the ratio of S/G, where G is the largest value of the height of the structure and half of its width.

Cr: is the velocity of the sound in the reflected medium.

$$\text{The fictitious length of the reflected wave } (t_{rf}) = \frac{2Ir}{Pr} \tag{9}$$

Table 2.3: Drag coefficient for roof and side.[8]

Peak dynamic pressure (Kpa)	Drag coefficient (C_D)
0-170	-0.4
170-350	-0.3
350-900	-0.2

The blast pressure-time history in the roof, side, and the rear-wall is different from the front wall. The blast wave leaves the front wall and travels across the roof and the side-walls, the peak reflected pressure reduce as well as the velocity of the wave. To simplify this, an equivalent pressure-time history is used instead of the step-by-step analysis of the wave propagation across the surface, as shown in the Figures below.

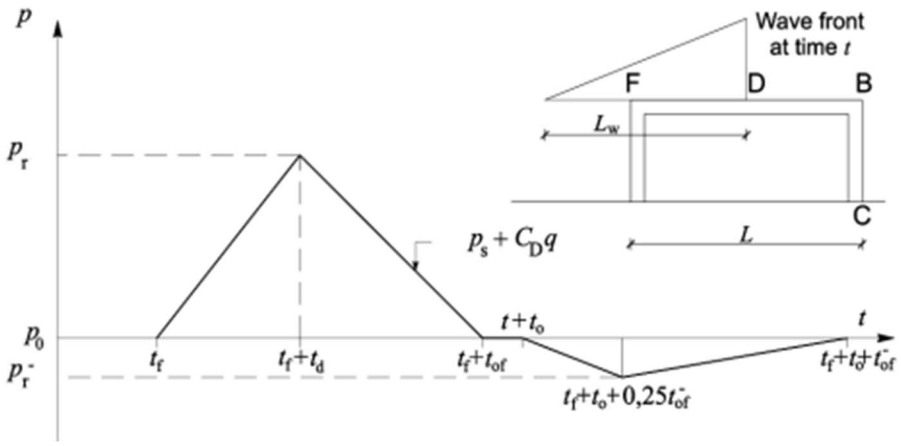

Figure 2.11: Triangular pressure-time history for the roof of the structure.[5]

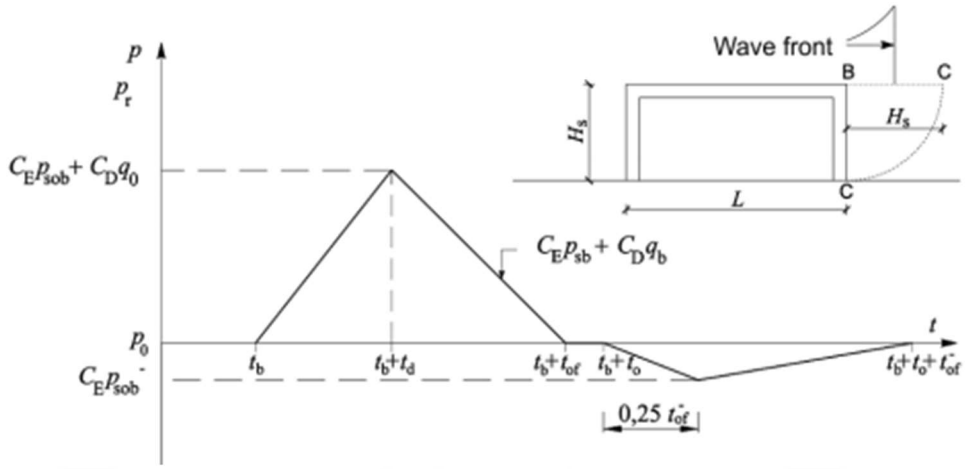

Figure 2.12: Triangular pressure-time history for the rear-wall of the structure.[5]

2.1.7 EFFECTS OF OPENINGS

Openings are a very important part of every structure, since an important part of the design is distribute the sunlight and also the fresh air to the whole building, and the process requires large windows for every part of the building, and modern buildings are identified by large windows and gates especially the front side.

Windows are the first parts to fail when the blast wave first reaches the building even if the structure was designed to withstand blast loads, these failed windows allow the blast pressure to pass through them, the passed pressure is reflected multiple times from the internal partition walls, by these reflections the peak pressure of the blast wave increases every time.

The waves that hit the external walls and the roof are heading towards the interior of the structure, however, the pressure on the interior side of the walls and the roof expanded after the failure of the windows are directed towards outside of the structure, this means the same element will experience opposite pressures from the two sides.

2.2 BLAST LOADED STRUCTURES' FAILURE MODES

The influence of the blast loading on the structural members may cause both global and local responses depending on the types of failure modes. The charge weight, standoff distance, and the direction of the explosive with respect to the structure generally control the type of the structural response.

Punching, direct shear, and flexure are the failure modes expected from the blast loading. Near-field explosions cause local responses represented by localized bleaching and spalling, whereas far-field explosions generate a global response and are normally characterized as a flexural failure.[10]

2.2.1 GLOBAL STRUCTURAL BEHAVIOUR

According to Mendis et.al, the relationship between the effective loading duration of the explosion and the fundamental period of the structure governs the structural responses for explosion loads, when the effective loading duration is long compared to the structural fundamental period a quasi-static design can be used. While, when the effective loading duration is short (less than one-third of the period) then the impulse of the load governs the design.

The global response of structural elements normally comes as a result of transverse loads with a long time duration (quasi-static loading), and it is usually associated with global flexure and shear responses. So, the global response of above the ground reinforced concrete structures exposed to blast loading is referred to as bending failure.

The second global failure mode is defined as shear failure. It was found that the influence of both static and dynamic loadings can be one of four types of shear failures; direct (dynamic) shear, punching shear, diagonal tension, and diagonal compression. The last three shear responses have fewer structural effects in the case of blast loading since it demands large lateral loads same as the earthquake load and can be neglected.

The first type of shear failure is mostly associated with short-duration transient dynamic loads that result from the blast effects, and it depends mainly on the amount of the wave pressure. The associate shear force is multiple times larger than the shear force associated with the flexural failure modes. The large shear stresses may cause direct global shear failure and it may take place very early when the shock wave first impinges the front face of the structure, which can be before any occurrence of significant bending deformation.

2.2.2 LOCAL STRUCTURAL BEHAVIOURS

Near-field explosions most of the time cause localized failure either shear or bending failure to the elements located very close to the detonation point. This mainly depends on the standoff distance between the explosive and the structure, and the relative capacity and ductility of the building elements. The local shear failure comes in the form of local punching and spalling, which cause initiate fragmentations in low and high speed. The influence of the punching is commonly known as "bleaching" (Byfield). Typical bleaching failures are followed by spalling and scabbing of the finishing, concrete cover in addition to the fragments.[3]

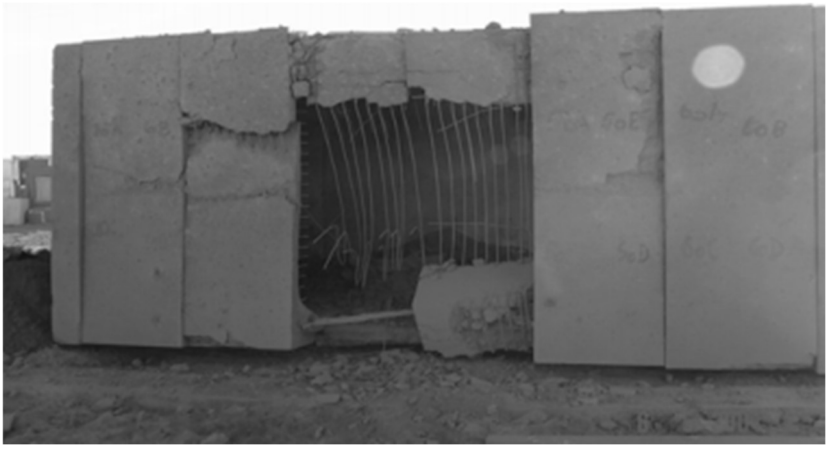

Figure 2.13: Breaching failure due to a close-in explosion of 6000kg TNT equivalent.[3]

2.2.3 PRESSURE-IMPULSE DIAGRAM (P-I)

The pressure-impulse (P-I) diagram is a simple method to mathematically connect a specific damage level to a combination of blast pressures and impulses enforced on a particular structural element. An example of a P-I diagram is shown in Figure 2.8 to predict levels of damage of a structural member. Structural members in the region (I) are maybe in severe damage and members in the region (II) may have negligible damages. Other P-I diagrams focus on the human response to blast in which case there are three categories of blast-induced injury, namely: primary, secondary, and tertiary injury.[3]

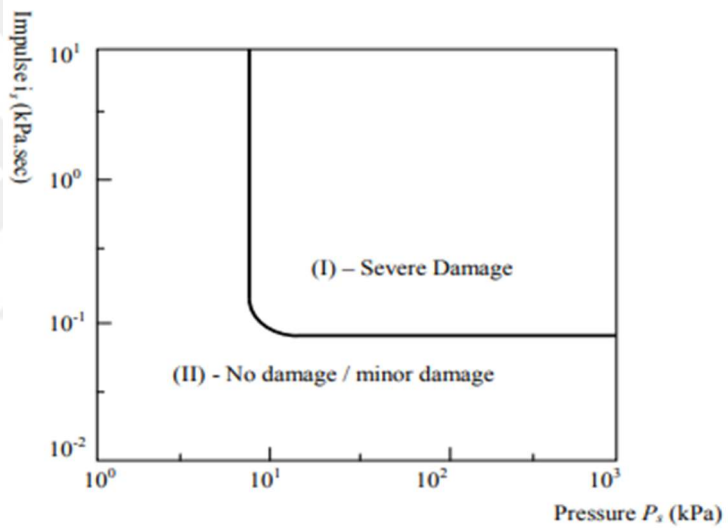

Figure 2.14: Pressure-impulse (P-I) diagram.[3]

2.3 MATERIAL PROPERTIES AT HIGH STRAIN-RATES

Different loading conditions have different strain-rate ranges; blast load is generally expected to increase the strain-rate from its static range value of (10^{-6} - 10^{-5})s^{-1} to high values in the range of (10^2 -10^4)s^{-1}, the material characteristics will change with the strain rate as well as the expected deformation. The strength of concrete and reinforcing steel bars increases whenever the reinforced concrete building experiences explosions due to the strain-rate. Figure 2.15 shows different strain-rate ranges for different loading conditions.

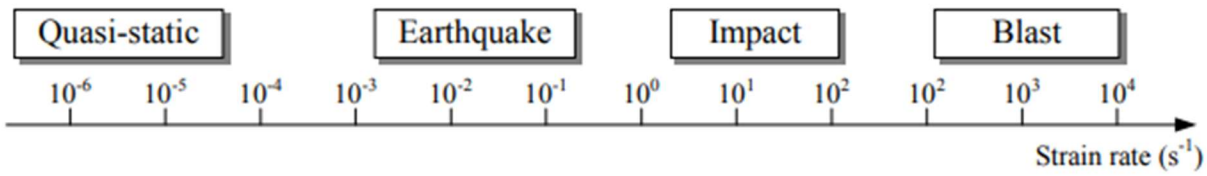

Figure 2.15: Strain-rate ranges for different loading conditions.[3]

2.3.1 DYNAMIC PROPERTIES OF CONCRETE AT HIGH STRAIN-RATES

The mechanical properties of concrete at high strain rates are different from its properties in the static strain-rates, the dynamic increasing factors (DIF) for the concrete can reach up to 6 in tension and 4 in compression in a strain rate of (10^2-10^3)s^{-1}.[11]

CEB- FIP (1990) proposed equations to get the dynamic properties of the concrete under known strain-rate; dynamic compressive strength, dynamic tensile strength, and dynamic modulus of elasticity.[12] [13]

For the concrete dynamic compressive strength Eq.10 and 11 are used:

$$\text{DIF} = \left(\frac{\dot{\varepsilon}}{\dot{\varepsilon}_S}\right)^{1.026\alpha} \qquad \text{for } \dot{\varepsilon} \leq 30\ s^{-1} \tag{10}$$

$$\text{DIF} = \gamma \left(\frac{\dot{\varepsilon}}{\dot{\varepsilon}_S}\right)^{1/3} \qquad \text{for } \dot{\varepsilon} > 30\ s^{-1} \tag{11}$$

Where $\dot{\varepsilon}$ = the strain-rate

$\dot{\varepsilon}_s$ = the static strain rate ($30\text{x}10^{-6}\ s^{-1}$)

Log γ = 6.156α-2

α = 1/ (5+9fc /fco)

fco = 10Mpa (1450 Psi)

And for concrete dynamic tensile strength under known strain-rate Eq. 12 and 13 are used.

$$\text{DIF} = \left(\frac{\dot{\varepsilon}}{\dot{\varepsilon}_S}\right)^{1.016\delta} \qquad \text{for } \dot{\varepsilon} \leq 30\ s^{-1} \tag{12}$$

$$\text{DIF} = \beta\left(\frac{\dot{\varepsilon}}{\dot{\varepsilon}_S}\right)^{1/3} \qquad \text{for } \dot{\varepsilon} > 30\ s^{-1} \tag{13}$$

Where: Log β = 7.112 δ -2.33

έ = the strain-rate

έs = the static strain rate (30x$10^{-6}\ s^{-1}$)

And for concrete dynamic modulus of elasticity Eq. 14 is used.

$$\text{DIF} = \left(\frac{\dot{\varepsilon}}{\dot{\varepsilon}_S}\right)^{0.026} \tag{14}$$

Where DIF = is the ratio of the dynamic modulus of elasticity to the static modulus of elasticity

έ = the strain-rate

$\acute{\varepsilon}_s$ = the static strain rate ($-30x10^{-6}\ s^{-1}$) for compression

$\acute{\varepsilon}_s$ = the static strain rate ($30x10^{-6}\ s^{-1}$) for tension

An increase of the strain-rate alters the compressive and tensile strength as well as the modulus of elasticity of the concrete as can be seen from Figure 2.16.

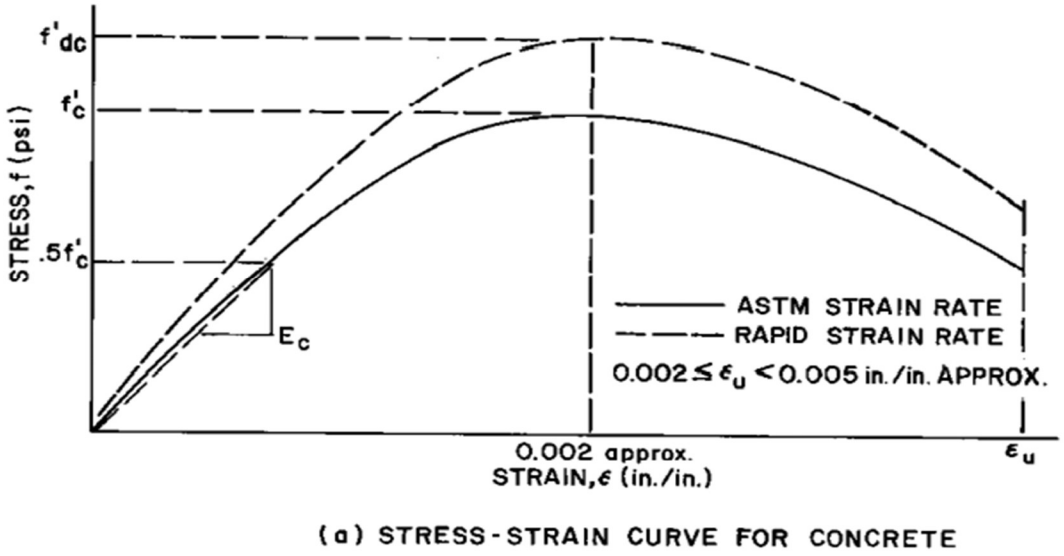

Figure 2.16: Strain-rate effects on the concrete stress-strain curve. [14]

2.3.2 DYNAMIC PROPERTIES OF STEEL AT HIGH STRAIN-RATES

Due to the isotropic characteristics of steel materials, their flexible and plastic reactions to dynamic loading can effortlessly be observed and evaluated. Norris et al (1959) examined steel with two diverse static yield strengths of 330 and 278 Mpa on tension under strain-rates ranging from 10^{-5}- $10^{-2}\ s^{-1}$. Strength increments of 9-21% and 10-23% were observed for the two types.

Malvar (1998) focused on the enhancement of steel reinforcing bars under high strain-rate effects, he analyzed the pre-existing data to estimate steel bars with yield strength at the range of 290-710 Mpa and found that the DIF drops for steel materials with high yield strengths also the DIF of the yield strength is higher than the ultimate strength.[15]

$$\text{DIF} = \left(\frac{\dot{\varepsilon}}{10^{-4}}\right)^{\propto} \quad (15)$$

Where $\propto = \propto fy$ when calculating for the yield stress.

$\propto fy = 0.074\text{-}0.04\ (fy/414)$

And $\propto = \propto fu$ when calculating for the ultimate strength.

$\propto fu = 0.019\text{-}0.009\ (fy/414)$

An increase in the strain-rate changes the yield strength and the ultimate strength of the steel but the modulus of elasticity remains the same as can be seen from Figure 2.17.

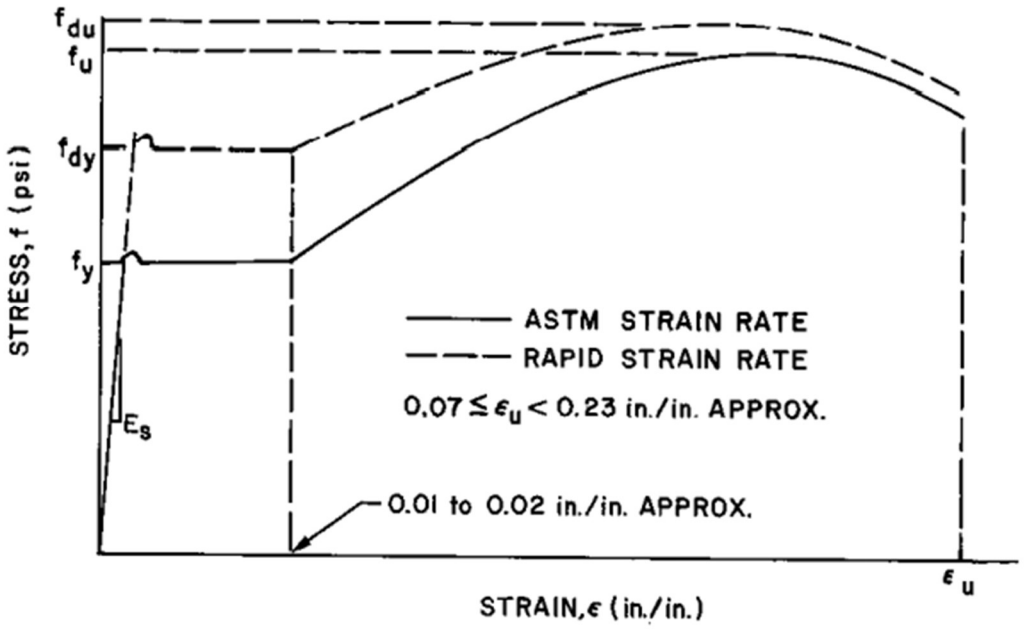

Figure 2.17: Strain-rate effects on the steel stress-strain curve.[14]

2.3.3 UNIFIED FACILITIES CRITERIA (UFC) CODE DIF RECOMMENDATIONS

Unified facilities criteria (UFC_340_02) recommends dynamic increasing factor values for the design of reinforced concrete elements depending on the type of stress

the structural element experiences and also the type of explosions it is designed for whether far-field or near-field explosions. The values recommended are always less than the actual values and this means the code takes into account the safety factor.

Table 2.4: Dynamic Increasing factors (DIF) for the design of reinforced concrete elements.[14]

Type of stress	Far Design range			Close-in design Range		
	Reinforcing bars		concrete	Reinforcing bars		concrete
	f_{dy}/f_y	f_{du}/f_u	f_{dc}/f_c	f_{dy}/f_y	f_{du}/f_u	f_{dc}/f_c
Bending	1.17	1.05	1.19	1.23	1.05	1.25
Diagonal TENSION	1.00	------	1.00	1.10	1.00	1.00
Direct shear	1.10	1.00	1.10	1.10	1.00	1.10
Bond	1.17	1.05	1.00	1.23	1.05	1.00
Compression	1.10	------	1.12	1.13	------	1.16

2.4 METHODS OF BLAST ANALYSIS

There are two commonly used methods for blast analysis, which are;

- The three-dimensional finite element method.
- The equivalent Single Degree Of Freedom (SDOF) method.[16]

2.4.1 EQUIVALENT SINGLE DEGREE OF FREEDOM ANALYSIS METHOD

In this method the structure is represented by an equivalent single degree of freedom system, then the blast load positive duration (t_d), and the fundamental natural vibration period of the structure is linked. few softwares use this method like NONLIN. This method is very simple compared to the three dimensional finite element method.

2.4.1.1 ELASTIC SINGLE DEGREE OF FREEDOM ANALYSIS

In this method the structure is modeled as a single mass, M, and stiffness, K, and the resistance of the structure is expressed in terms of the vertical displacement, Y_m, and the stiffness of the spring, K, as shown in Figure 2.18.[17]

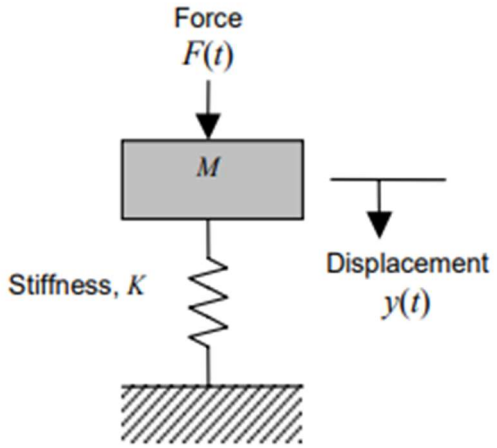

Figure 2.18: Single degree of freedom system.[17]

The blast load is also simplified as a triangular pulse with a peak force equal to F_m, and positive duration of t_d, and the function of the force is calculated by the equation below.

$$F_{(t)} = F_m \left(1 - \frac{t}{t_d}\right) \tag{16}$$

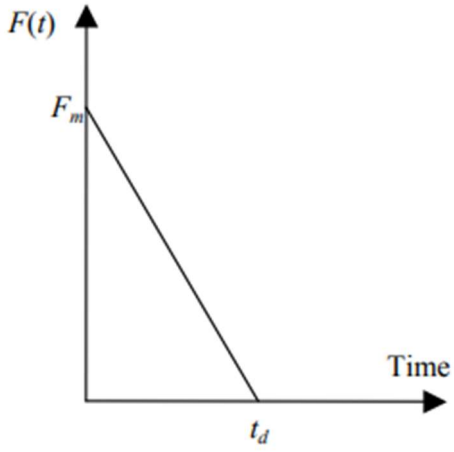

Figure 2.19: Positive phase triangular blast load time history.

And the area under the force function which is the blast impulse is given by Equation 17.

$$I = \frac{1}{2} F_m \, t_d \tag{17}$$

The equation of motion of the un-damped single degree of freedom for a time between 0 to t_d is given by Biggs (1964).[28]

$$M_{\ddot{y}} + K_y = F_m \left(1 - \frac{t}{t_d}\right) \tag{18}$$

And the general solution of the displacement is given by:

$$y_{(t)} = \frac{F_m}{K} (1\text{-}cos\omega\, t) + \frac{F_m}{K t_d} \left(\frac{sin\omega t}{\omega} - 1\right) \tag{19}$$

While for the velocity is given by:

$$\dot{y}_{(t)} = \frac{dy}{dt} = \frac{F_m}{K} \left[\omega sin\omega t + \frac{1}{t_d} (cos\omega t - 1)\right] \tag{20}$$

Where; ω is the natural circular frequency of the vibration, and

T is the natural period of the vibration of the structure.

The maximum dynamic deflection y_m can be found by setting the Equation 20 equal to zero.

2.4.1.2 ELASTO-PLASTIC SINGLE DEGREE OF FREEDOM ANALYSIS

The Ideal Equivalent Elasto-plastic single degree of freedom proposed by Biggs (1964) is commonly used, and the process depends on the required ductility factor, $\mu = \frac{y_m}{y_e}$.

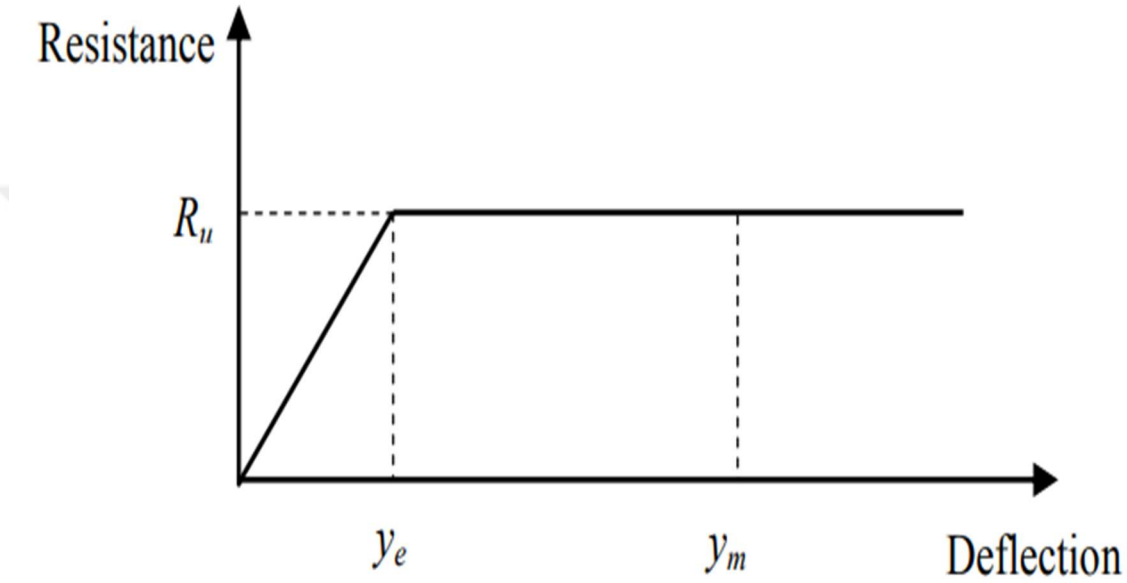

Figure 2.20: Resistance function for an Elasto-plastic SDOF system.[17]

The response of an ideal bilinear elasto-plastic system can be estimated for the triangular load pulse with rapid rise and linear decay, with maximum value F_m and duration, t_d. The result for the maximum displacement is found from chart given in (TM 5-1300), as a family of curves for selected values of R_u /F_m showing the required ductility μ as a function of td/T, in which Ru is the structural resistance of the member and T is the natural period.[17]

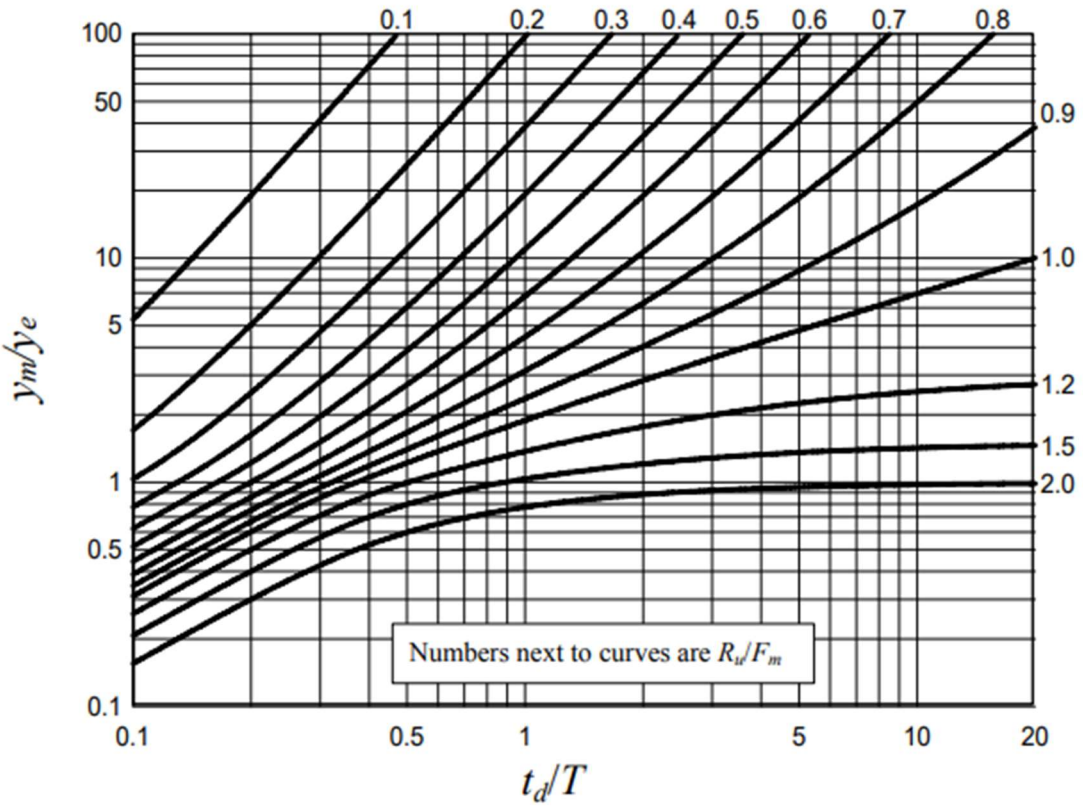

Figure 2.21: Maximum deflection of Elasto-plastic SDOF system under triangular blast load.

2.4.2 THE THREE DIMENSIONAL FINITE ELEMENT ANALYSIS METHOD.

The structural members are expected to experience large nonlinear deformations caused by blast loads, the exact dynamic response of the structure is possible only by step by step solution demanding nonlinear dynamic finite element software.

This method is the most accurate and reliable analysis method for monitoring the behavior of structures under blast loads, also the performance of structural members, the geometric and material nonlinearity can also be considered, and the sequence of the plastic hinges formation can be captured. This method demands high-performance computer software that can solve too much equivalent equations, such as; ANSYS, ABAQUS and LS-Dyna.

2.4 PROGRESSIVE COLLAPSE PHENOMENON

Progressive collapse is a term given to when local damage leads to global damage and this occurs when one of the vertical load-carrying members fail, the load carried by the failed member is distributed to the other parties of the structure depending on their relative location and stiffness, the other parties may collapse due to the extra load, this phenomenon is known as progressive collapse.

Different load types may lead to progressive collapse events such as; earthquakes, gas explosions, explosions used in the demolition process and impact loads like car or aircraft collision. Normally after the column failure the roof supported by the column experience large deflections, therefore, the adjacent columns experience extra loads, the structure will redistribute these loads and reach equilibrium or global collapse will take place.

2.5 PROGRESSIVE COLLAPSE DESIGN METHODS

Several design methods were recommended to protect the structure from the progressive collapse caused by the unpredictable loads for new and existing buildings, these methods are classified into three methods which are;

a) Event control.
b) Indirect design method and
c) Direct design method.

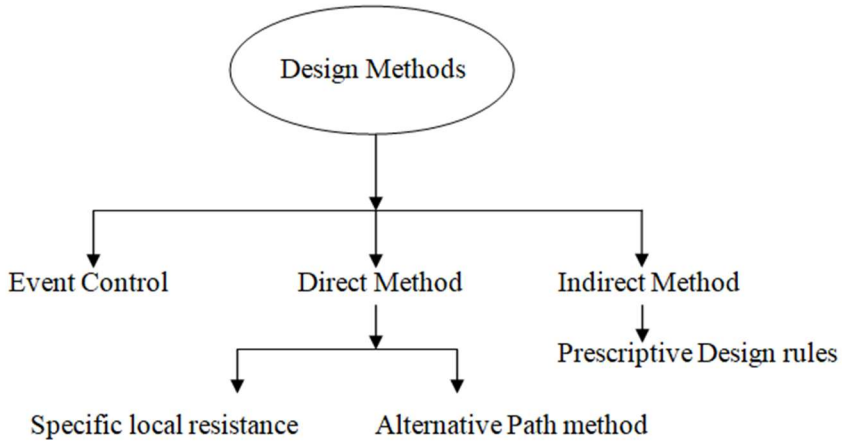

Figure 2.22: Progressive collapse design methods

The Event control method is not a well-known procedure for designing structures against progressive collapse, while the other methods are advanced and special in the design and estimation of progressive collapse for new and existing buildings, these methods are also mentioned in most of the design codes and guidelines such as; the American Society of civil engineering (ASCE 2002), General Service Administration (GSA 2003) and Department of Defense (DOD 2016).

2.5.1 EVENT CONTROL

The event control method is the most economical method to protect the buildings from the abnormal loads that may cause the progressive collapse; this method is based on suggestions of researchers and structural engineers to minimize the possibility of the progressive collapse occurrence, such as; parking zone isolation and also providing large standoff distance by building the fence away from the main building to minimize explosive hazards. This method is a good choice economically but impractical.

2.5.2 INDIRECT DESIGN METHODS

All indirect design methods are independent of the hazards that may lead the progressive collapse, the idea of this design method is based on increasing the total integrity of the structure without taking into account the abnormal loads expected to cause the progressive collapse.

To increase the general integrity and stability of the building, continuous interconnection across joints are used to develop redundancy and increase the ductility, also some codes recommend using tie forces, this will provide the structural elements proper connections that will hold the structural elements together even after the failure of some vertical load-carrying elements.

2.5.3 DIRECT DESIGN METHODS

In these design methods, the abnormal loads are taken into account by using specific ways to design the structural elements and connections to improve their performance for the progressive collapse. The alternative path method is the most used direct design method and it is recommended by most of the codes.

2.5.3.1 ALTERNATIVE PATH METHOD

This method is followed in this study for analyzing the structures for the progressive collapse. Also most of the studies that focus on this topic follow this method, since the most two used guidelines recommend using this method which are the Department Of Defense[14] and General Services Administration (GSA,2003).

The concept of this method is to allow small deformations but prevent the total or partial collapse of the structural system by using alternative load paths in the adjacent elements to transmit the loads carried by the failed components.

The procedure followed in this method starts with applying the design loads as normal then various instantaneous removals of vertical load-carrying members in the center, corner, and the side of the structure is performed one after another, after each time the remaining part of the structure is designed to resist such failure, at the end the structure will be apple to resist progressive collapse occurrence.[18]

2.6 METHODS OF PROGRESSIVE COLLAPSE ANALYSIS

To estimate the response of structures for the progressive collapse there are few methods of analysis, these methods are different in terms of time-consuming and accuracy of the results required. These methods used for the prediction of the structural behavior are linear static analysis (LS), linear dynamic analysis (LD), nonlinear static analysis (NS), and Nonlinear dynamic analysis (ND).

Researchers in this field investigate the advantages and disadvantages of each method. Both DOD and GSA recommend using the simple analysis method for estimating the behavior of new and existing buildings of low and moderate-rise buildings, as result of that the most used analysis method for the prediction of the progressive collapse is the linear static method.[19]

2.6.1 LINEAR STATIC METHOD

This procedure is the easiest and fundamental structural analysis method, it assumes the structural materials to remain in their linear elastic condition and neither material nor geometric nonlinearities are taken into account, so the prediction of the response of the structures for blast loads and progressive collapse by this method will not give precise results since these hazards are nonlinear dynamic events. As per GSA guidelines, this method is not applicable for irregular structures and also structures with more than ten stories.

In this procedure the structure is modeled then one of its vertically load-carrying members is removed from the model, the remaining part of the structure is loaded with a gravity load which is according to the GSA guideline which is used in this study (DL+0.25LL), and (1.2DL+0.5LL) according to the UFC guideline, then the analysis is carried out. The most advantage of this method is that the analysis finishes very quickly, after that the demand-capacity ratio (DCR) is calculated for each element. The dynamic effects are considered by using a gravity load amplification factor of 2, this means the gravity load used in this method is 2(DL+0.25LL) or 2(1.2DL+0.5LL) according to GSA and UFC guidelines respectively.

2.6.2 LINEAR DYNAMIC METHOD

This method is more advanced and accurate compared to the previous method. Similar to the previous method this method is also based on the assumption that the structural materials remain in the linear elastic zone during and after the event, but unlike the previous method it considers the dynamic properties of the loads, therefore there is no need for gravity amplification factor, meaning the gravity load in this method is (DL+0.25LL) or (1.2DL+0.5LL) according to GSA and UFC guidelines respectively. Also in this method, we calculate the DCR of the elements after the removal of the critical vertically load-carrying element.

2.6.3 NONLINEAR STATIC METHOD

This method is known as pushover analysis; it is mostly used in the analysis of lateral loads such as earthquakes. When this method is used for the progressive collapse estimation it is named pushdown analysis. It is more precise than the linear static method since it allows the structural materials to undergo the plastic condition by assigning plastic hinges on the members, also it considers the material and geometric nonlinearities in its analysis, however, it does not consider the dynamic properties of the load, so to take it into account gravity amplification factor of 2 is used same as the linear static method.

In this method, the gravity load is incrementally increased in each step until the maximum load is reached or the structure fails. This method does not need to calculate the DCR of the members since the hinge status shows the member condition.

2.6.4 NONLINEAR DYNAMIC METHOD

This method is the most advanced precise and complicated of all methods, it is known as Time History analysis in the structural engineering field, where the load is modeled as a function of time also the results are functions of time as well.

This method consumes a lot of time and the engineer is needed to know the properties of the structure to use this method. In this method both material and geometric nonlinearities are taken into account also the dynamic properties of the load

are considered, therefore the gravity load amplification factor is not needed, the DCR is not calculated as well since plastic hinges are assigned on the members. Structural engineers mostly do not use this method because of its time consumption and complexity.

CHAPTER 3

MODELING DESIGN AND ANALYSIS

3.1 INTRODUCTION

To analyze blast load effects and Progressive collapse on a structure two five-story 2D reinforced concrete frames were designed according to the EUROCODE 2-2004 using structural analysis and design software SAP2000 version 20.

The two frames have similar properties, loadings, and dimensioning except the compressive strength of the concrete, in frame A concrete Grade C30 is used while frame B is used Grade C10 to represent both low and relatively high levels of concrete compressive strengths.

Both structures are five-story 2D reinforced concrete frame buildings of 3m story heights and three bays of 4m width.

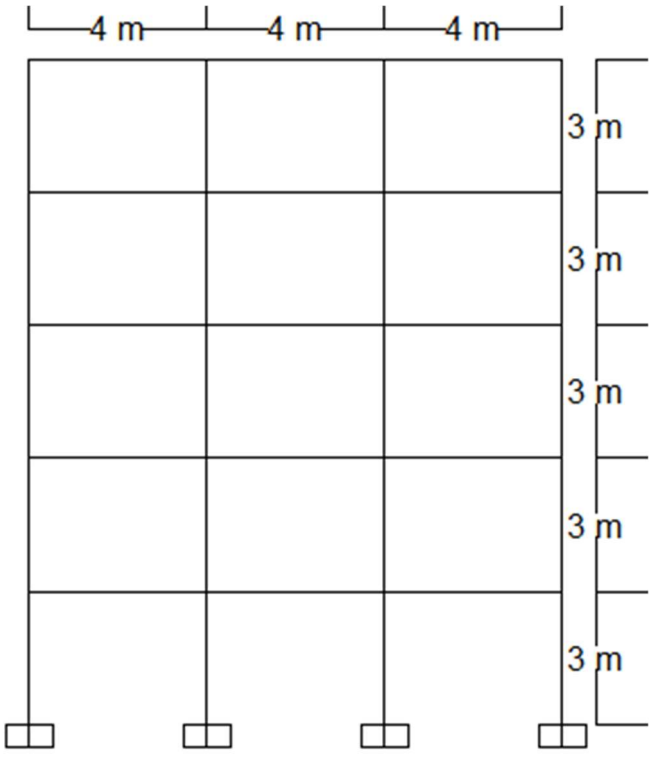

Figure 3.1: Elevation view and dimensions of the frames.

3.2 MATERIAL PROPERTIES OF THE FRAMES

Both frames were modeled as reinforced concrete structures. Frame A was modeled with concrete with compressive strength of 30Mpa and modulus of elasticity of 33Gpa, while Frame B was modeled with grade 10 concrete with a modulus of elasticity of 23Gpa, both frames were reinforced with steel rebar with a yield strength of 415Mpa and ultimate strength of 485Mpa.

Table 3.1: Material properties of both structures in detail.

	Frame A	**Frame B**
Grade of concrete	C30	C10
Density of concrete	25KN/m^3	25KN/m^3
Modulus of elasticity of concrete	33Gpa	23Gpa
Poisons ratio of concrete	0.2	0.2
Grade of steel	fe415	fe415
Yield strength of steel	415Mpa	415Mpa
The ultimate strength of steel	485Mpa	485Mpa
Modulus of elasticity of steel	200Gpa	200Gpa
Poisons ratio of steel	0.3	0.3

3.3 DESIGN ASSUMED LOAS INTENSITIES

The structures are assumed and designed as residential buildings with a Dead load of 16KN/m and a Live load of 6KN/m representing the gravity load. For the Earthquake loading TSC-2018 is used as an equivalent lateral load with these assumptions:

- The map spectral accelerations $\mathbf{S_1}$ =0.226 and $\mathbf{S_s}$ =0.788
- Site class=ZC
- Response reduction factor, **R** = 8
- System over-strength, **D** = 3
- Importance factor, **I** = 1

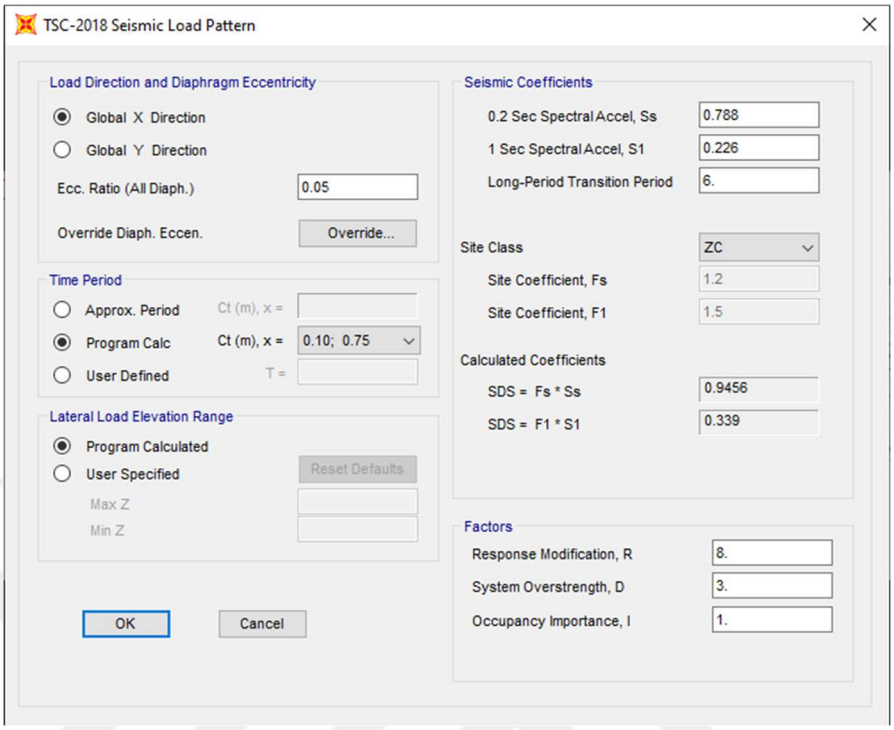

Figure 3.2: Earthquake load definition in SAP2000 as an equivalent lateral load as per TSC-2018

3.4 DESIGN LOAD COMBINATIONS

a) 1.35DL

b) 1.35DL +1.5 LL

c) DL + 0.3LL + EQ

d) DL + 0.3LL – EQ

e) DL + EQ

f) DL – EQ

3.5 STRUCTURAL DETAILING OF THE MEMBERS

The required area of the reinforcement from the SAP2000 was divided by the area of the chosen rebar type to get the number of rebars in each member.

Table 3.2: Members reinforcement details.

	Reinforcements	
	Frame A	**Frame B**
Column 500x500mm	Long= 8Ø20mm	Long= 8Ø20mm
	Shear= 3Ø8 @85mm b/w	Shear= 3Ø8 @110mm b/w
Beam 450x300mm	Top= 4Ø14mm	Top= 4Ø14mm
	Bottom= 3Ø14mm	Bottom= 2Ø14mm

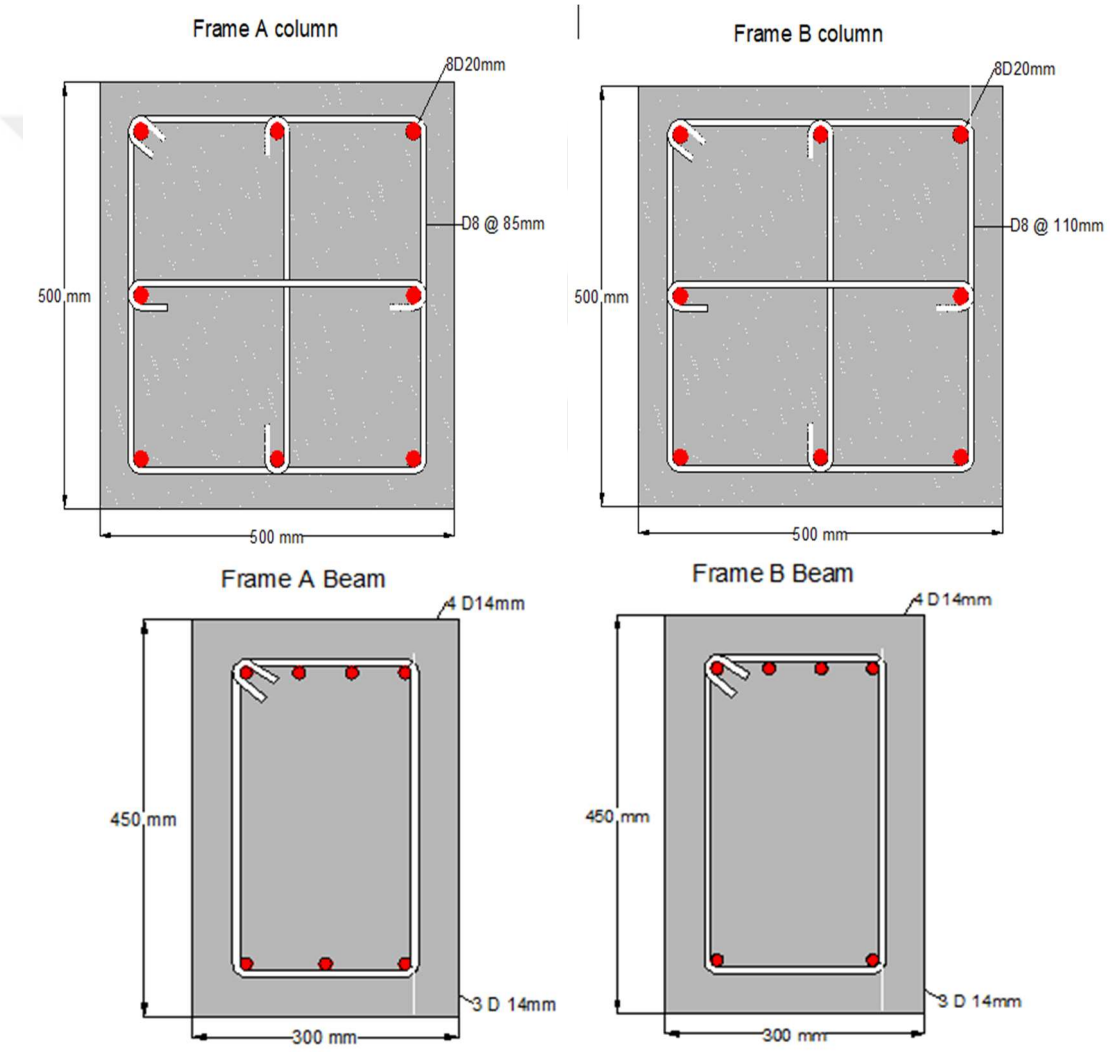

Figure 3.3: Reinforcement detailing of the reinforced concrete members.

The natural period of frame A was 0.687s while frame B had a 0.82s period.

3.6 MODEL ASSUMPTIONS

1) All connections are assumed to be moment connections.
2) Connections of the columns to the foundation are assumed to be fixed.
3) All floors are considered rigid diaphragms.

3.7 STRAINS-RATE EFFECTS ON CHARACTERISTICS OF THE STRUCTURAL MEMBERS

To monitor the influence of the strain-rate value on the properties of the structural members, a random column was detailed as shown in Figure 3.4, concrete grade 30 was used with modulus of elasticity of 25742960Mpa, for the longitudinal steel bars the yield strength was 440Mpa and the ultimate strength was 550Mpa, while for the stirrups it was used steel bars with yield strength of 275Mpa and ultimate strength of 430Mpa.

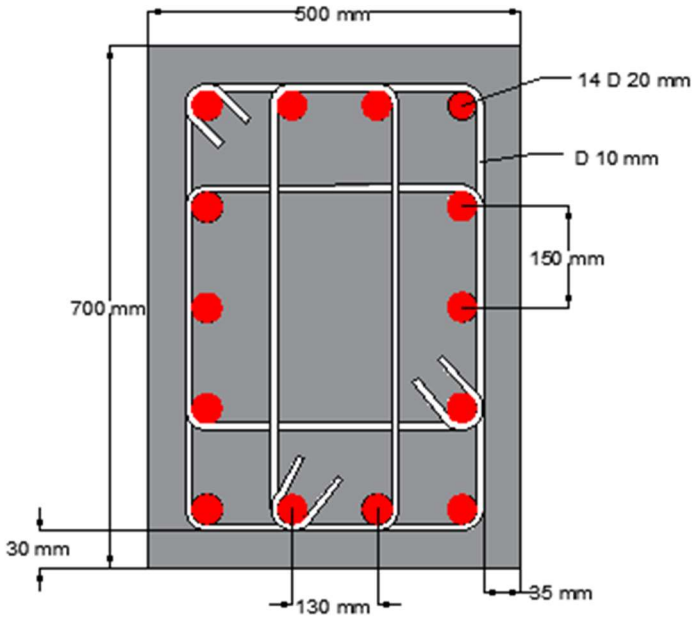

Figure 3.4: reinforcement details of the column.

Different strain-rate values were selected and according to those values the Dynamic Increasing Factor (DIF) for each material property was computed using the Equations (10 to 15) from the CEB-FIP-1990 code. The column was modeled in

SAP2000 V20 in the Section designer, and the steel bars were modeled as line bars as illustrated in Figure 3.5.

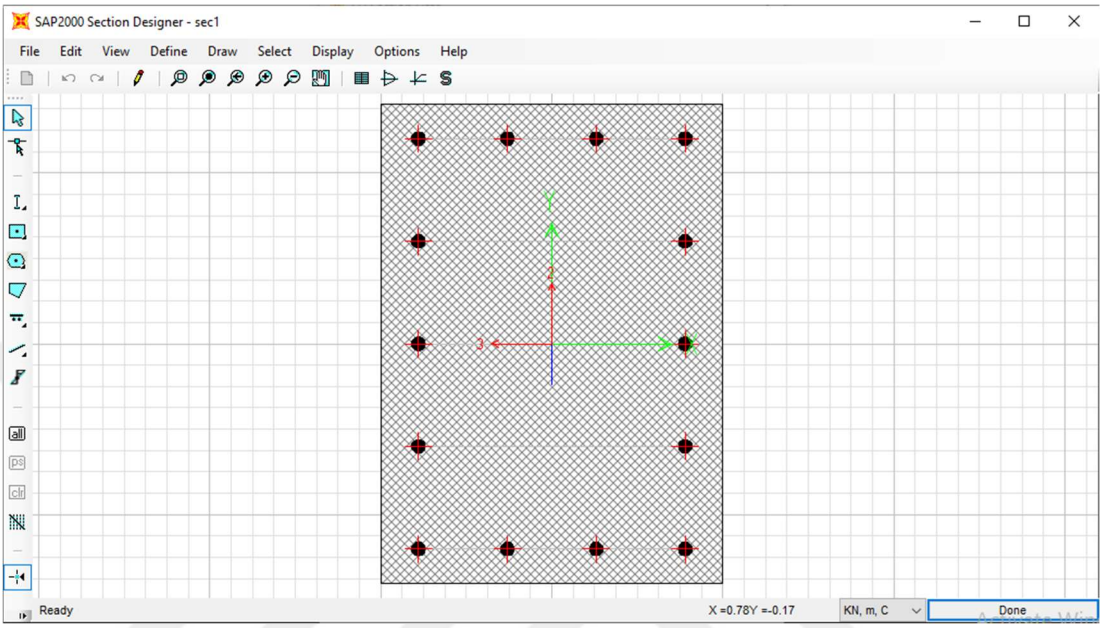

Figure 3.5: SAP2000 section designer.

Then the moment-curvature curve is displayed as Caltrans idealized model as shown in Figure 3.6. This process was repeated for each strain-rate value and the moment-curvature curves were compared to find out the effect of the strain-rates on the strength of the member.

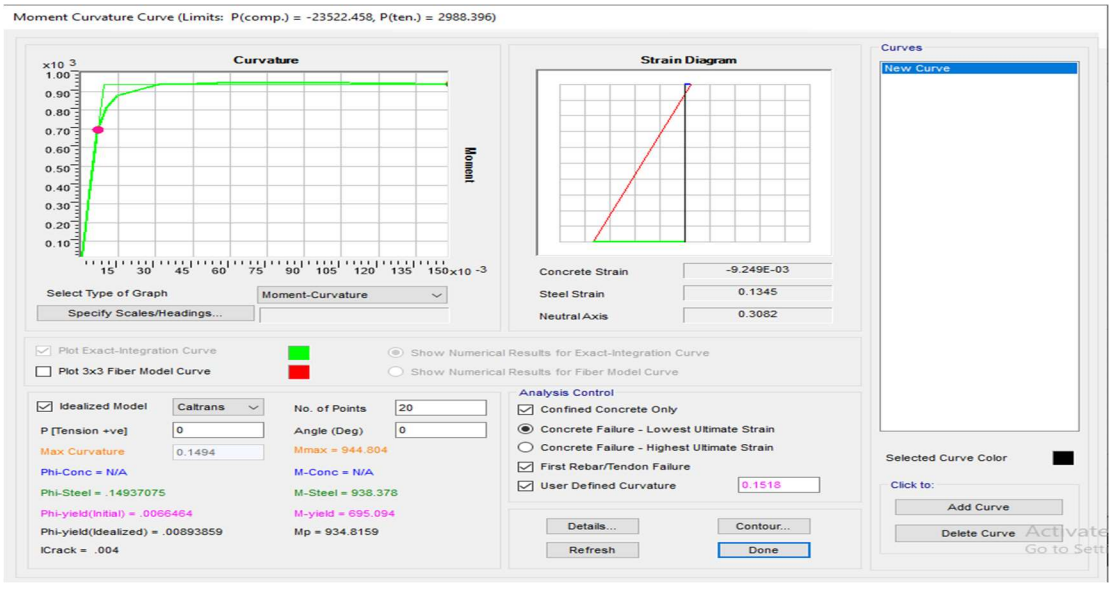

Figure 3.6: Moment-Curvature curve in SAP2000.

3.8 STRAINS-RATE EFFECTS ON THE OVERALL BEHAVIOR OF THE STRUCTURES

To investigate the influence of the strain-rate value on the overall performance of structures, the two frames were analyzed under different strain-rate values. First different strain-rate values were selected and according to those values the Dynamic Increasing Factors (DIFs) for each material property were computed using the Equations (10 to 15) from the CEB-FIP-1990 code. A separate model was created for the same structure under different strain-rates and Pushover analysis was carried out at each condition.

Table 3.3: Calculated Dynamic Increasing Factors at each strain-rate.

strain-rate	fcd/fc	Ed/E	fyd/fy	fud/fu
static	1	1	1	1
$1x10^{-3}$	1.118993	1.0955	1.0752	1.022
$1x10^{0}$	1.396416	1.311	1.3364	1.0908
$1x10^{2}$	2.33	1.478	1.545	1.1392
used strain-rate	1.25	1.1	1.23	1.1

The gravity load used to represent the static load carried by the structure at the moment the hazard takes place was Dead load plus thirty percent of live load (DL+0.3LL); also the geometric nonlinearity was considered in the gravity load by applying the P-Delta effects.

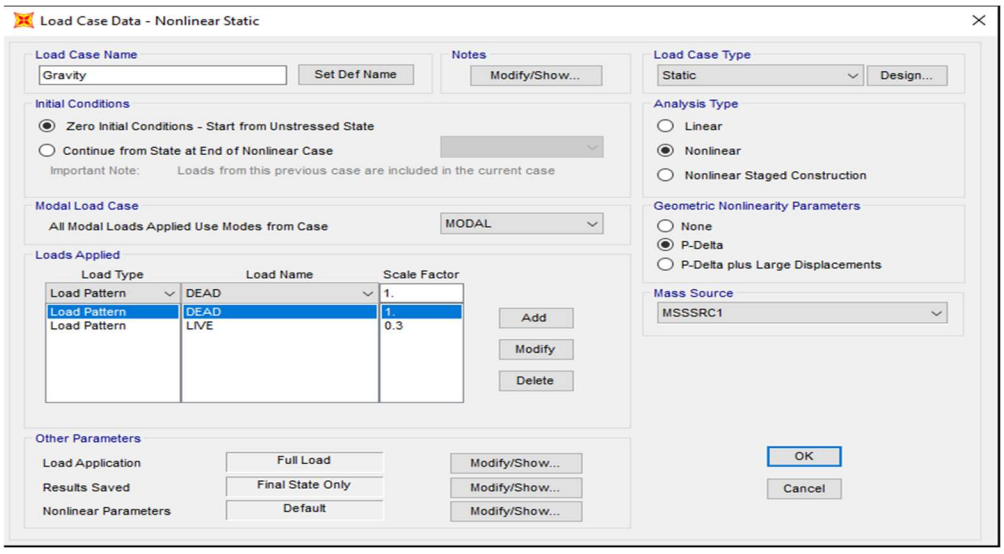

Figure 3.7: Nonlinear static gravity considered in the pushover analysis.

3.8.1 HINGE PROPERTIES DEFINITION ON THE ELEMENTS

Plastic hinge properties were assigned at a distance of 10 and percent of the member length from both edges. The auto-hinge type from ASCE 41-13 code was used and (P-M2-M3) were considered as degrees of freedom for the hinges assigned to the columns, while (M3) was considered for those on the beams.

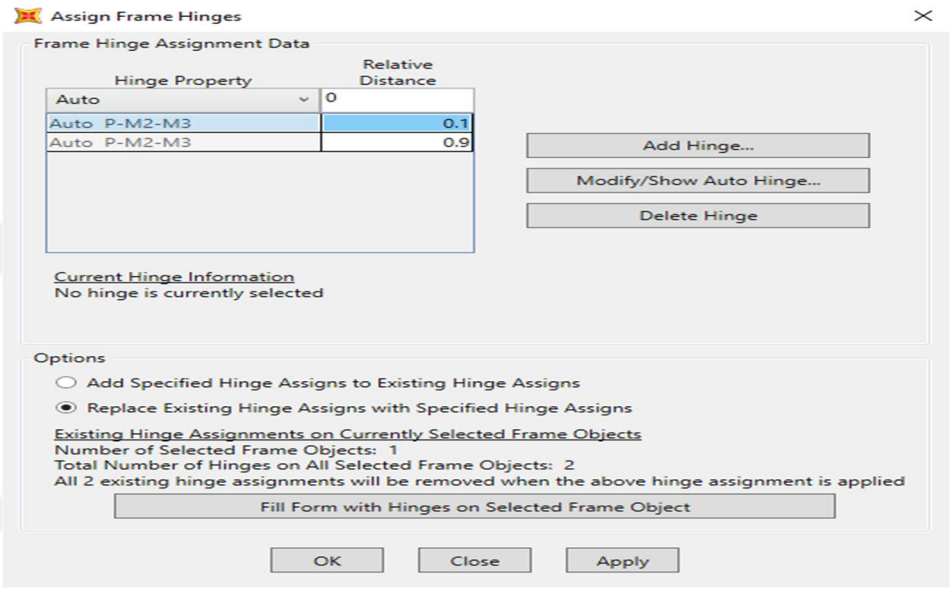

Figure 3.8: Assigned hinges to the columns.

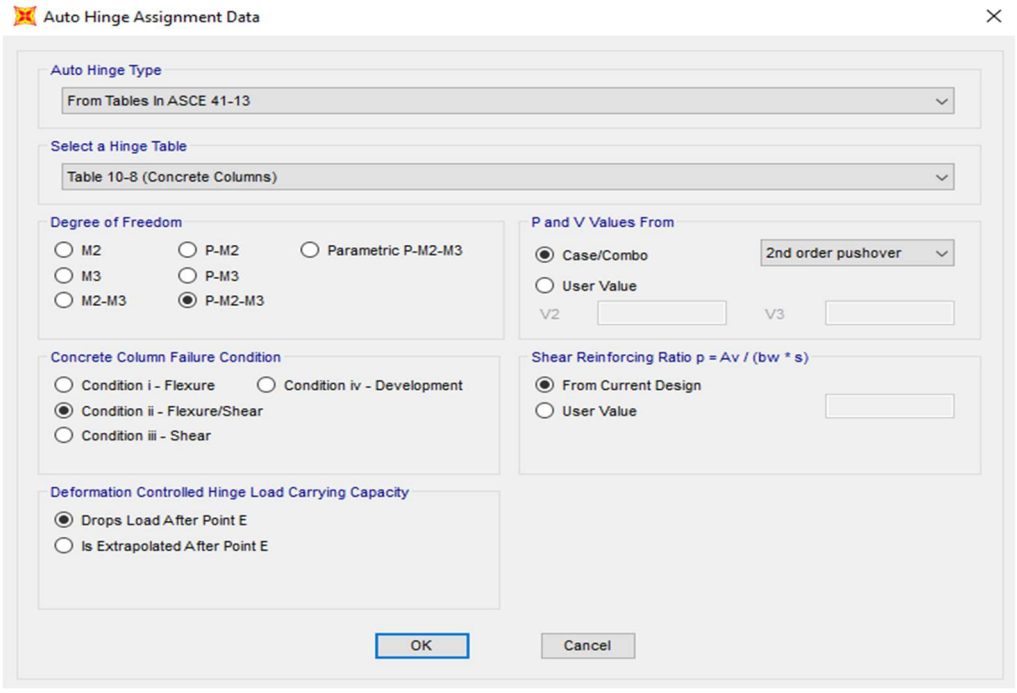

Figure 3.9: Assigned hinges to the columns for the second-order pushover.

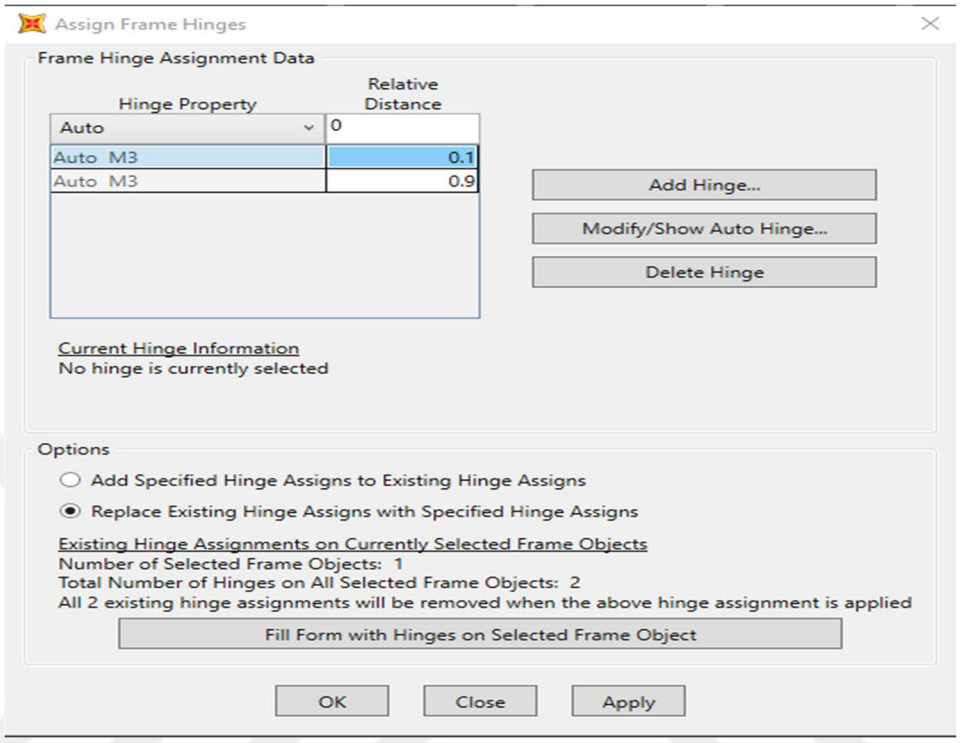

Figure 3.10: Assigned hinges to the beams.

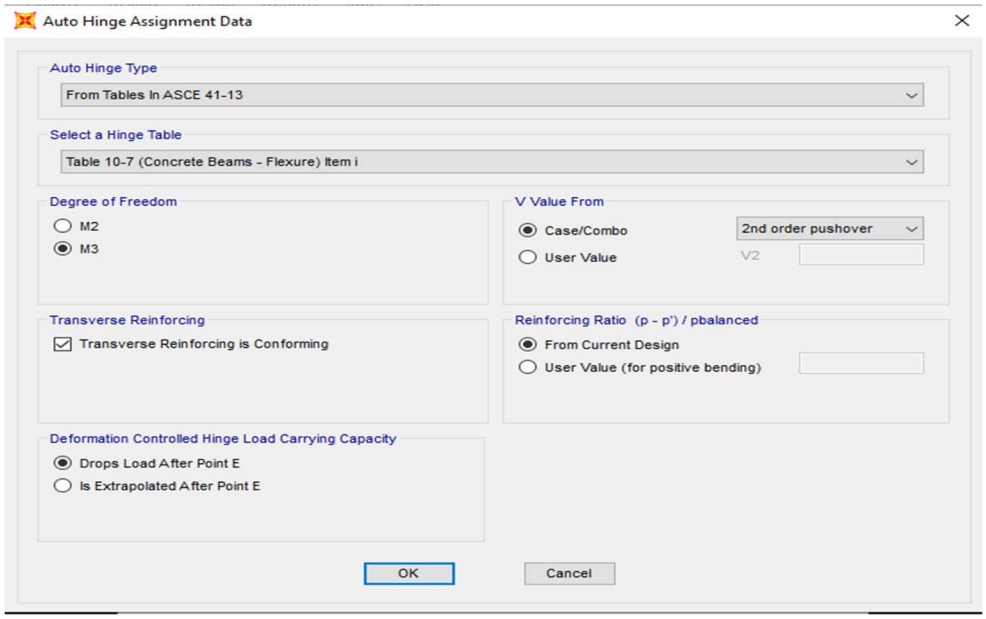

Figure 3.11: Assigned hinges to the beams for the second-order pushover

3.8.2 SECOND ORDER PUSHOVER ANALYSIS

Nonlinear static (Pushover) analysis was executed for the structure as it holds the gravity load. The load was applied as a displacement control on the global X-direction of a joint in the roof. The geometric nonlinearity was also taken into account by applying the P-Delta effects, and the mass source of the dynamic action was assumed as dead load plus 30 percent live load.

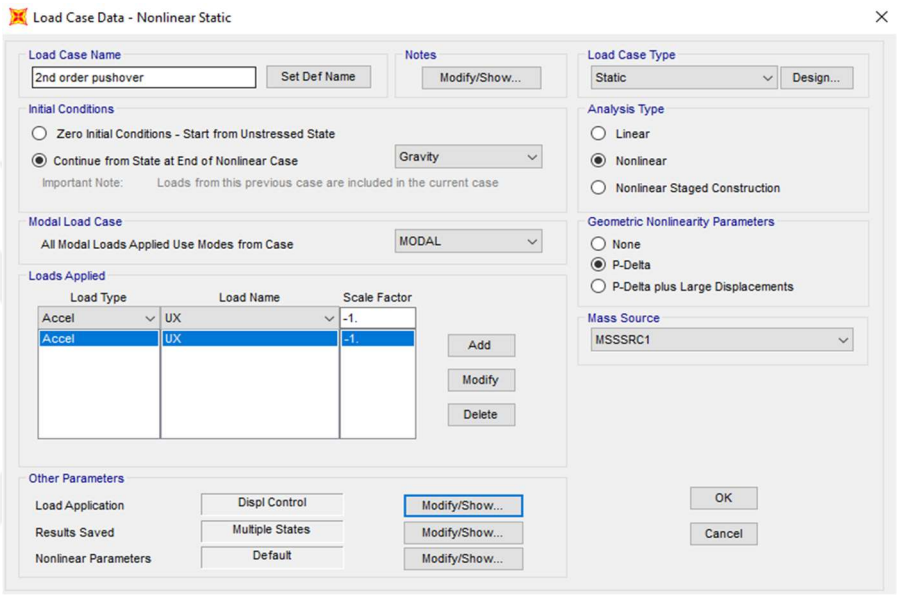

Figure 3.12: Second order pushover analysis definition.

3.9 BLAST ANALYSIS

Several parameters govern the global response of the building structure under blast load. The response out-puts also are affected by the assumptions made during the analysis, therefore it is necessary to check the influence of these parameters and the validity of the assumptions and simplifications made in the analysis.

To examine the resistance capacity of the structures two hemispherical (ground) scenarios of different TNT charge weights (100 and 300 kg) at a standoff distance of 10 meters from the structure were analyzed for both frames by nonlinear dynamic method (Time history analysis).

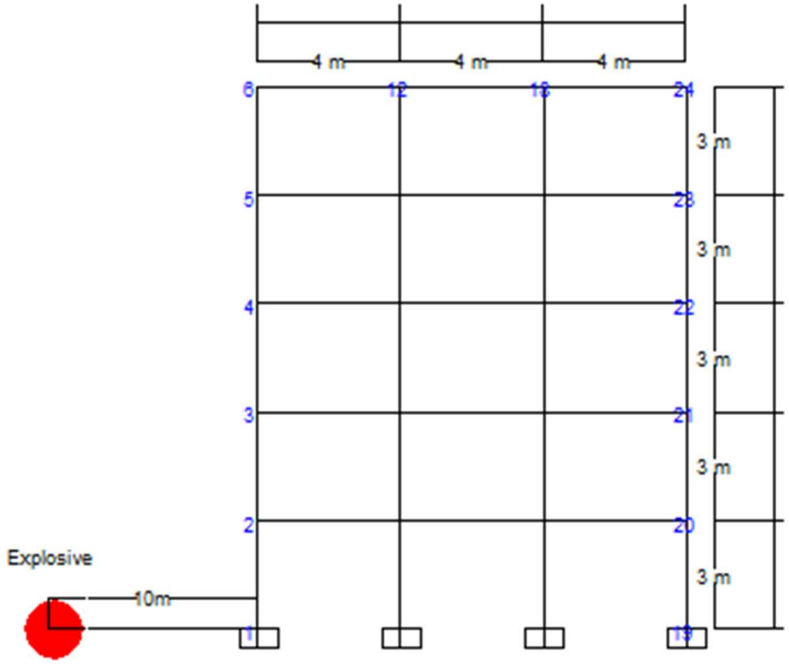

Figure 3.13: The Explosive location relative to the structure.

3.9.1 MATERIAL MODEL

Concrete material was modeled in Sap2000 as Takeda hysteresis with Mander stress-strain curve model, and the steel material was modeled as Kinematic hysteresis with simple stress-strain curve model, Dynamic increasing factors of 1.25 for the concrete compressive strength and 1.23 for the yield strength of the steel reinforcing bars and 1.1 for all other material strengths.

3.9.2 BLAST LOADING PATTERNS

To calculate the blast pressures on a structure the surface is divided into rectangles and at the center of each rectangle, there is a joint as shown in the figure below.

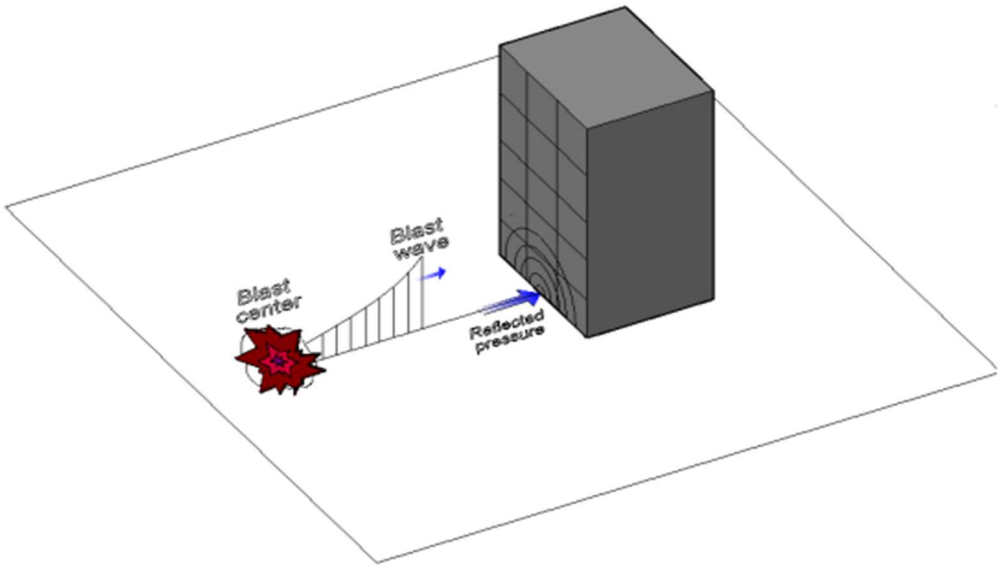

Figure 3.14: Surface division for the blast pressure calculation.[8]

Three different blast load patterns were used and compared for each scenario as below:

1) **Exact progressive loading**: this kind of loading can be used for both 2D and 3D analysis.

   Blast Loads are assigned on beam-column joints on all faces of the structure. The blast pressure-time history of each joint on the front face is calculated based on the explosive charge weight, distance, and angle of the incident then multiplied to the tributary area to change the pressure into a load, Also the load at every joint start at its exact arrival time. The loads on Joints at the other faces are calculated as equivalent loads. This type of loading is closest to the real load the structure experiences.

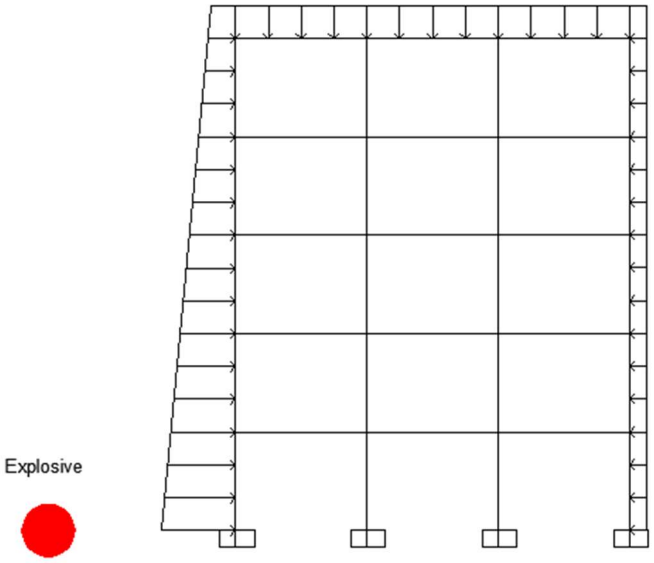

Figure 3.15: Exact progressive loading pattern.

2) **<u>Progressive loading</u>**: this kind of loading can be used for 2D analysis.

Blast Loads are assigned on beam-column joints on the front and the roof of the structure. The blast pressure-time history of each joint on the front face is calculated based on the explosive charge weight, distance, and the angle of incidence then multiplied to the tributary area to change the pressure into a load, Also the load at every joint start at its exact arrival time. The loads on Joints at the other faces are calculated as equivalent loads.

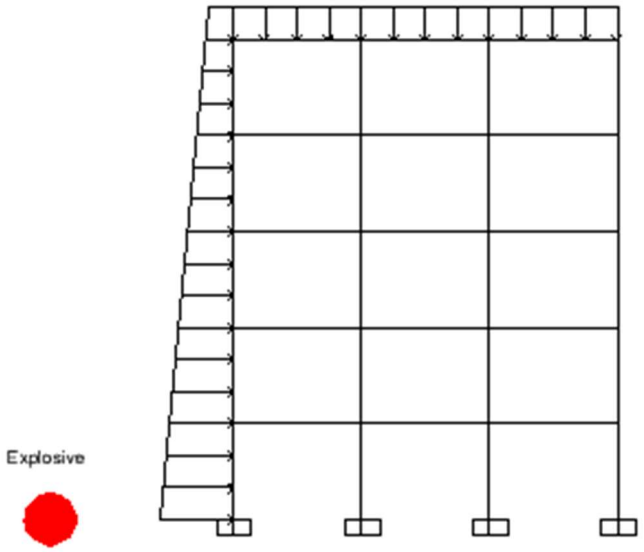

Figure 3.16: Progressive loading pattern.

3) **Simplified progressive loading**: this kind of loading can be used for 2D analysis.

Blast Loads are assigned only on beam-column joints on the front face of the structure. The blast pressure-time history of each joint on the front face is calculated based on the explosive charge weight, distance, and angle of incident then multiplied to the tributary area to change the pressure into a load, Also the load at every joint starts at its exact arrival time. The loads on Joints at the other faces are calculated as equivalent loads.

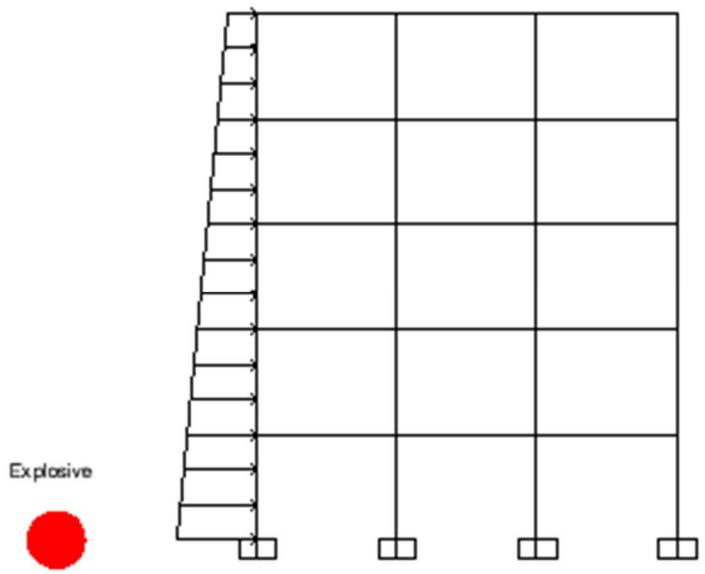

Figure 3.17: Simplified progressive loading pattern.

3.9.3 CALCULATION OF THE BLAST LOAD PARAMETERS

Blast load parameters can be computed manually using the diagrams given in the UFC_3_340_02 guideline, or by using the blast load calculating softwares. In this study OVERPRESSURE software was used which calculates the blast parameters of the ground explosions following the above-mentioned guideline. This software gives more accurate values and makes the process easier and faster as well. This software demands the standoff distance, the angle of incidence, and also the weight of the TNT charge.

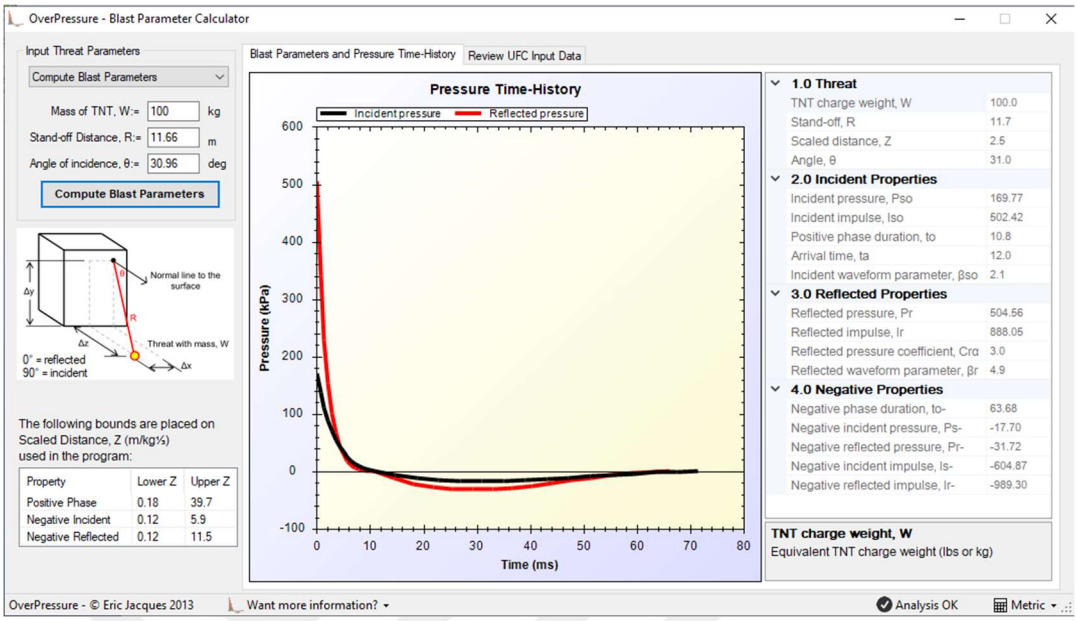

Figure 3.18: Blast load parameters calculation using OVERPESSURE software. [27]

3.9.4 Blast pressure- time functions of the joints.

Two different TNT weights were assumed at a standoff distance of 10m from the structure and the blast pressure-time history was calculated for each joint according to its standoff distance, and angle of incidence.

Table 3.4: Parameters affect the blast pressure-time history.

Joint	Standoff distance(R) in(m)	The angle of incidence(degrees)	AREA(m^2)
2	10.44	16.7	12
3	11.66	30.96	12
4	13.45	41.99	12
5	15.62	50.19	12
6 front	18.03	56.31	12
6 roof	18.03	0	8
12	-	-	16
18	-	-	16
24 roof	30.03	0	8
24 rear	30.03	0	6
23	-	0	12
22	-	0	12
21	-	0	12
20	-	0	12

3.9.4.1 SCENARIO ONE (100kg of TNT)

In this scenario, a 100kg of TNT explosive was considered on the ground at a distance of 10 meters from the structure. The blast parameters were found by OVERPRESSURE software using the actual standoff distance and angle of incidence. Then the blast load is found by multiplying the pressure-time function to the tributary area.

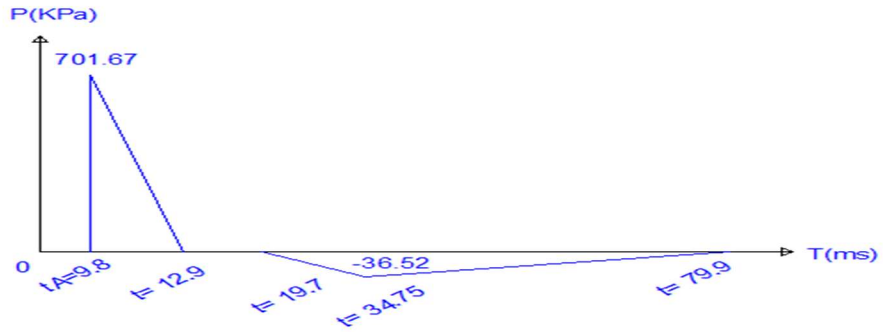

Figure 3.19: Blast pressure-time history at joint (2) from scenario one.

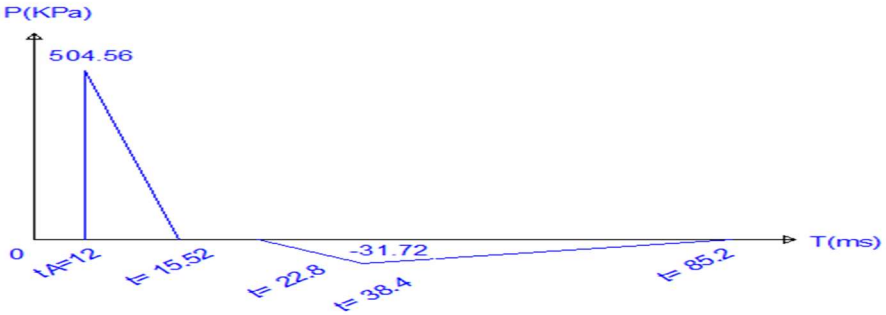

Figure 3.20: Blast pressure-time history at joint (3) from scenario one.

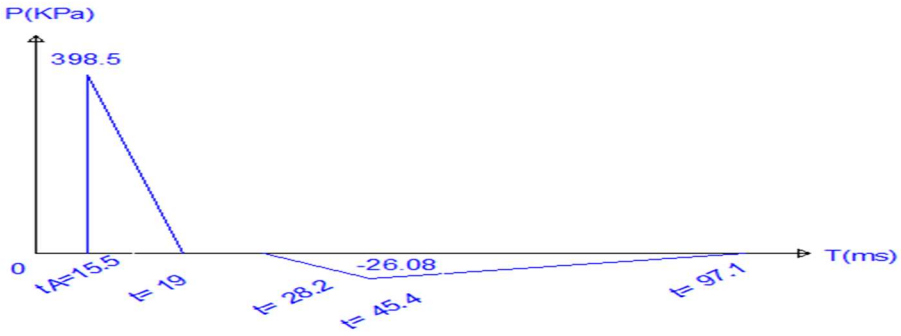

Figure 3.21: Blast pressure-time history at joint (4) from scenario one.

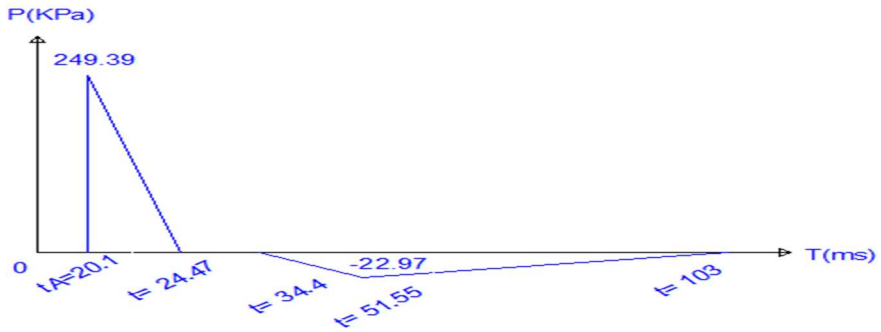

Figure 3.22: Blast pressure-time history at joint (5) from scenario one.

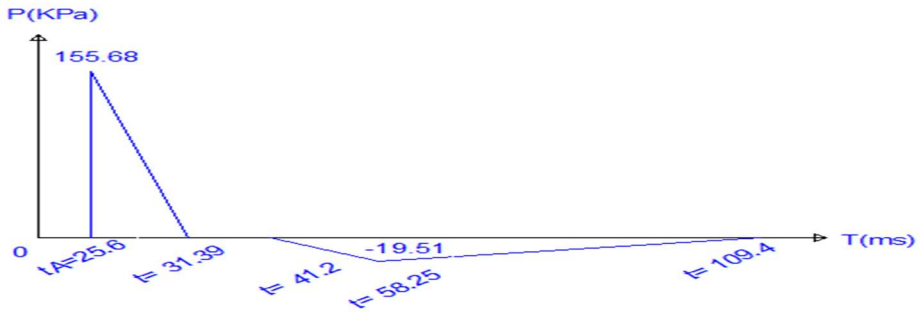

Figure 3.23: Blast pressure-time history at joint (6) from scenario one.

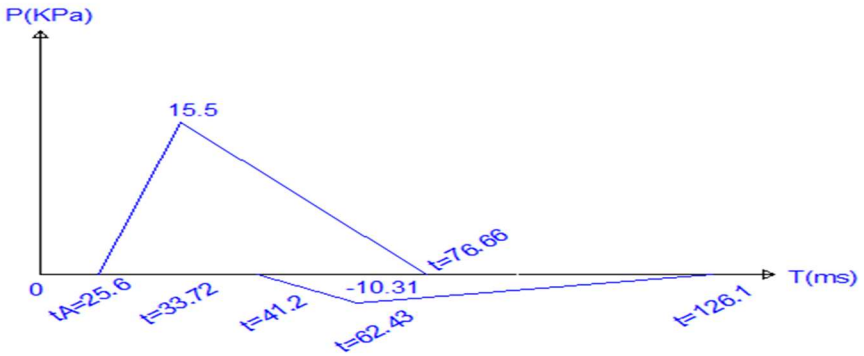

Figure 3.24: Equivalent blast pressure-time history at the joints on the roof from scenario one.

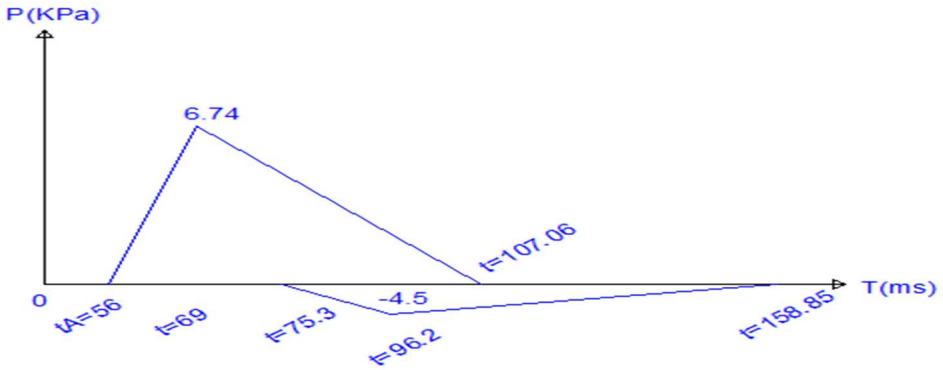

Figure 3.25: Equivalent blast pressure-time history at the joints on the rear-wall from scenario one.

3.9.4.2 SCENARIO TWO (300kg of TNT)

In this scenario, a 300kg of TNT explosive was considered on the ground at a distance of 10 meters from the structure. The standoff distance and the angle of incidence remain the same as scenario one.

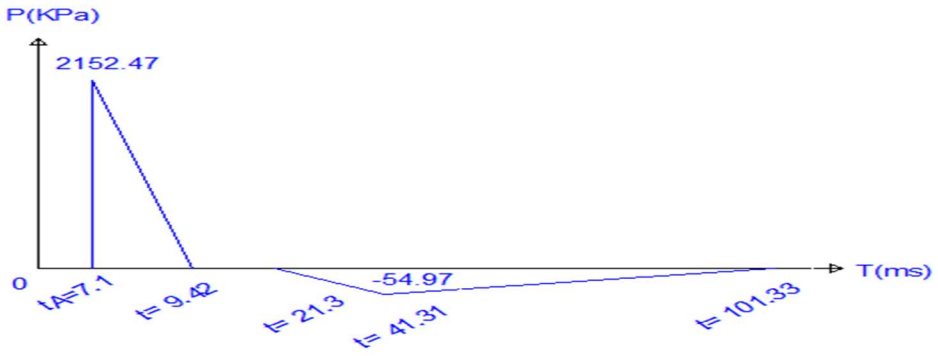

Figure 3.26: Blast pressure-time history at joint (2) from scenario two.

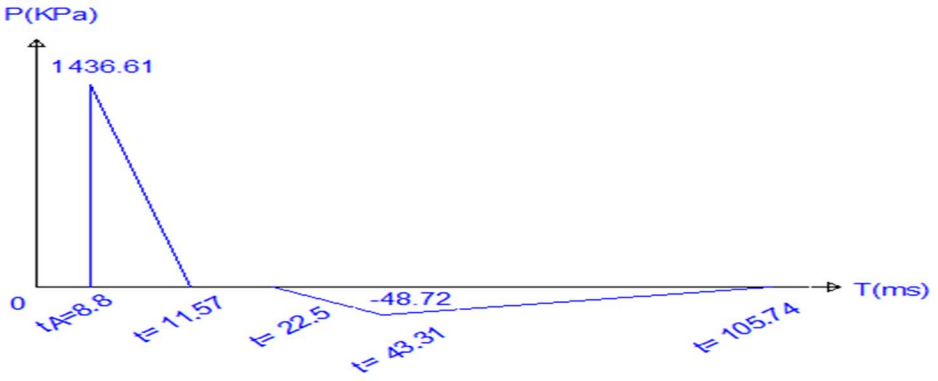

Figure 3.27: Blast pressure-time history at joint (3) from scenario two.

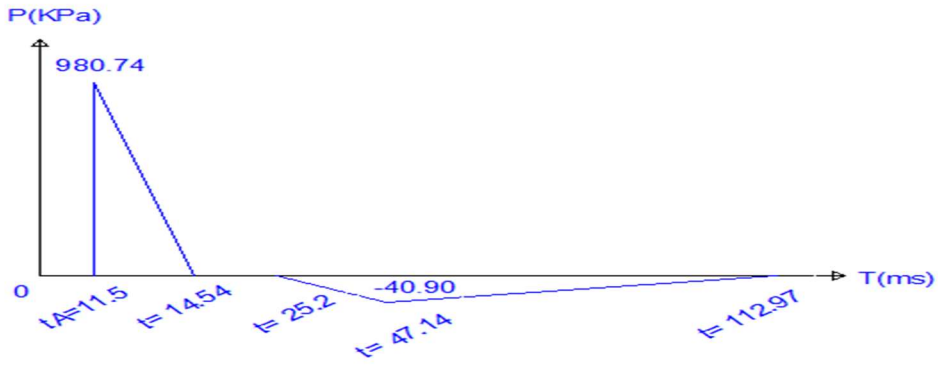

Figure 3.28: Blast pressure-time history at joint (4) from scenario two.

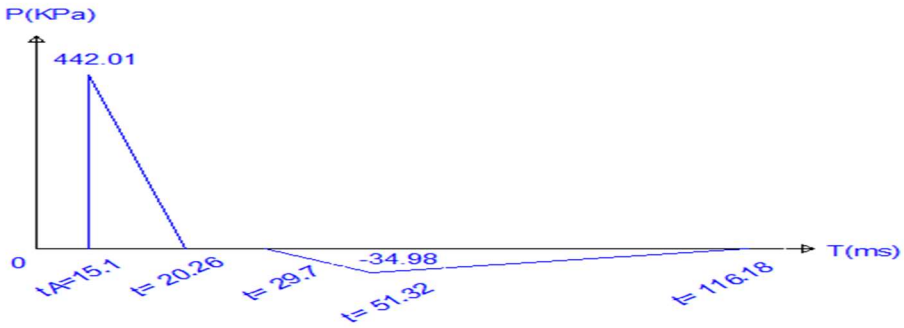

Figure 3.29: Blast pressure-time history at joint (5) from scenario two.

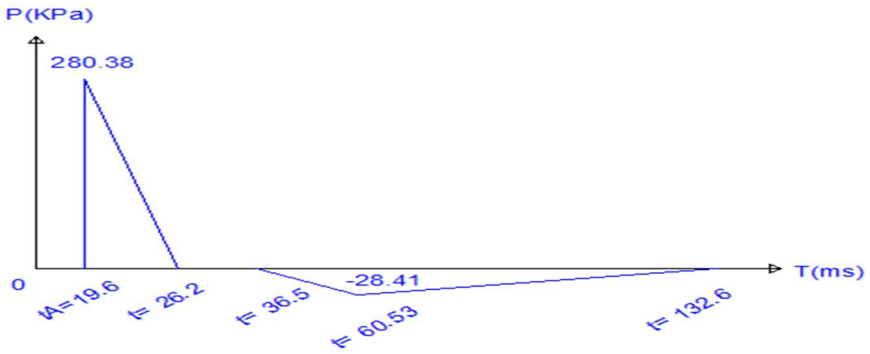

Figure 3.30: Blast pressure-time history at joint (6) from scenario two.

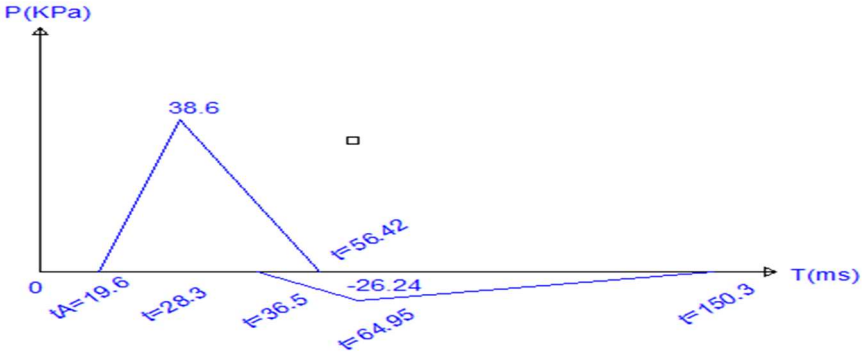

Figure 3.31: Equivalent blast pressure-time history at the joints on the roof from scenario two.

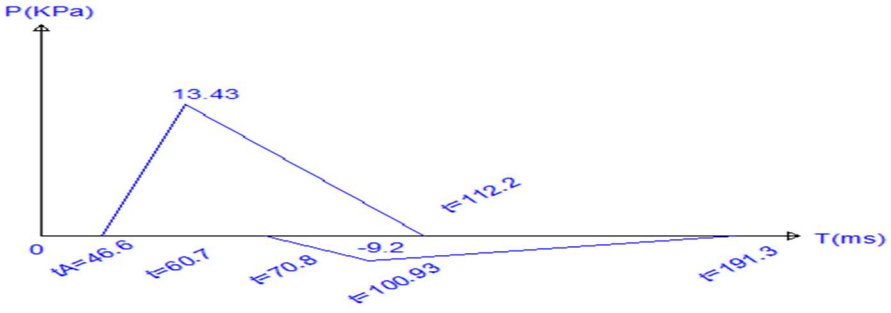

Figure 3.32: Equivalent blast pressure-time history at the joints on the rear-wall from scenario two.

3.9.5 NONLINEAR DYNAMIC ANALYSIS

The P-Delta effect on the columns was taken into account in the analysis to consider the second-order effect on the frames. The structures were assumed to be carrying the dead load and 30% of the live load at the moment the explosion takes place. Dynamic analyses were performed for the three different patterns of blast loads mentioned above for both frames.

The blast pressure-time history of each joint is defined as a time history function in the SAP2000 as in the Figure below.

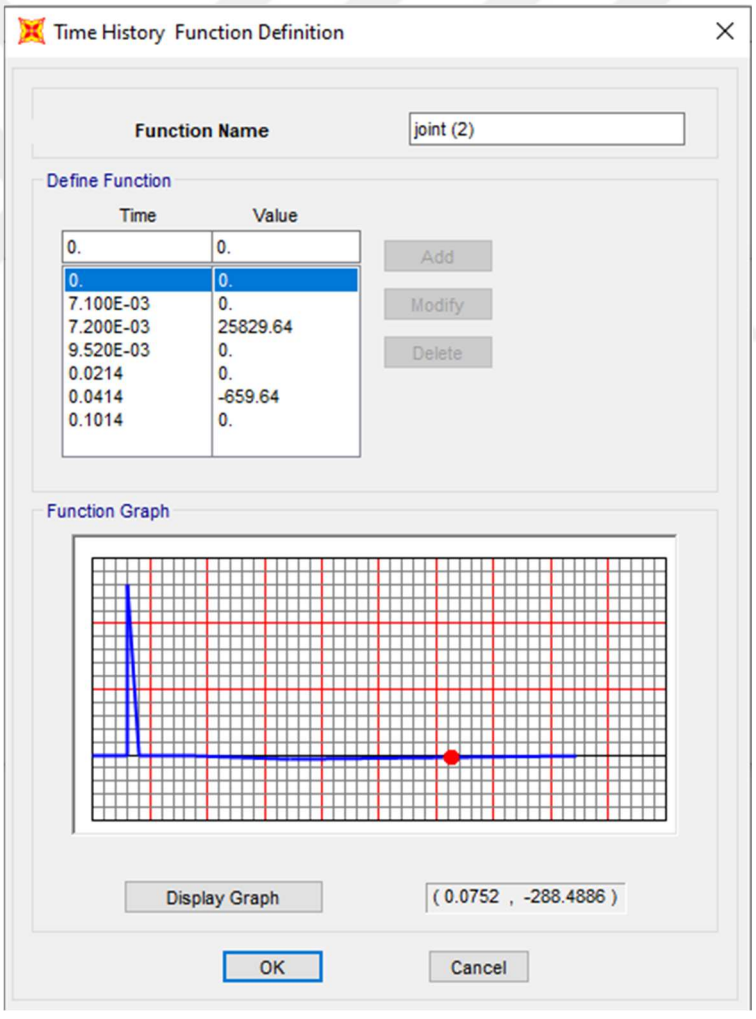

Figure 3.33: Joint blast pressure-time history definition in SAP2000.

To allow the structure to undergo the plasticity region plastic hinges were placed at the edges of the members. Only moment M3 is considered to cause the plastic hinge to the flexural members and the axial-moment interaction (P-M3) is considered to cause the plastic hinge in a column.

The dynamic analysis was carried out by step-by-step integration using Newmark's average method. Mass and stiffness proportional Rayleigh damping was taken into account in the analysis. A damping ratio of 5% was assumed for modes 1 and 4. The nonlinear iterative procedure was executed using the modified Newton-Raphson methodology. The analysis time step was 0.1 millisecond and the analysis was considered a total time of 4 seconds.

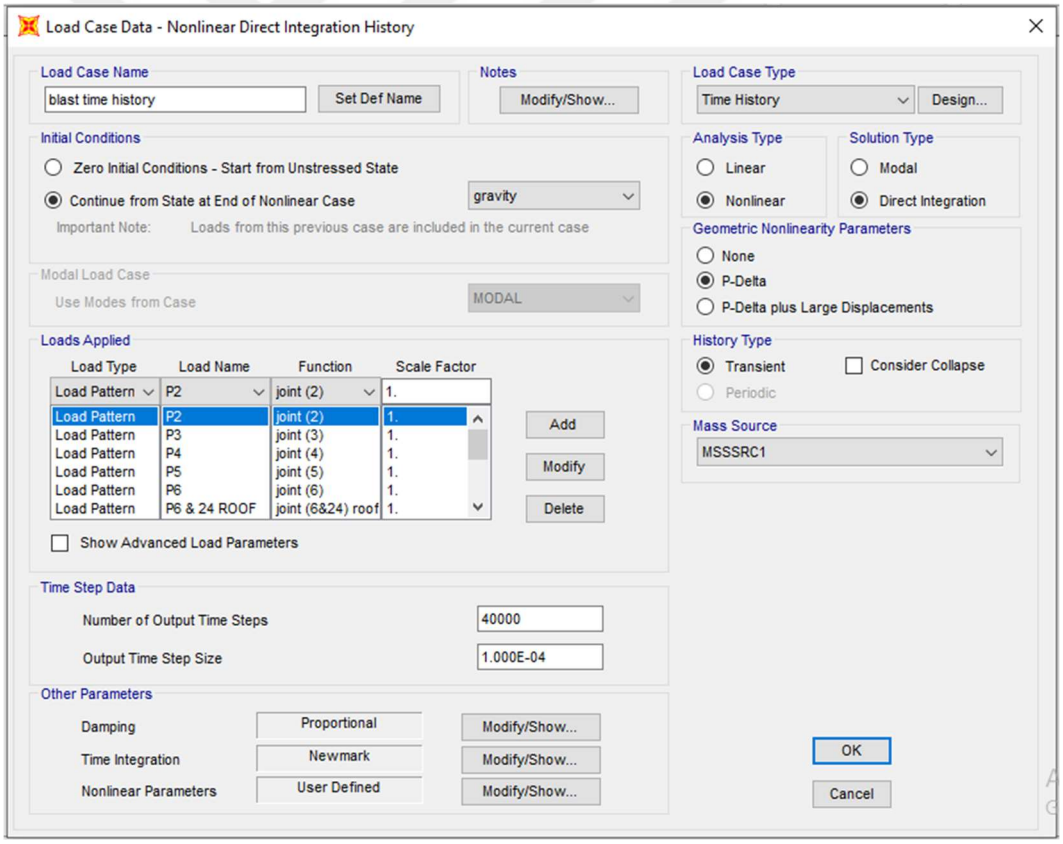

Figure 3.34: Blast nonlinear dynamic load case definition in SAP2000.

3.10 PROGRESSIVE COLLAPSE ANALYSIS

Progressive collapse is a dynamic phenomenon that occurs when one or more vertical load-carrying elements fail. This failure is caused by abnormal loads such as bombings, gas explosions, earthquakes...etc. The structure starts to redistribute the loads after the failure of the vertical load-carrying member until it finds equilibrium.

In this study, the two pre-defined frames (A and B) were tested for their resistance capacity to the progressive collapse using the structural analysis and design software SAP2000. The nonlinear dynamic procedure is performed for the progressive collapse analysis which is the most efficient method of analysis in which a vertical load-carrying member is removed dynamically and the structural members are allowed to undergo nonlinear behavior.

3.10.1 REMOVED COLUMN LOCATIONS

Three different probabilities progressive collapse may initiate which are all on the ground floor were taken into considerations for each structure which are:

- Corner column failure.
- Internal column failure.
- Failure of two consecutive internal columns.

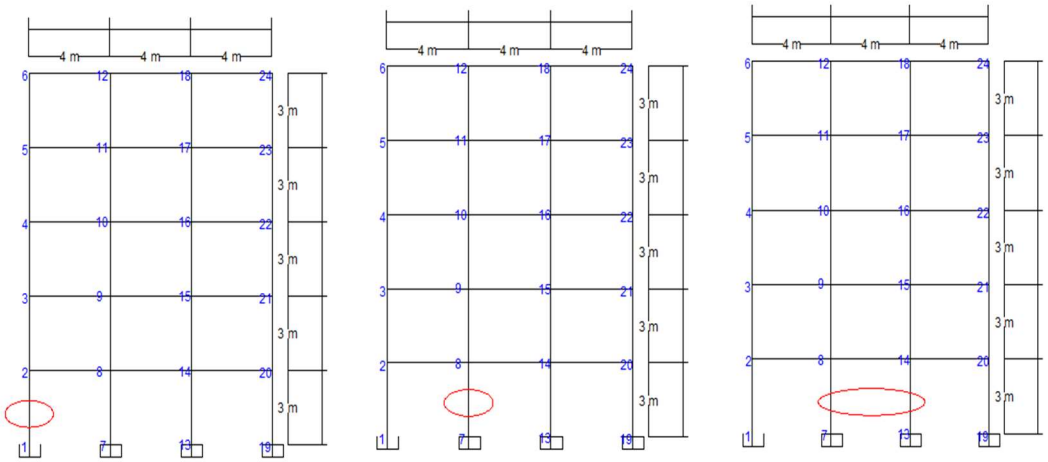

a) Scenario one. b) Scenario two. c) Scenario three.

Figure 3.35: locations of the removed column for the three scenarios.

3.10.2 GRAVITY LOADS AND DYNAMIC COLUMN REMOVAL PROCESS

The gravity load and also the mass source was defined as Dead load plus 25 percent of the live load as per GSA, the second-order effect was considered by taking into account the P-delta effects, The internal forces of the members to be removed caused by the gravity load was found out.

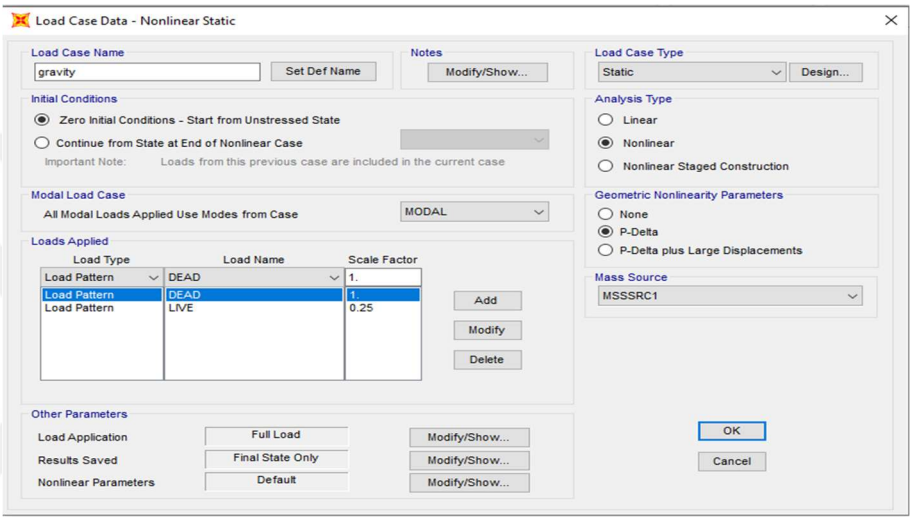

Figure 3.36: The gravity load on the structure as per GSA.

The critical members were removed dynamically from the structure and the forces carried by the removed members were represented as joint loads on the joint above the removed column in the opposite direction.

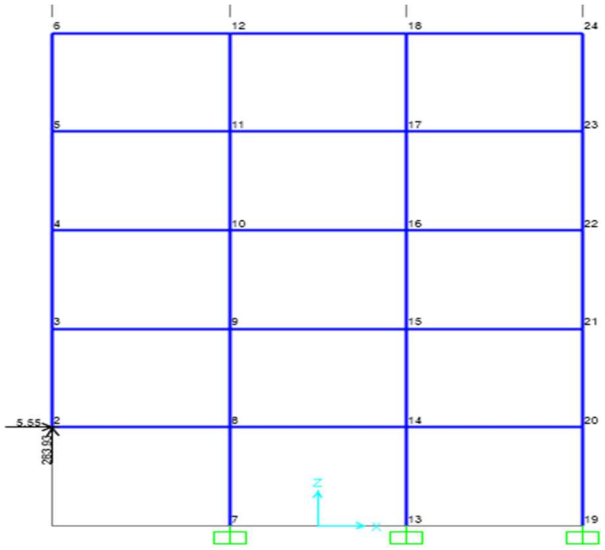

Figure 3.37: Joint loads representing the removed column.

A new load case was defined combining the gravity load of the damaged structure and the joint loads.

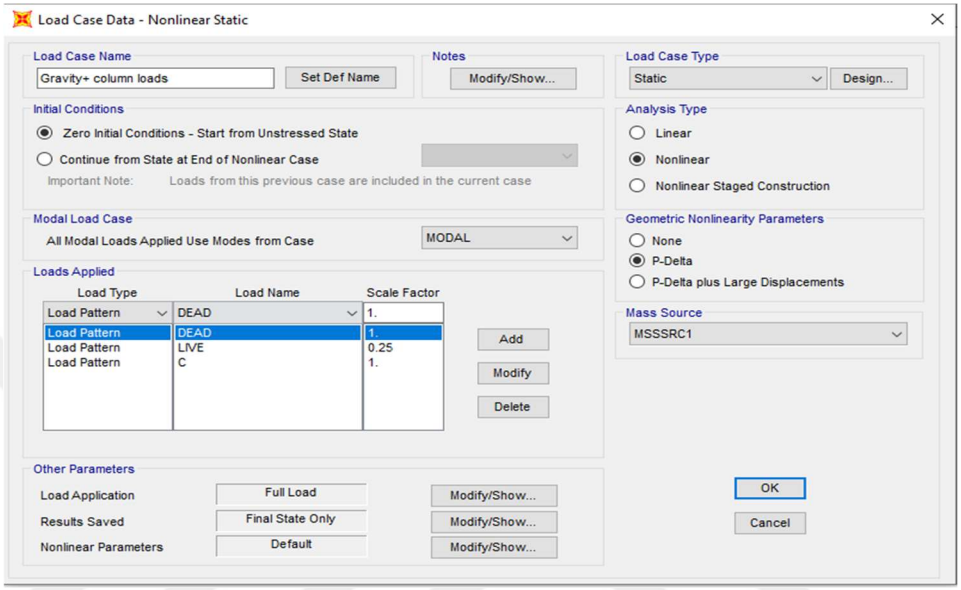

Figure 3.38: Combination of the Gravity load and the joint load.

The combination of the gravity load and the joint load represents the undamaged structure holding the gravity load, the figure below the bending moment diagram of the structure under this load case.

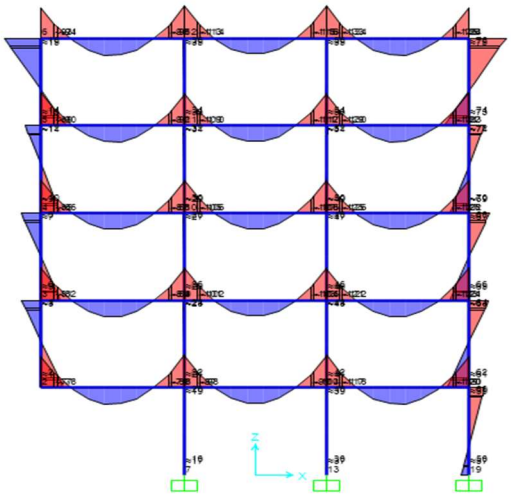

Figure 3.39: Bending moment diagram of a combination of the gravity load and the column representing joint loads.

A ramp time history function was created as column removal function and the column removal duration was set to $\frac{T}{15}$ where T is the period of the first mode that exhibits vertical motion at the position of the removed column after the column was removed.

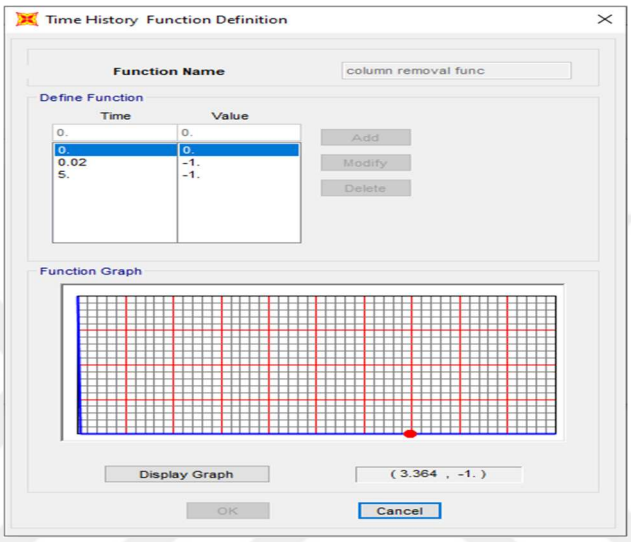

Figure 3.40: Column removal time history function.

3.10.3 NONLINEAR DYNAMIC ANALYSIS

A nonlinear direct integration time history was created for the progressive collapse which continues from the (Gravity + column loads) load case and by the column removal function the column loads were removed dynamically and nonlinear plastic hinges were assigned at 10 percent of the members' length away from the edges of the members. Only moment M3 is considered to cause a plastic hinge to the flexural members and the axial-moment interaction (P-M3) is considered to cause a plastic hinge in a column.

The dynamic analysis was carried out by step-by-step integration using Newmark's average method. Mass and stiffness proportional Rayleigh damping was taken into account in the analysis. A damping ratio of 5% was assumed for the first two modes to exhibit vertically on the position of the removed column. The nonlinear iterative procedure was executed using the modified Newton-Raphson methodology. The analysis time step was 0.01 seconds, and the analysis was considered a total time of 5 seconds.

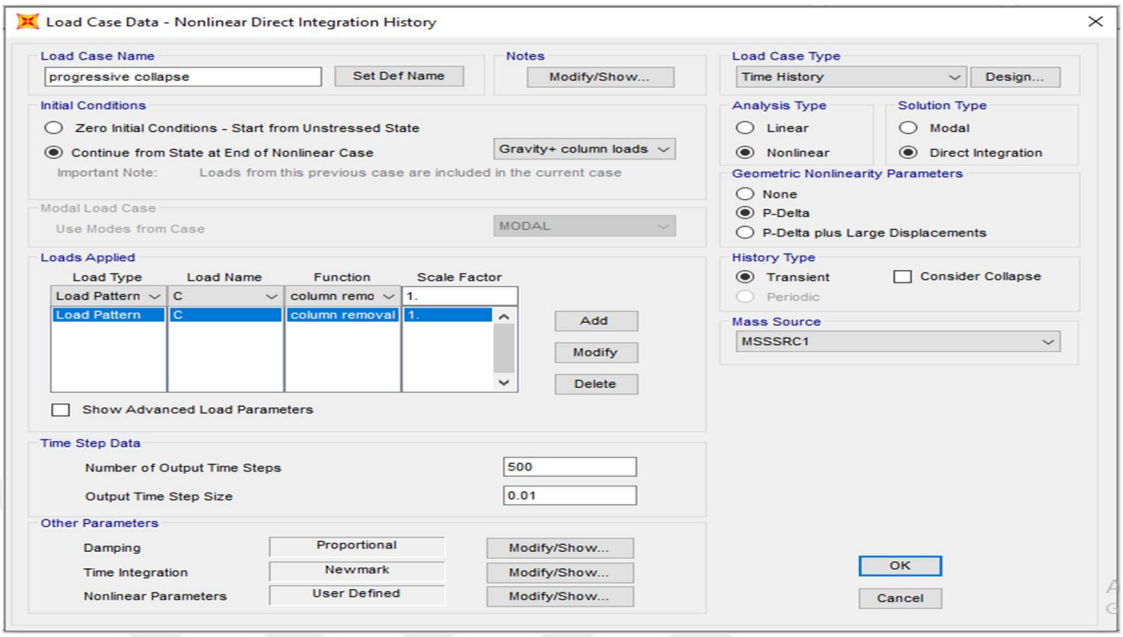

Figure 3.41: Progressive collapse nonlinear dynamic load case definition in SAP2000.

CHAPTER 4

RESULTS AND DISCUSSION

In this study, five-storey two-dimensional structures were designed as per EUROCODE 2-2004 with concrete grade 10 in the first structure and named (Frame

A), and concrete grade 30 in the second one and named (Frame B) using SAP2000 v20.

The strain-rate effects on the global response of the structures were observed by using different strain-rate values including the UFC_3_340_02 recommended values, and in each strain-rate, second-order pushover analyses were performed for the two structures as detailed in chapter 3 (section 3.8).

Also, the above mentioned two frames were investigated for their performances under the blast loads in two cases; **case one** 100kg of TNT at the ground and 10 meters away from the structures, **case two** 300kg of TNT at the ground at a standoff distance of 10 meters, and the analyses were performed by nonlinear dynamic method (time history analysis). The process is explained in detail in section 3.9.

4.1 RESULTS of THE STRAIN-RATES ON THE STRENGTH OF THE STRUCTURAL MEMBERS

Various strain-rate values were chosen and according to those values the dynamic increasing factors were calculated as per CEB-FIP-1990 code. The moment-curvature curves of the column section at the different strain-rates were compared.

As shown in the Figure below, the strength of the section increased respectively as the strain-rate value increases. Also from the curves, it was observed that the strain-rate increases the yield strength more than the ultimate strength.

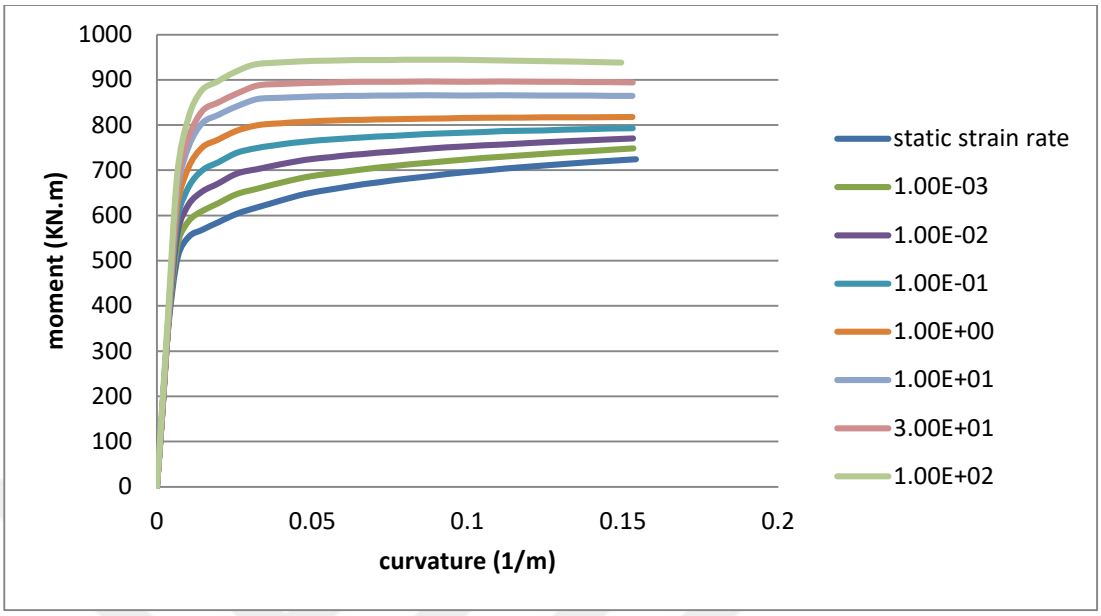

Figure 4.1: Moment-Curvature curves at different strain-rate values.

4.2 RESULTS OF THE STRAIN-RATE EFFECTS ON THE OVERALL STRUCTURAL RESPONSE

Different values of strain-rates were considered including the static value, and also the UFC guideline-recommended values.

The results obtained from the analyses of both frames show that with the increase of the strain-rate value the material strengths increase; therefore increase in strength of the whole structure. The base-shear resistance capacity increased from 514kN to 808kN in the case of Frame A as shown in figure 4.1, and from 413kN to 664kN in the case of Frame B when the strain-rate value increased from the static value to $1x10^2/s$.

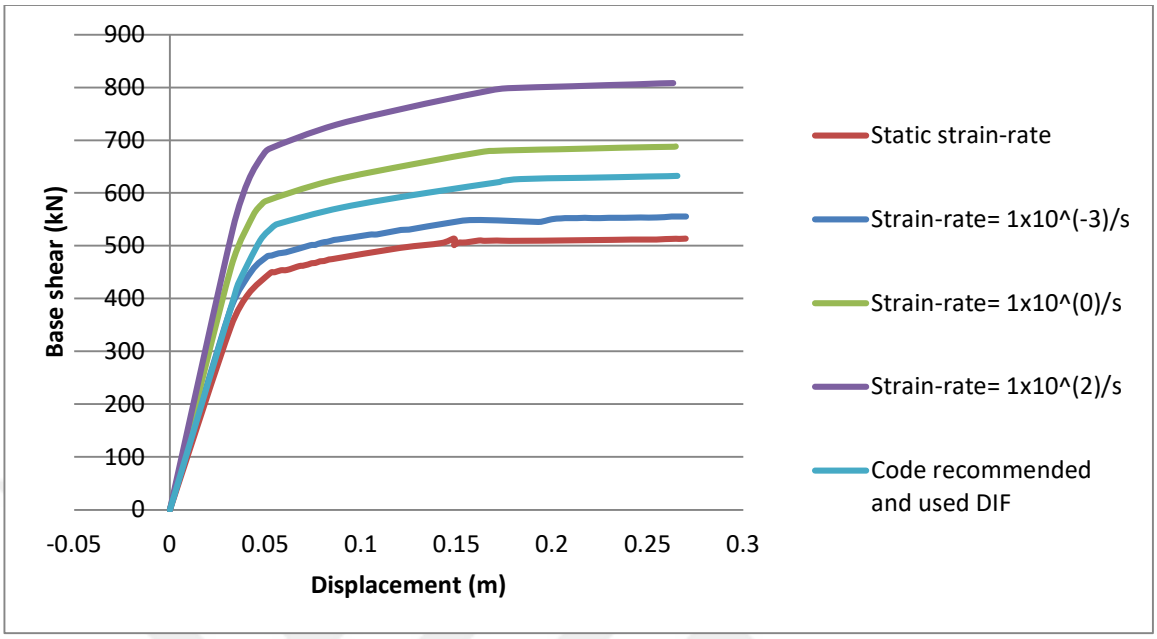

Figure 4.2: Frame A pushover curves under different strain-rates.

The unexpected instantaneous high pressure of the explosions normally causes strain-rates at the range of 10^2 -10^4 per second and as can be seen from both Figures 4.1 and 4.2 the values recommended by the UFC-3-340-02 are less than those values and this means the guideline take the safety factor into account.

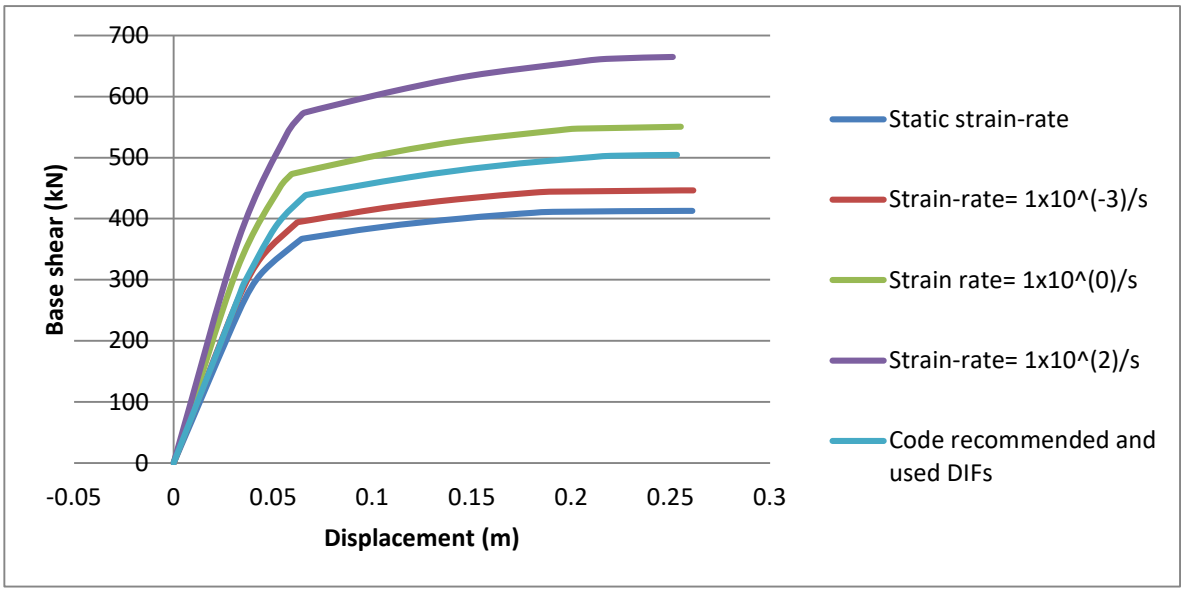

Figure 4.3: Frame B pushover curves under different strain-rates.

Also the influence of the second-order effects on the results was investigated under the pre-mentioned strain-rates, and this is done by comparing the maximum displacement and base-shear of the structures from their pushover curves at the different strain-rates, and their fundamental natural periods are as shown in Table 4.1.

Table 4.1: Fundamental natural periods of the structure at the different strain-rates.

Strain-rates$(1/s)$	Frame A (s)	Frame B (s)
Static strain-rate	0.687	0.823
$1x10^{-3}$	0.656	0.786
$1x10^{0}$	0.6	0.718
$1x10^{2}$	0.565	0.677
UFC code recommended DIFs	0.655	0.784

Table 4.2 illustrates the values of the base-shear for both Frames (A and B) at different strain-rates, from the results it can be observed that because of the second-order effects the structure will take not only the axial loads, but also moments caused by the sway of the structure, therefore, the base-shear resisted by the structure in the second-order method is less than the one it resists in first-order method.

Table 4.2: Maximum base-shears resisted by the structures at different strain-rates.

	Frame A (kN)		Frame B (kN)	
Strain-rates$(1/s)$	1st order	2nd order	1st order	2nd order
Static strain-rate	549.02	514.09	446.07	413.22
$1x10^{-3}$	588.41	555.8	479.36	446.63
$1x10^{0}$	722.28	688.51	583.14	550.7
$1x10^{2}$	842.5	808.66	697.08	664.83
UFC code recommended DIFs	666.45	632.42	537.58	504.75

Also the impact of the second-order effects on the ultimate displacements reached by the structures under different strain-rates was examined. As mentioned previously the structure in the second-order method holds more loads than the first-order method because of the moments produced by the P-delta effects, so, it was observed from the

results in Table 4.3 that the deformations reached at the collapse of the structures in the first-order method is more than those in the second-order method.

Table 4.3: Maximum displacements observed from the structures at different strain-rates.

	Frame A (mm)		**Frame B** (mm)	
Strain-rates($1/s$)	**1st order**	**2nd order**	**1st order**	**2nd order**
Static strain-rate	271.42	270	263.34	260.9
$1x10^{-3}$	269.42	270.02	263.36	261.32
$1x10^{0}$	267.53	264.62	257.2	255.05
$1x10^{2}$	265.9	263.44	253.5	251.05
UFC code recommended DIFs	268.39	265.6	257.37	253.2

Since the hinges formed on the same structure under the different strain-rates appear almost similar, the static strain-rate is taken as an example. In the second order analysis the plastic hinges on the Frame A first formed on the beams at the middle to the first floors, then the ground floor columns, due to the gravity loads, then formed on the all beams and finally on some other columns.

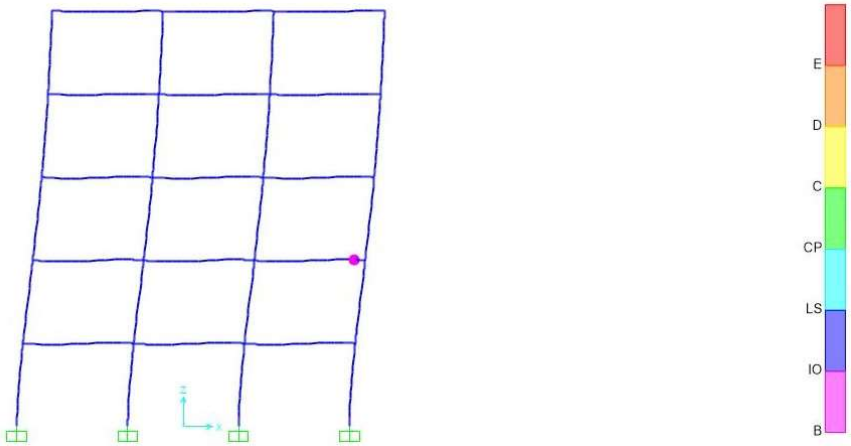

Figure 4.4: Formed plastic hinges on Frame A at step 1.

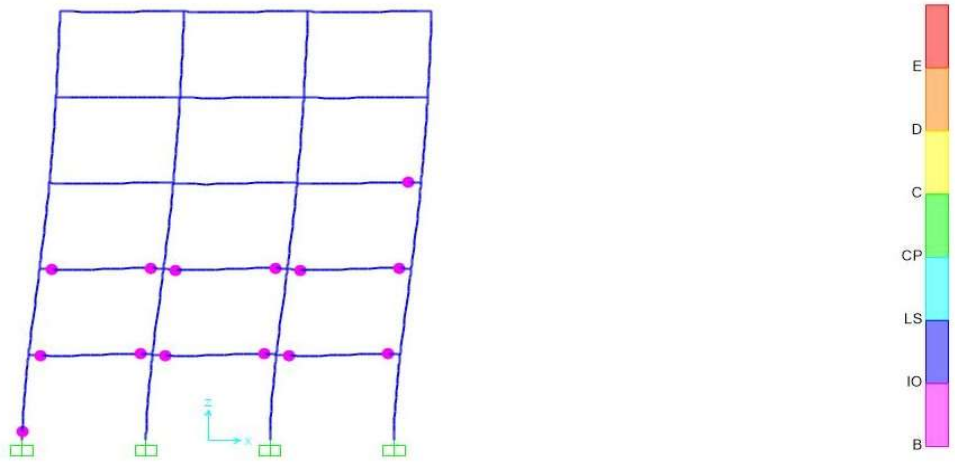

Figure 4.5: Formed plastic hinges on Frame A at step 2.

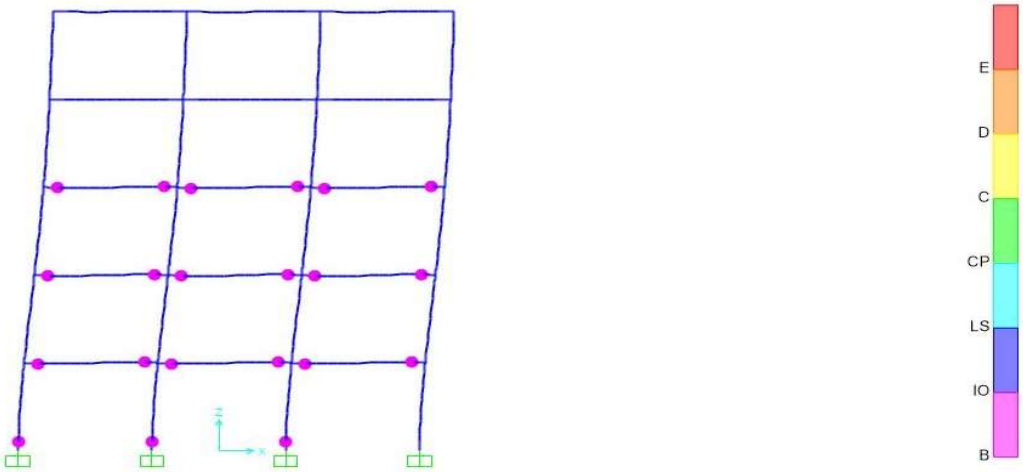

Figure 4.6: Formed plastic hinges on Frame A at step 3.

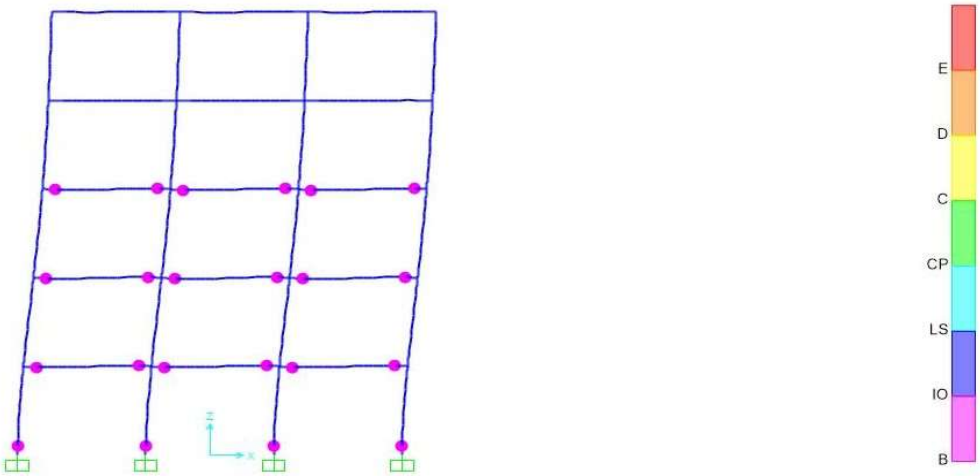

Figure 4.7: Formed plastic hinges on Frame A at steps 4 to 11.

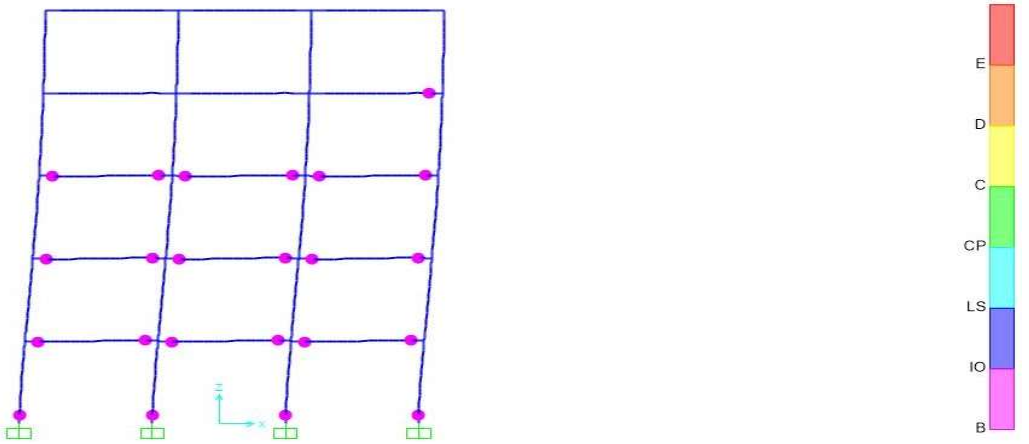

Figure 4.8: Formed plastic hinges on Frame A at steps 12 to 13.

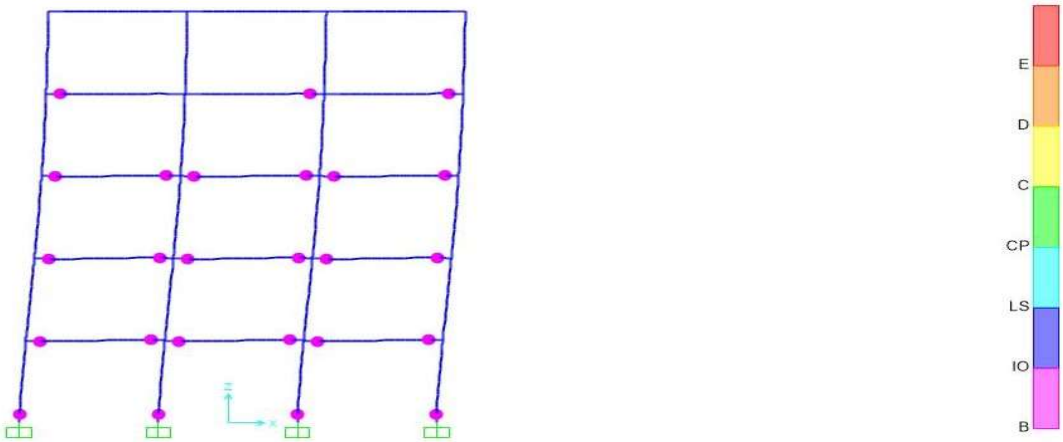

Figure 4.9: Formed plastic hinges on Frame A at step 14.

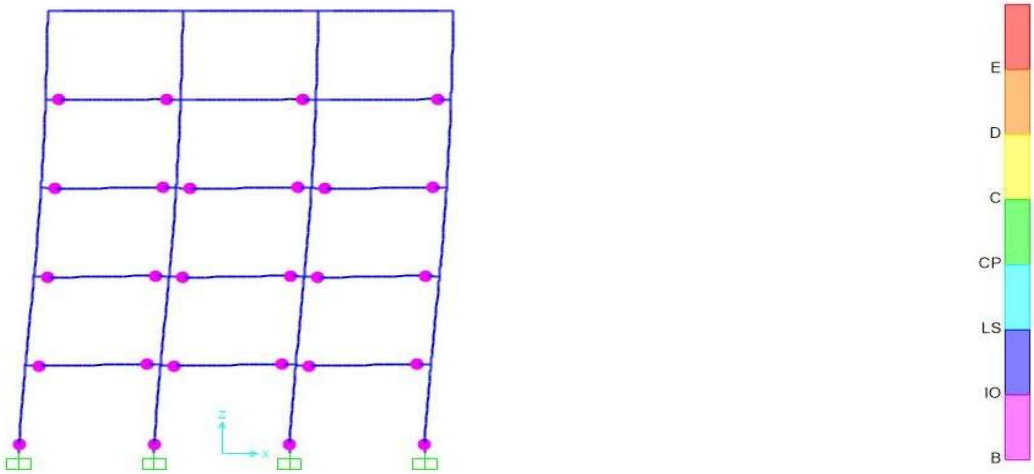

Figure 4.10: Formed plastic hinges on Frame A at step 15.

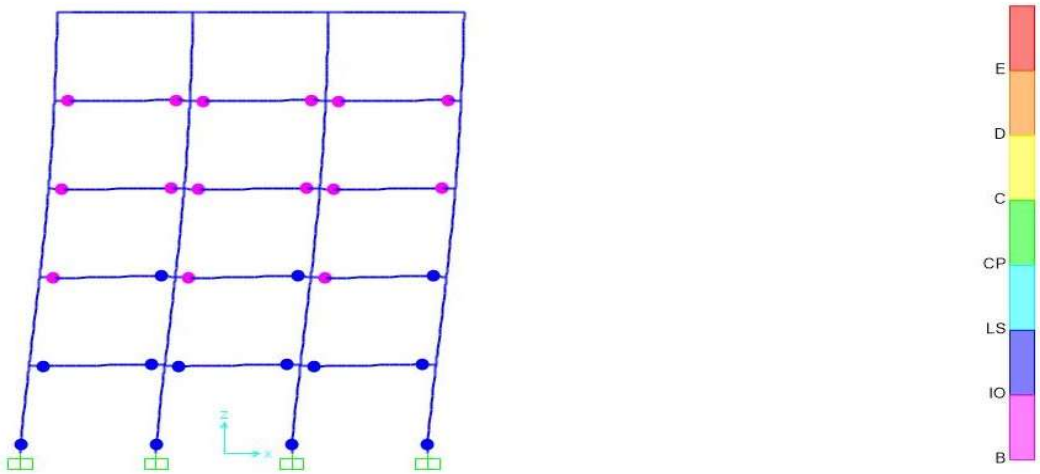

Figure 4.11: Formed plastic hinges on Frame A at step 16.

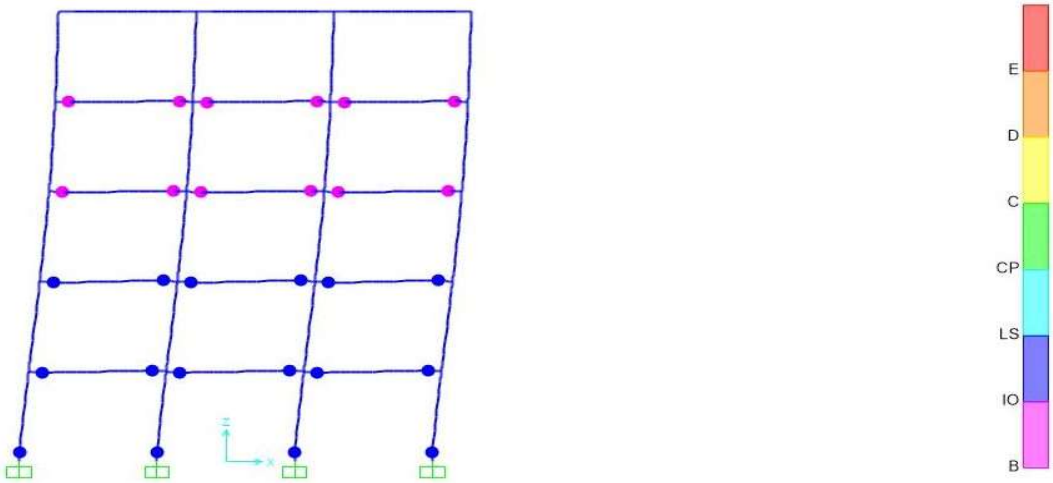

Figure 4.12: Formed plastic hinges on Frame A at step 17.

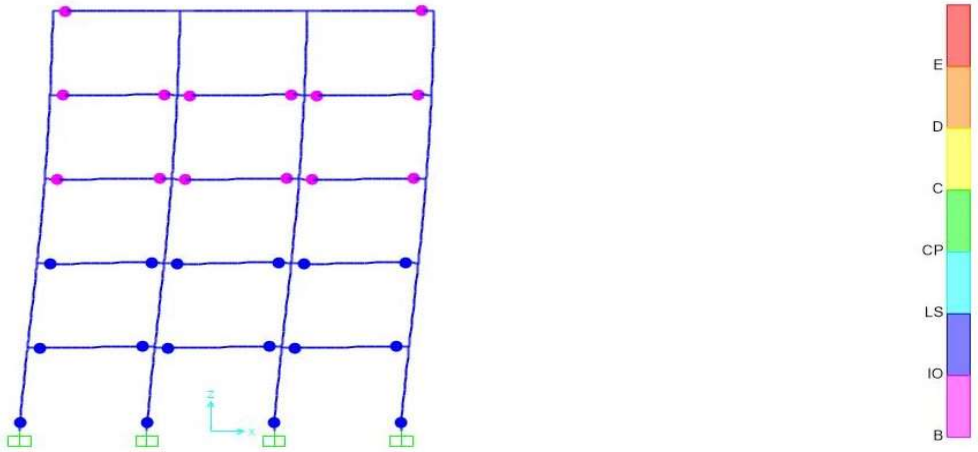

Figure 4.13: Formed plastic hinges on Frame A at steps 18 to 23.

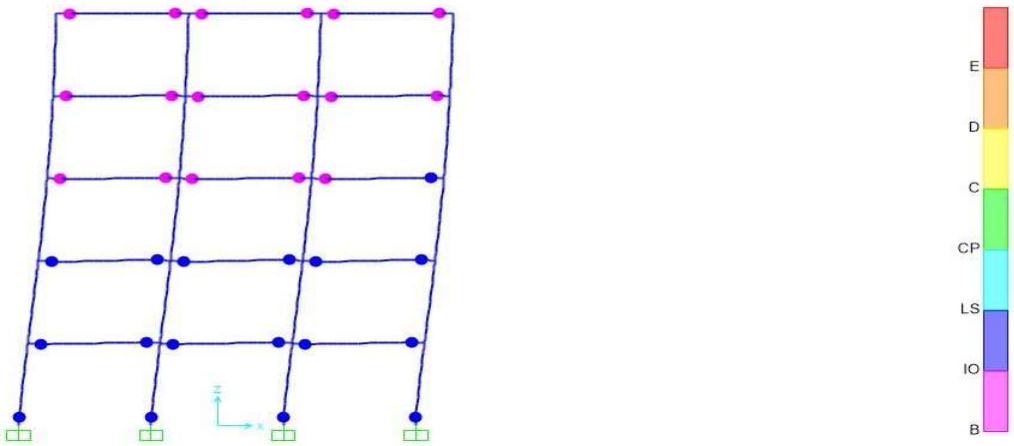

Figure 4.14: Formed plastic hinges on Frame A at step 24.

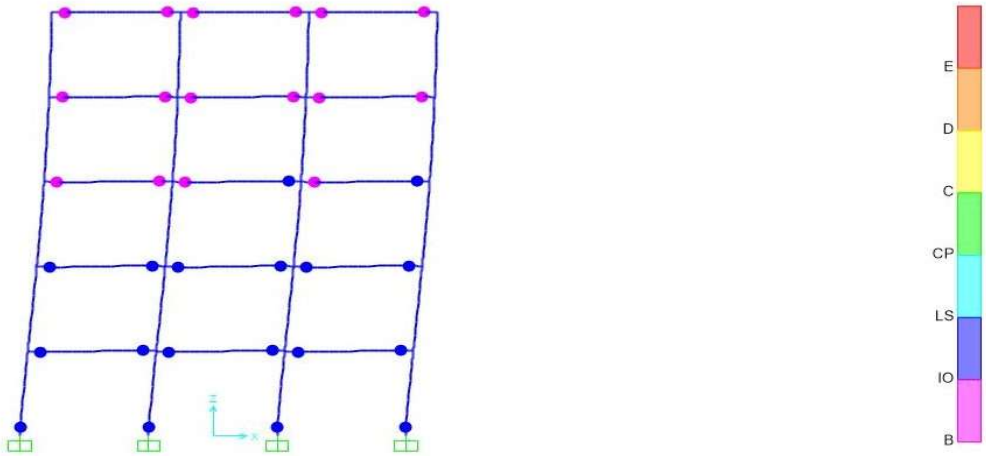

Figure 4.15: Formed plastic hinges on Frame A at step 25.

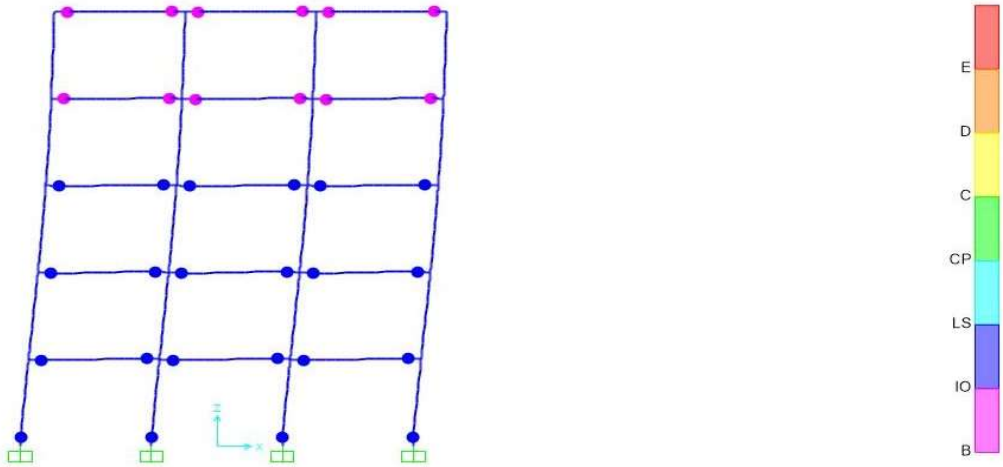

Figure 4.16: Formed plastic hinges on Frame A at steps 26 to 28.

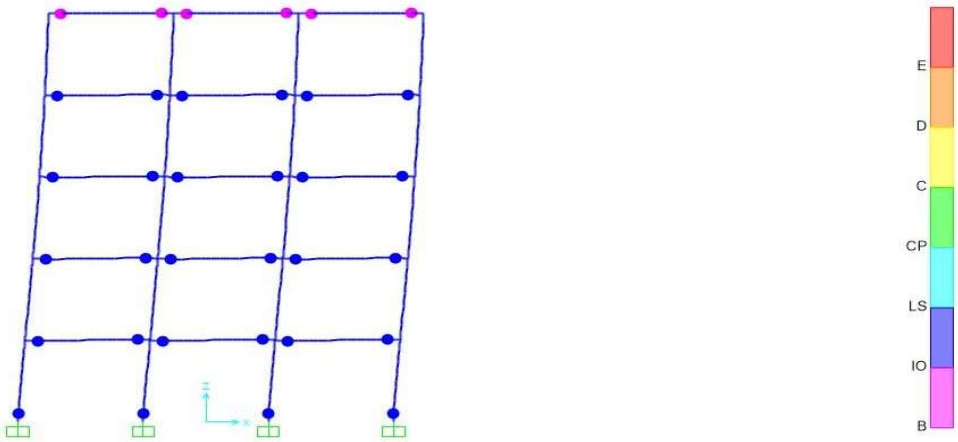

Figure 4.17: Formed plastic hinges on Frame A at step 29.

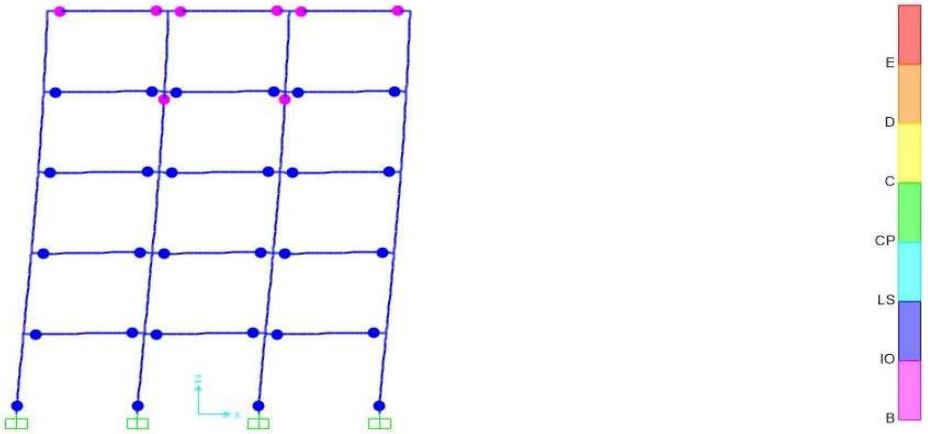

Figure 4.18: Formed plastic hinges on Frame A at step 30.

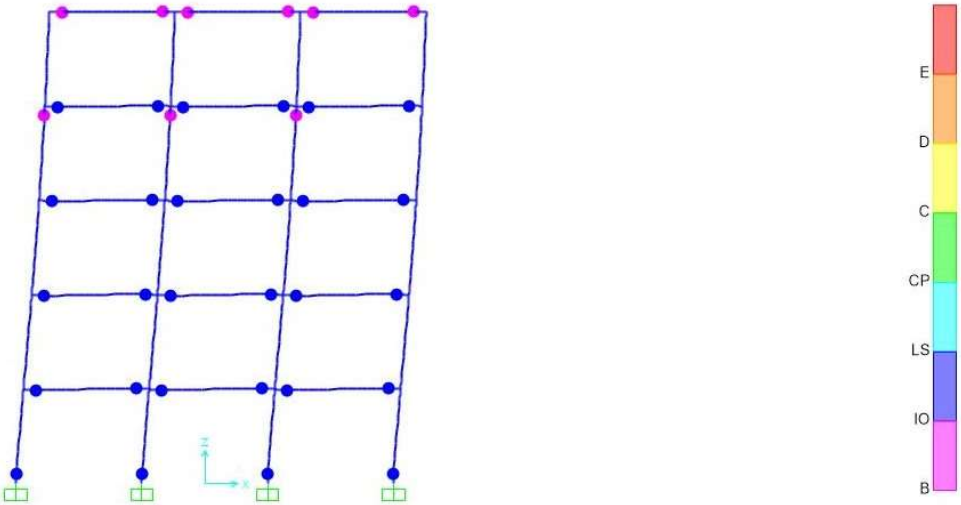

Figure 4.19: Formed plastic hinges on Frame A at steps 31 to 32.

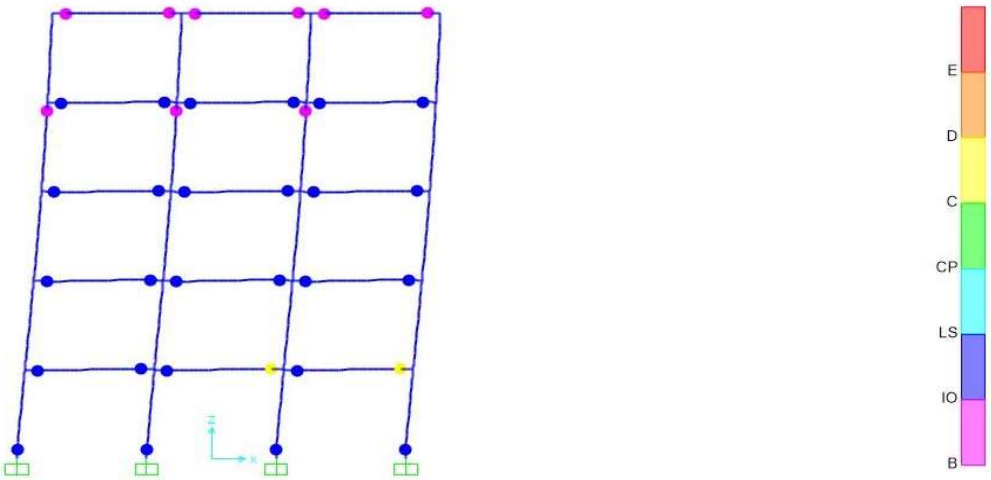

Figure 4.20: Formed plastic hinges on Frame A at step 33.

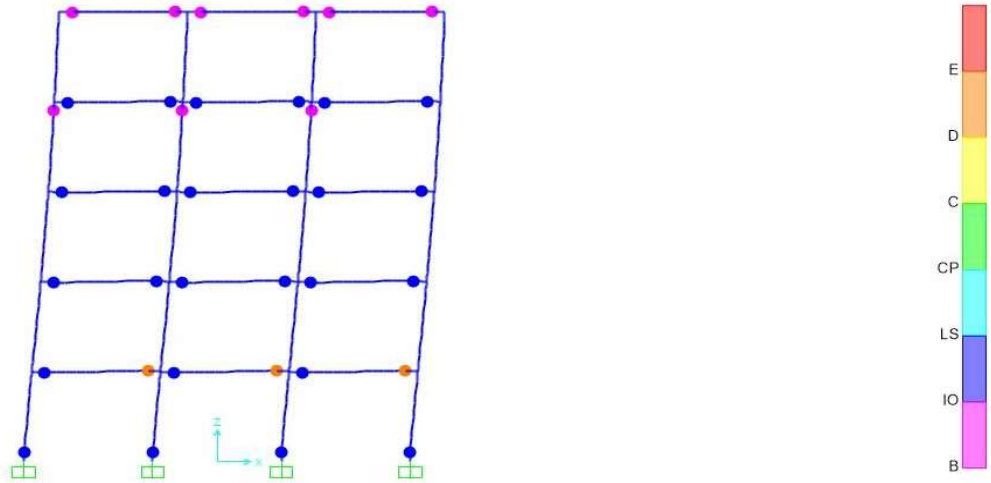

Figure 4.21: Formed plastic hinges on Frame A at steps 34 to 35.

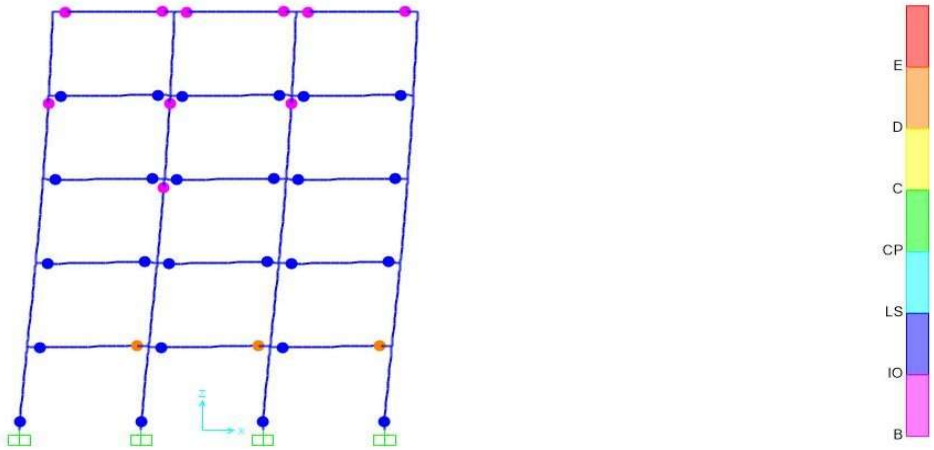

Figure 4.22: Formed plastic hinges on Frame A at step 36.

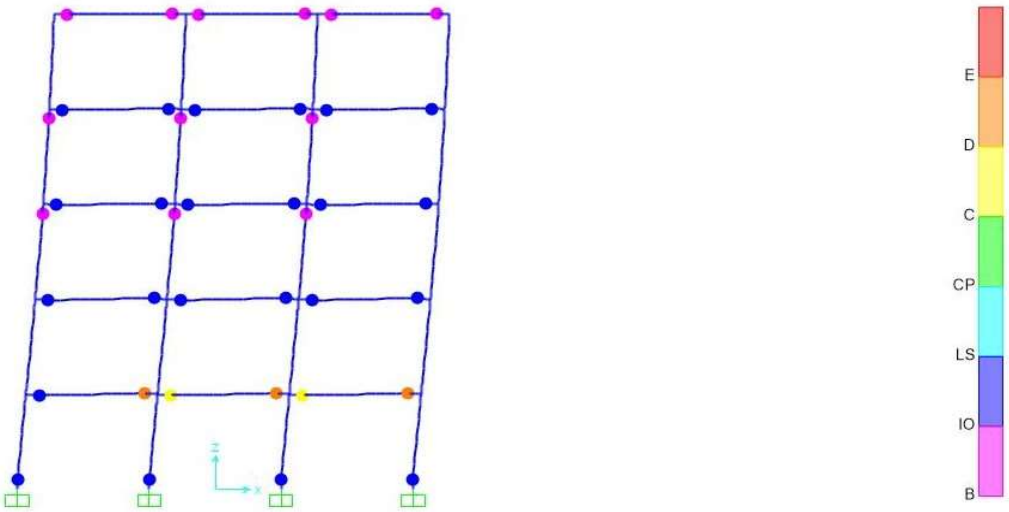

Figure 4.23: Formed plastic hinges on Frame A at steps 37 to 38.

In the case of Frame B, the plastic hinges appeared on the beams in the first to the third floors, then at ground floor column, then on the whole beams, but did not form on the other columns as shown below.

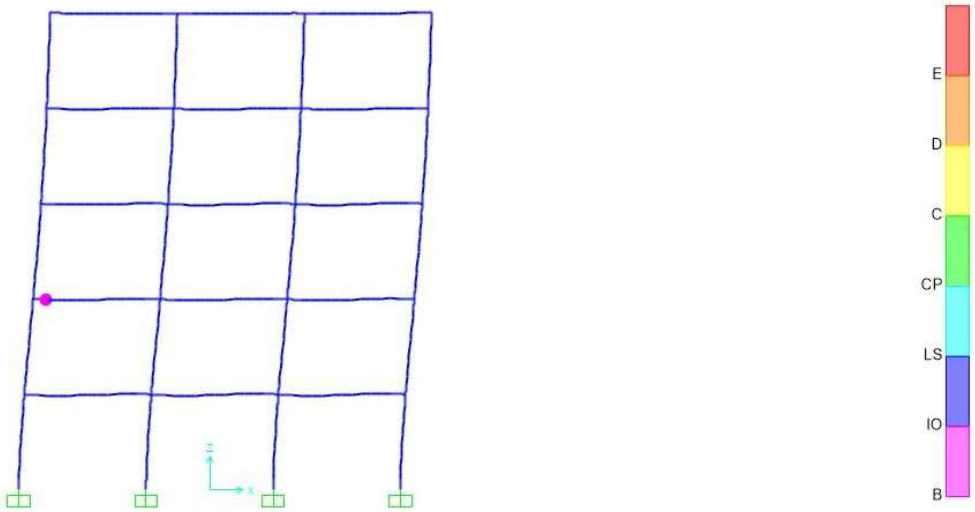

Figure 4.24: Formed plastic hinges on Frame B at step 1.

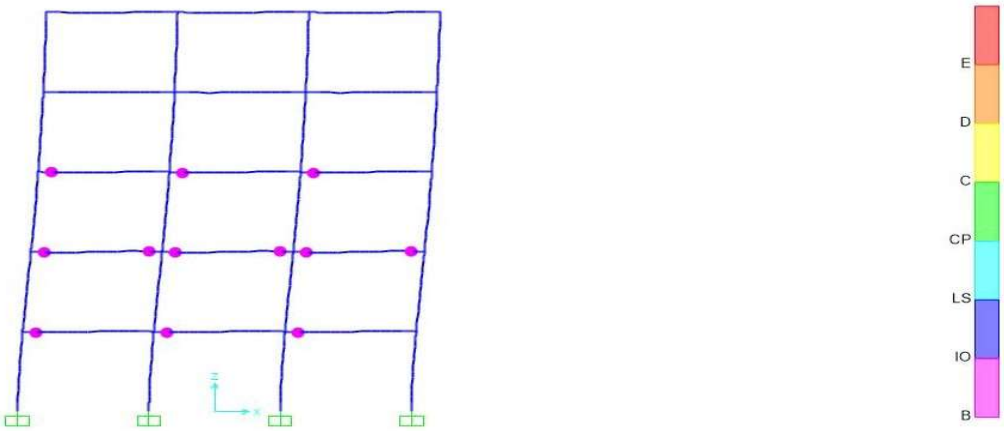

Figure 4.25: Formed plastic hinges on Frame B at step 2.

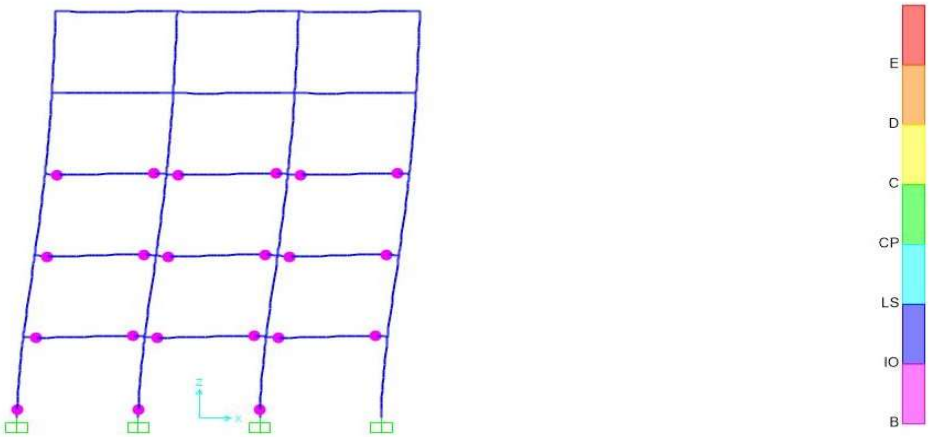

Figure 4.26: Formed plastic hinges on Frame B at step 3.

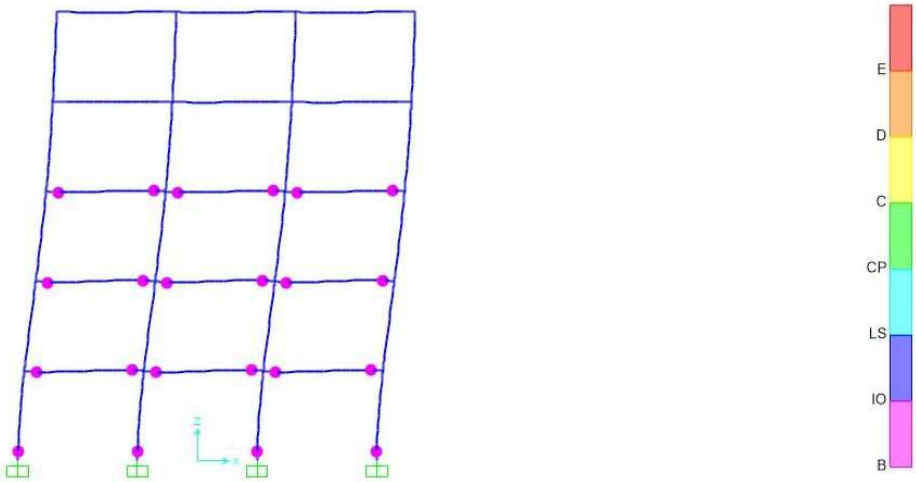

Figure 4.27: Formed plastic hinges on Frame B at step 4.

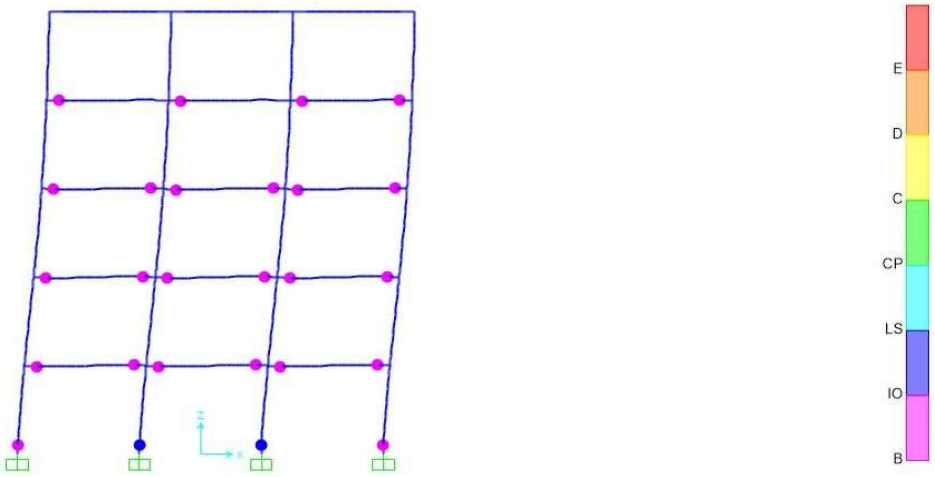

Figure 4.28: Formed plastic hinges on Frame B at step 5.

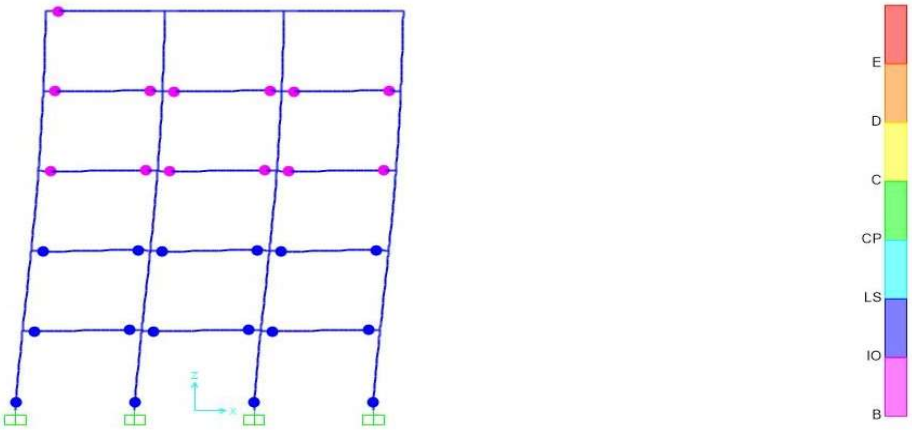

Figure 4.29: Formed plastic hinges on Frame B at step 6.

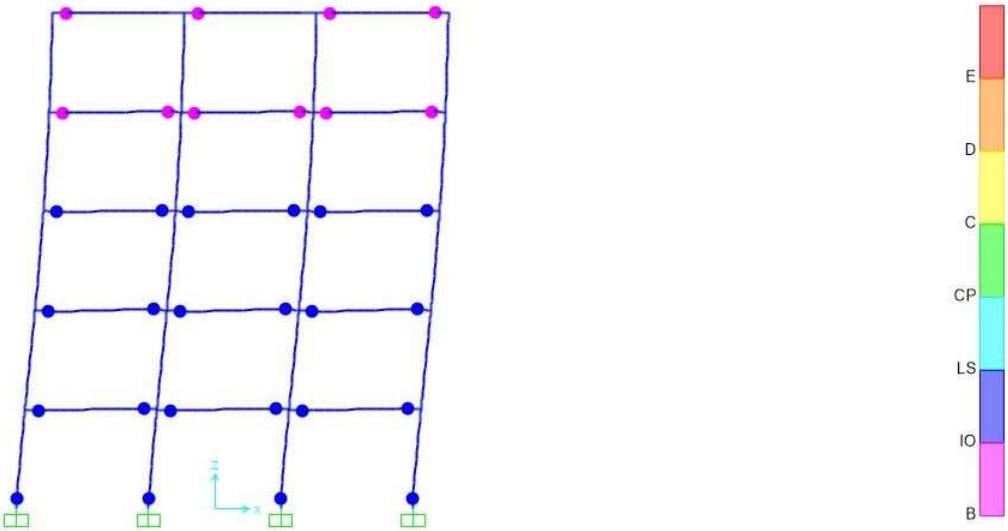

Figure 4.30: Formed plastic hinges on Frame B at step 7.

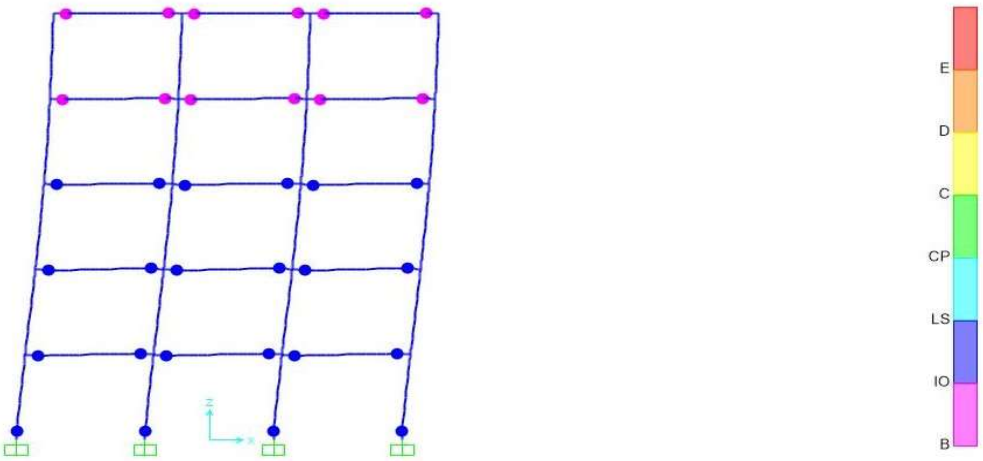

Figure 4.31: Formed plastic hinges on Frame B at step 8.

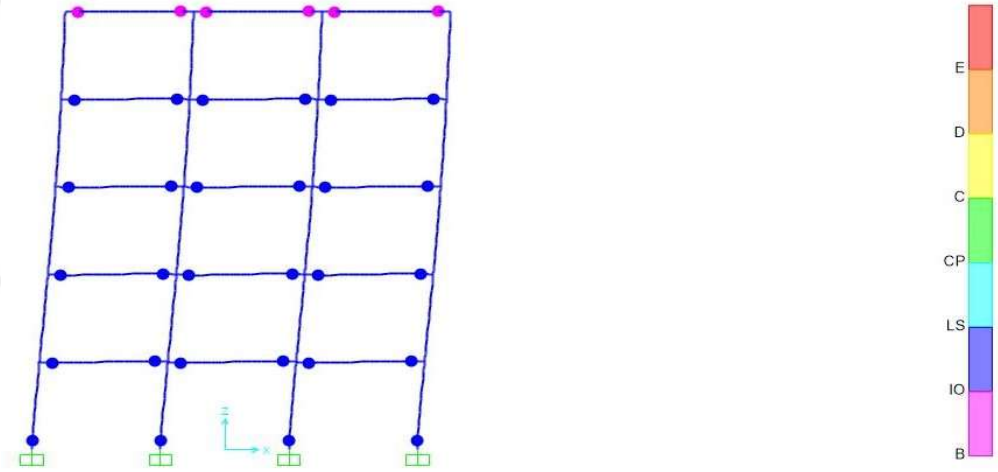

Figure 4.32: Formed plastic hinges on Frame B at step 9.

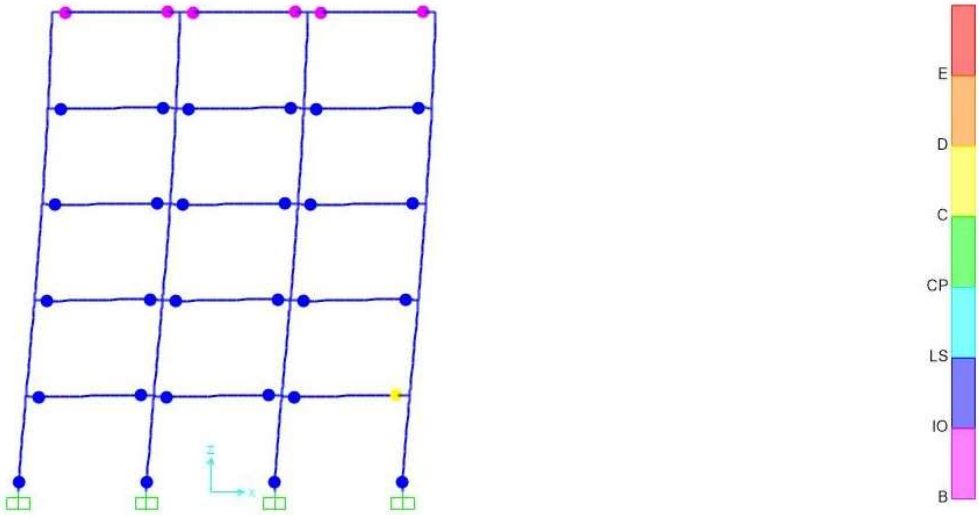

Figure 4.33: Formed plastic hinges on Frame B at step 10.

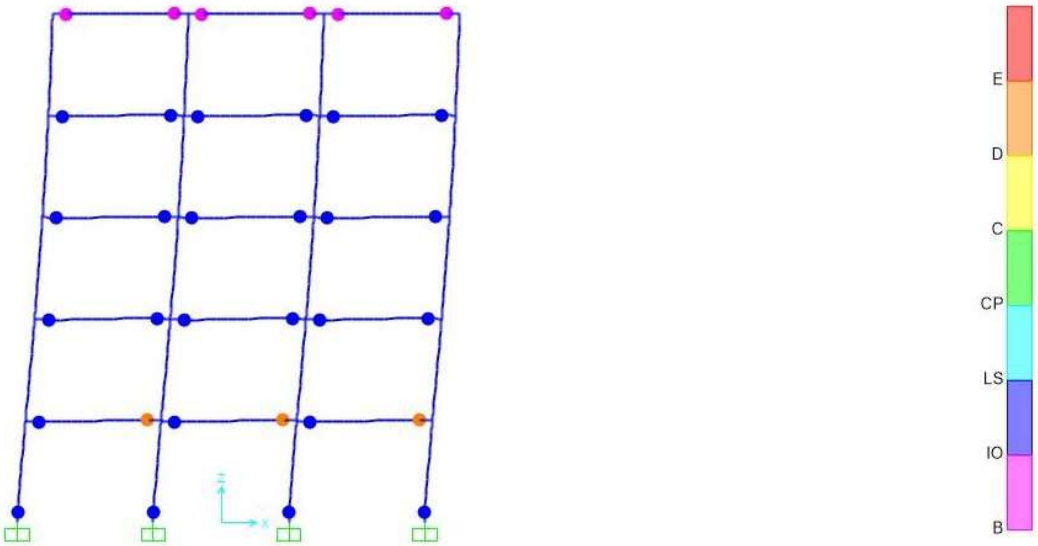

Figure 4.34: Formed plastic hinges on Frame B at step 11.

4.3 RESULTS OF THE BLAST ANALYSIS

The 2D structures are a good choice for estimating the global response of the structure as it gives quite accurate results and reduces the computational time and efforts.[4]

The actual concept of the explosions is that the blast pressure encloses everything that comes on its way; therefore the blast pressure should be assigned on every external surface. However, to simplify the process there are other ways to model the blast loads on the structure which are:

a) Exact progressive method: in this method, the blast load is applied in all directions of the structure.
b) Progressive method: in this method, the blast load is applied on the front and roof surfaces.
c) Simplified progressive method: in this method, the blast load is only applied on the front side of the structure.

These three loading patterns are compared for the two Frames in two ground explosion scenarios.

4.3.1 COMPARISON OF THE THREE LOADING PATTERNS.

The results as can be seen from the figures below the progressive and the simplified progressive methods give Maximum storey drift ratios that are almost the same and very consistent with the results found by Danesh Nourzadeh in 2015 [4], though they show a slight difference in the case of Frame B under the 300kg of TNT scenario and this.

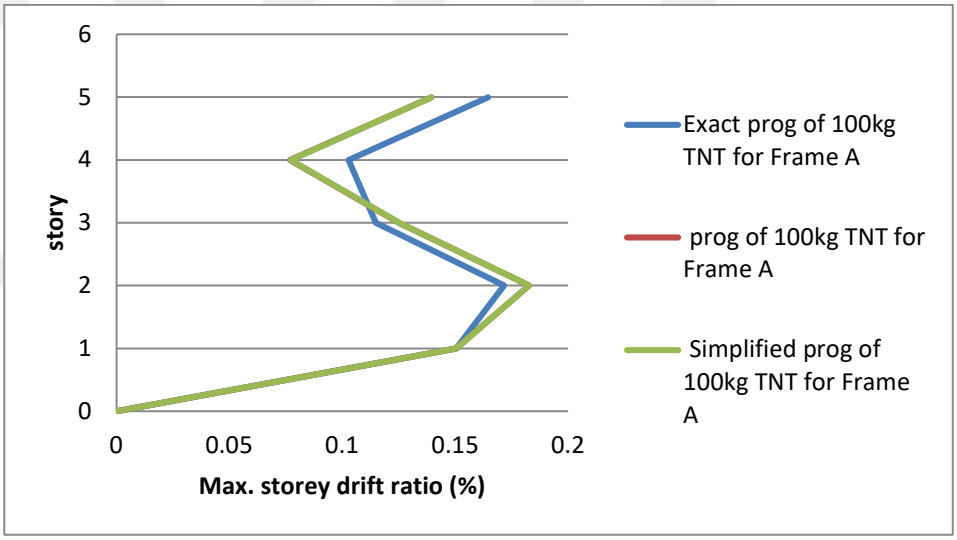

Figure 4.35: Maximum storey drifts ratio of frame A (100kg TNT) for different types of loading patterns.

.

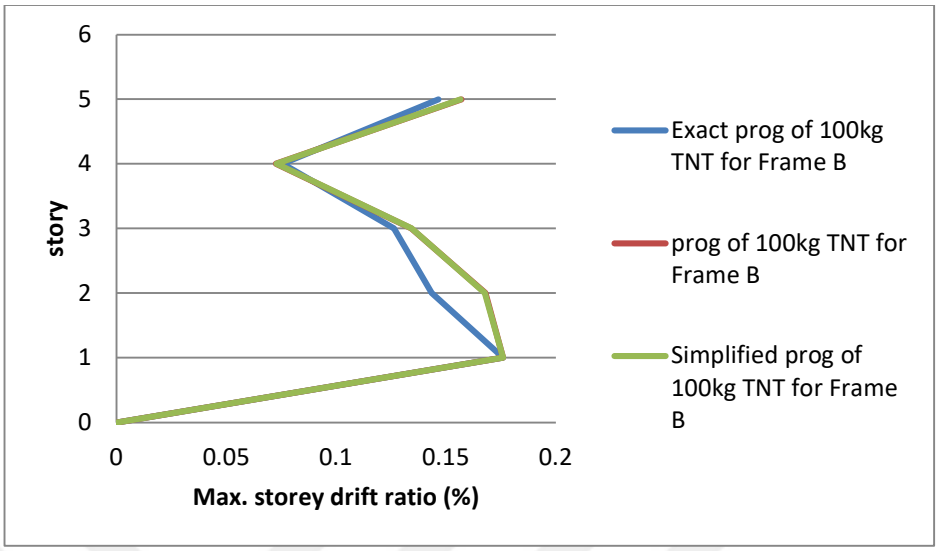

Figure 4.36: Maximum storey drifts ratio of frame B (100kg TNT) for different types of loading patterns.

The bottom storey experience larger storey drifts than the other storeys, since the large effect of the blast load reaches the things that are closer to the explosive. It can be seen from Figures 4.35 to 4.38 that the progressive method and the simplified progressive method give very close results to the real one in determining the global response in addition to time saved in the calculation of the blast pressure-time function of each node in the structure.

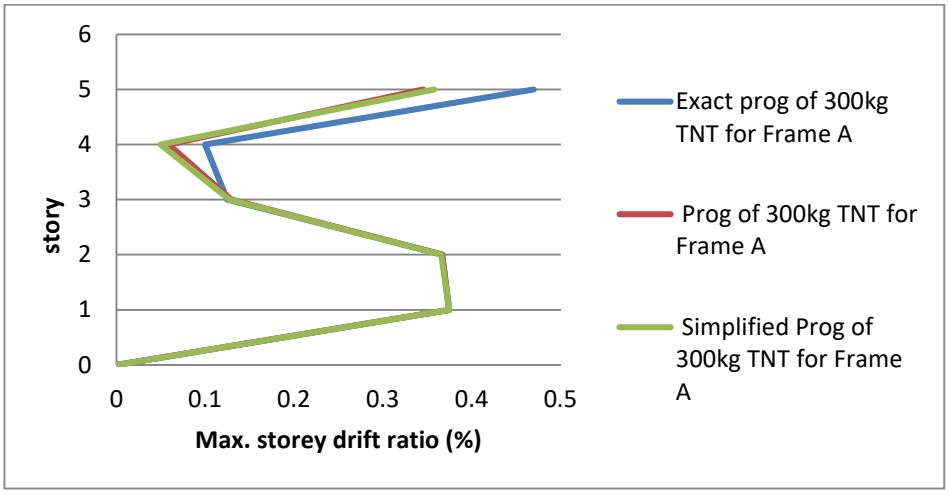

Figure 4.37: Maximum storey drifts ratio of frame A (300kg TNT) for different types of loading patterns.

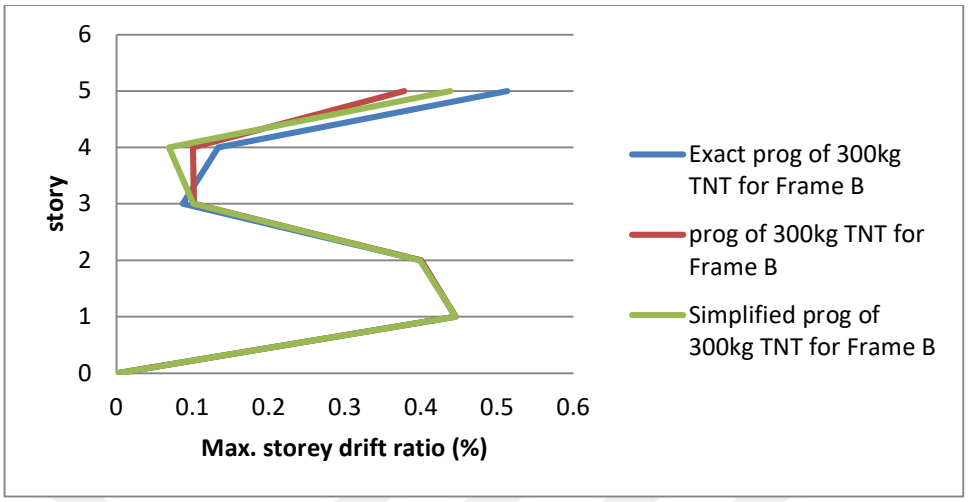

Figure 4.38: Maximum storey drifts ratio of frame B (300kg TNT) for different types of loading patterns.

4.3.2 Comparison of the response of the two structures

The figure below compares the storey drift ratios of Frame A and Frame B in the 300kg of TNT scenario, and as it is clear in that figure frame B which is designed with concrete grade 10 appears to have storey drifts which are apparently larger than that of frame A which is designed with concrete grade 30.

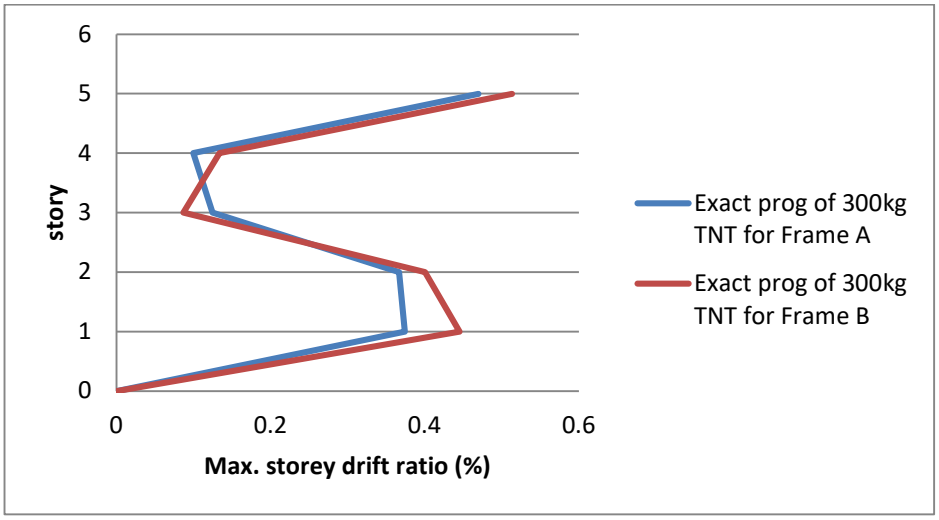

Figure 4.39: Maximum storey drifts ratio of frame A and B (300kg TNT) for exact progressive loading patterns.

The two Figures below illustrate the plastic hinges that appeared on both Frames A and B at the last step of the nonlinear dynamic analyses of the 100kg of TNT scenario. It can be seen from the figures that two hinges appeared from Frame A, while from Frame B appeared three hinges. Both structures resisted the 100kg of TNT scenario loads without any failure.

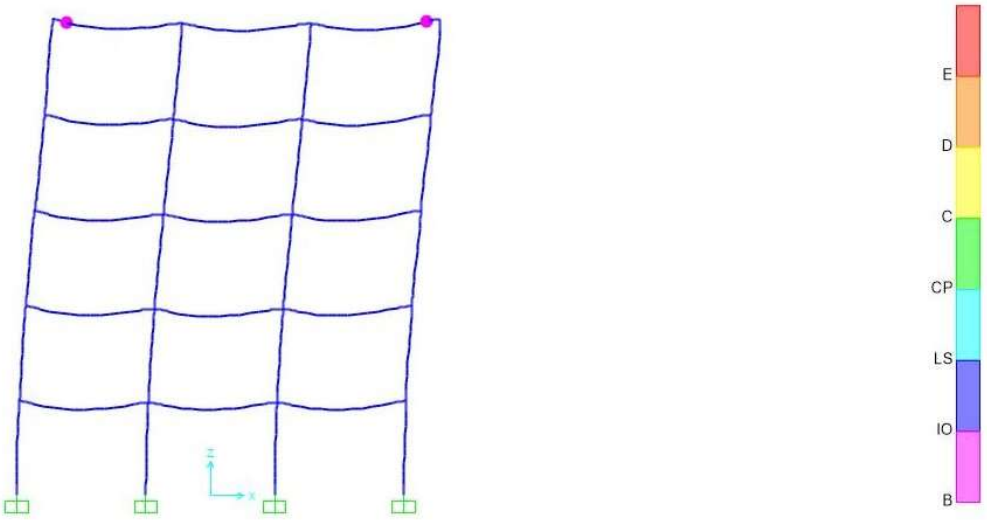

Figure 4.40: Hinges formed on frame A from the 100kg TNT scenario.

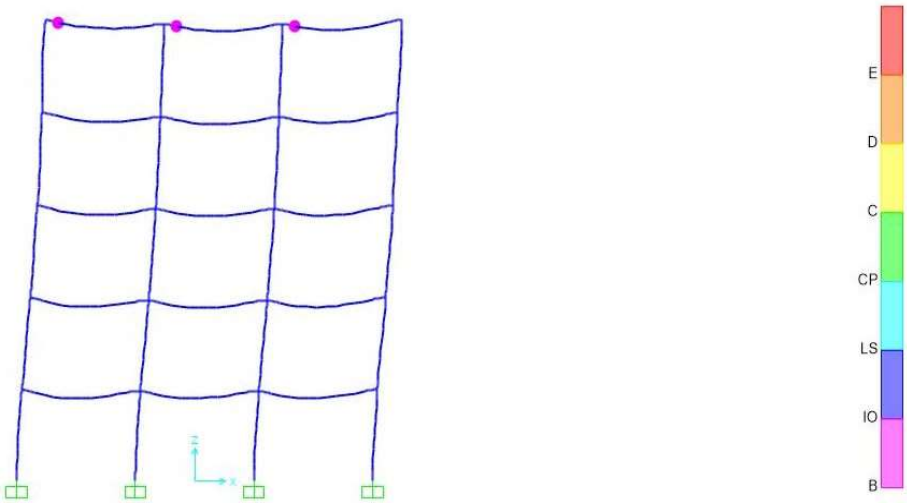

Figure 4.41: Hinges formed on frame B from the 100kg TNT scenario.

.

4.4 RESULTS OF THE PROGRESSIVE COLLAPSE

Progressive collapse resistance of a structure is its ability to redistribute the loads after the failure of one or more vertically load-carrying members without collapse, the more members the structure has the more it can redistribute the loads and resist failure.

Plastic hinges are found out on the frames i.e. IO, LS, CP, etc. If the hinges go beyond the Collapse prevention state, hinges are considered to be collapsed. Plastic hinge rotations beyond CP state are 0.025 radians. So when the plastic hinge rotations exceed 0.025 radians for any member, it is considered as collapsed.

4.4.1 Comparison of the two structures

The two previously defined frames were examined and compared for their progressive collapse resistance capacity using the alternative path method in three cases; corner column removal case, internal column removal case, and two consecutive columns removal case. The analyses were performed by the nonlinear dynamic method. The details of this process are given in section 3.10.

4.4.1.1 Corner column removal case

In this case, a corner column at the ground floor was removed dynamically from both frames using a ramp function, and the analyses were performed by the nonlinear dynamic method.

As can be seen from Figure 4.42, Frame A resisted the progressive collapse without any collapse, hinges in the immediate occupancy state have appeared from the span supported by the removed column while there are other hinges in the other parts of the structure except one hinge in its first state. On the other hand Figure 4.43 illustrates partial collapse that occurred in Frame B at the span supported by the

removed column. In this case Frame B failed, while Frame A resisted the progressive collapse.

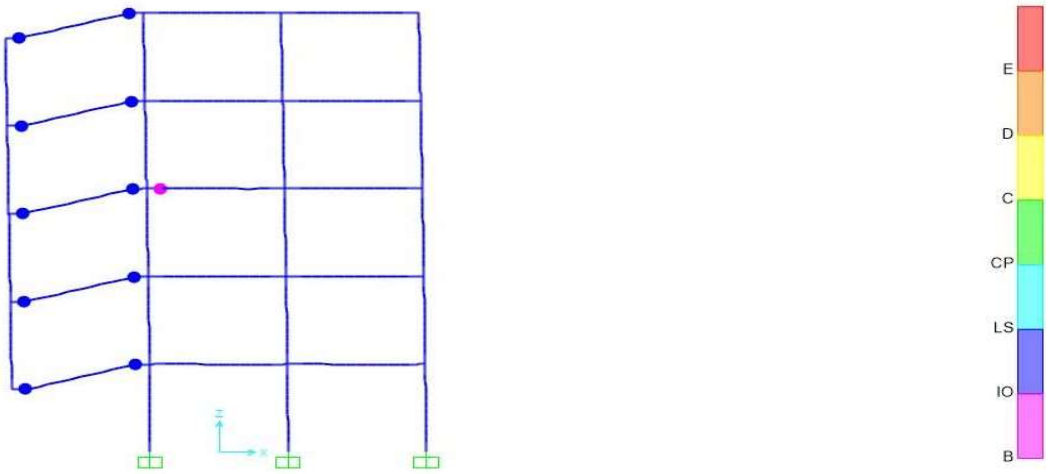

Figure 4.42: Frame A corner column removal formed hinges.

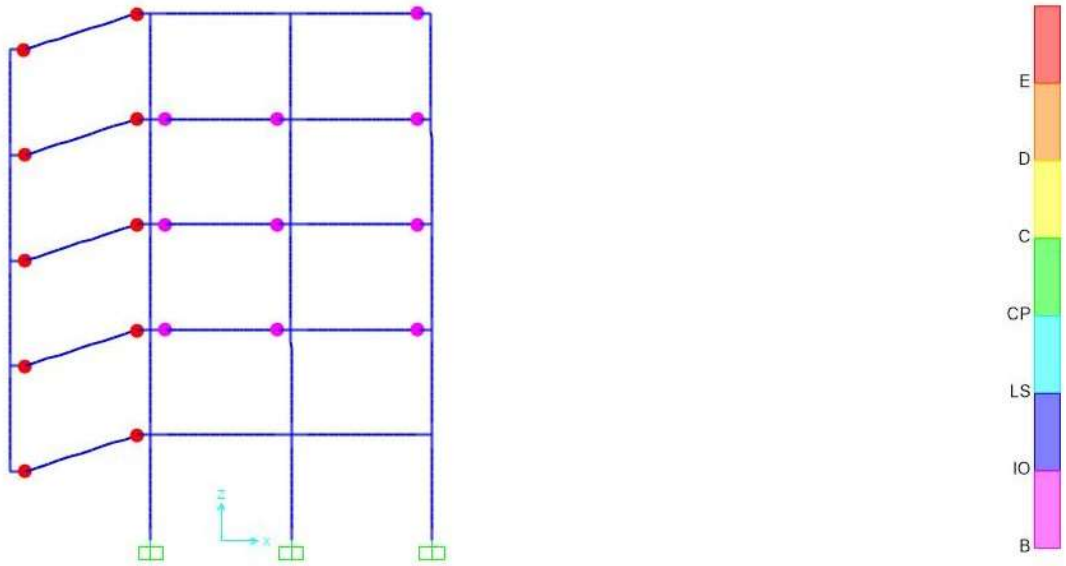

Figure 4.43: Frame B corner column removal formed hinges.

Figure 4.44 reveals the vertical displacement of the joint above the removed column per time. And it is clear that in Frame B the vertical displacement of the joint increases immediately, while in Frame A the joint displacement increases with time.

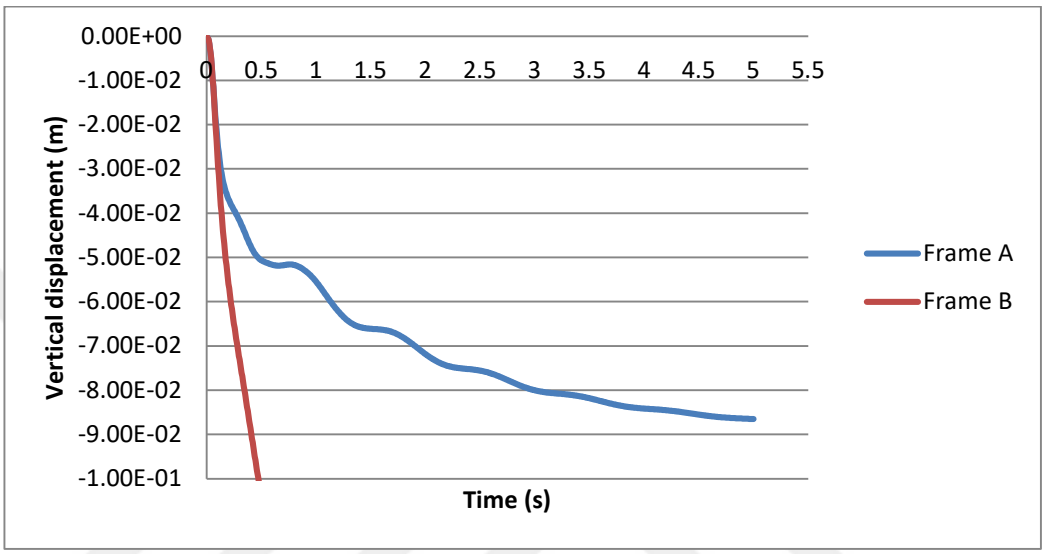

Figure 4.44: Vertical displacement time history of the joint above the removed column in the corner column removal case

4.4.1.2 Internal column removal case

In this case, one internal column at the ground floor was removed from each structure and progressive collapse analyses were performed. And as illustrated in Figure 4.45 Frame A redistributed the loads carried by the removed column and found a new equilibrium, therefore it succeeded in resisting the progressive collapse, while the plastic hinges that appeared in Frame B are the failure state, therefore Frame B experienced partial collapse.

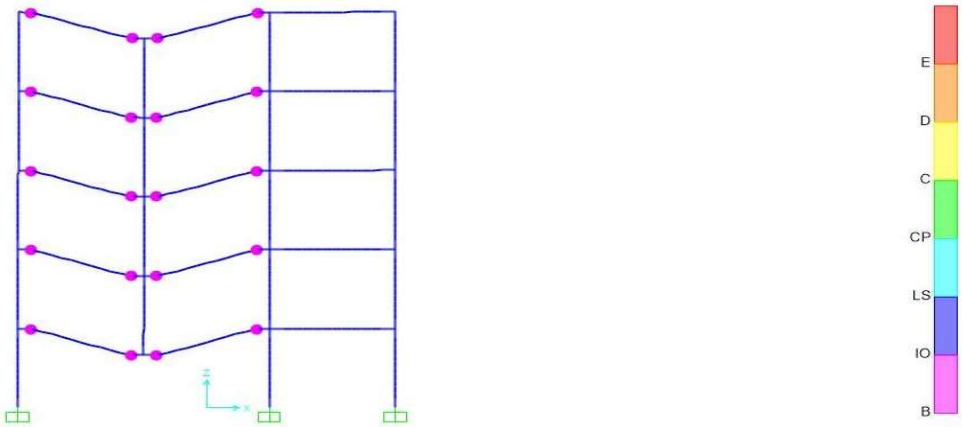

Figure 4.45: Frame A internal column removal formed hinges.

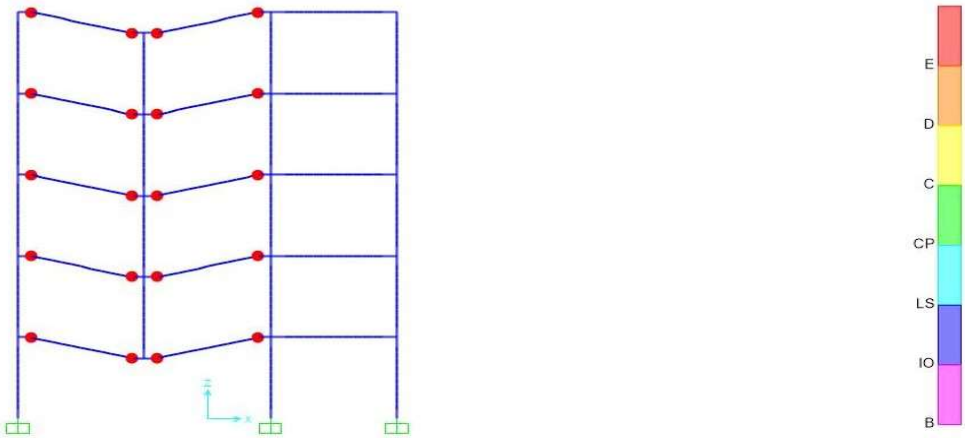

Figure 4.46: Frame B internal column removal formed hinges.

The maximum deflection achieved by the joint in Frame A was 34.81mm at 0.25sec as shown in Figure 4.47, however in Frame B the vertical displacement of the joint increases immediately till the failure.

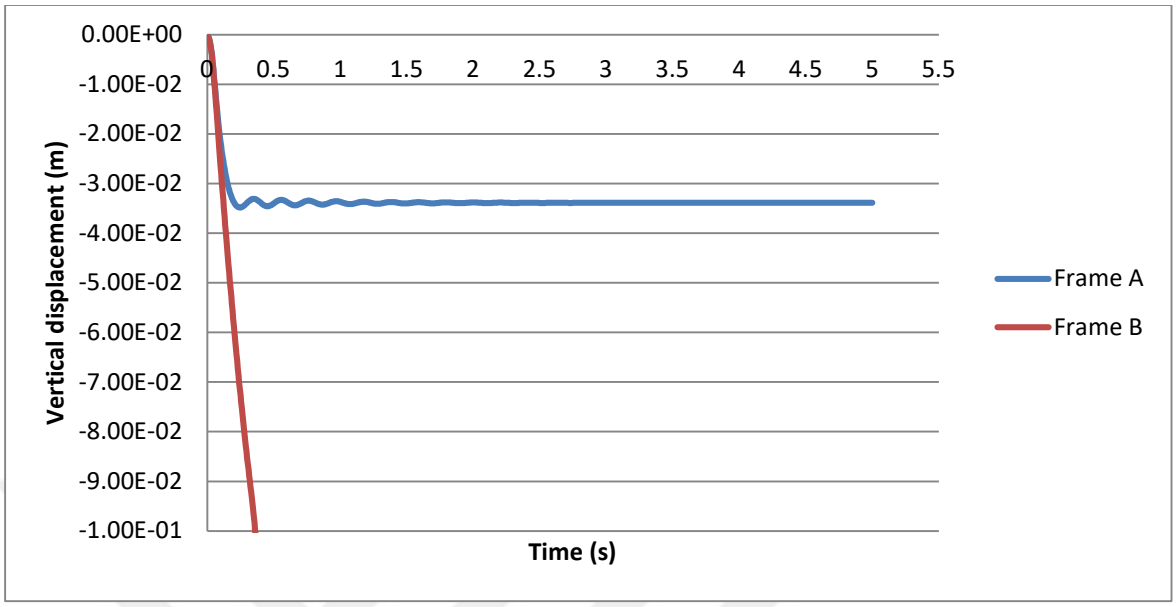

Figure 4.47: Vertical displacement time history of the joint above the removed column in the internal column removal case.

4.4.1.3 Two internal columns removal case

In this case, the two internal columns at the ground floor were removed from the structures then progressive collapse analyses were performed and the results were found as shown in Figures 4.48 and 4.49 total collapses occurred in both frames due to the large span and lack of alternative paths to redistribute the loads.

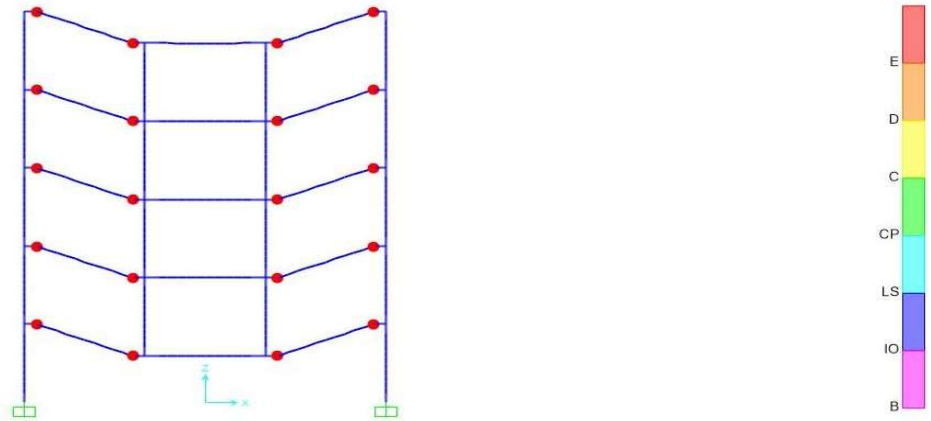

Figure 4.48: Frame A two internal column removal formed hinges.

.

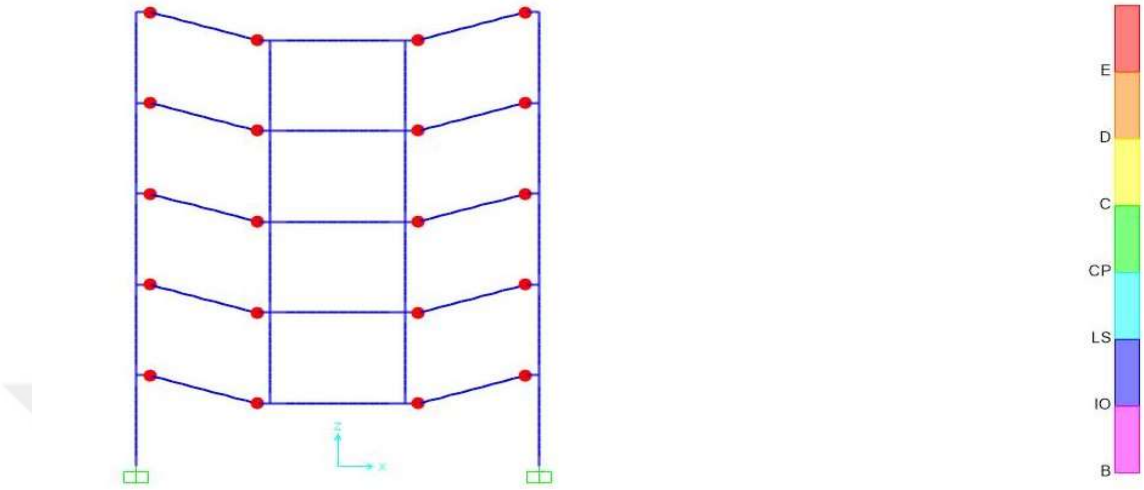

Figure 4.49: Frame B two internal column removal formed hinges.

Also, the vertical displacement time history plot in Figure 4.50 depicts that the vertical displacement of both joints keeps increasing till the failure.

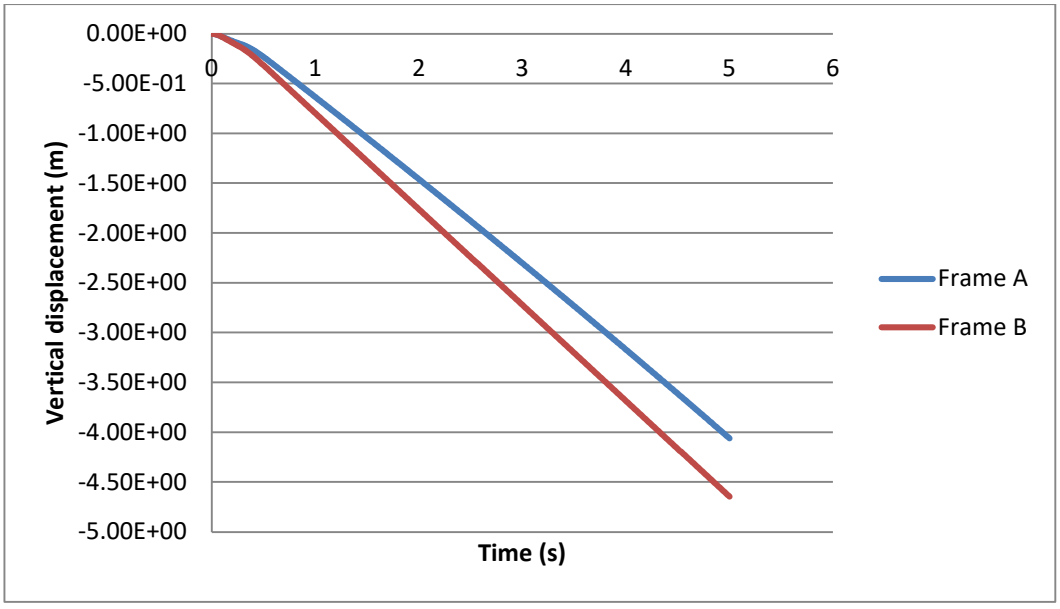

Figure 4.50: Vertical displacement time history of the joint above the removed column in the internal column removal case.

CHAPTER 5

5.1 CONCLUSIONS

- To analyze blast load effects and Progressive collapse on structures, two five storey 2D reinforced concrete frames were designed according to the EUROCODE 2-2004 using structural analysis and design software SAP2000 version 20.

  The two frames have similar properties, loadings, and dimensioning except the compressive strength of the concrete, in frame A concrete Grade C30 is used while frame B is used Grade C10 to represent both low and relatively high levels of concrete compressive strengths.

  Both structures are five-story 2D reinforced concrete frame buildings of 3m story heights and three bays of 4m width.

- A reinforced concrete column section was modeled in the section designer using SAP2000 V20, the moment-curvature curves of the section at different strain-rates were compared and it was observed that the strength of the section increases when the strain-rate values increase, precisely the moment resistance capacity of the section increased 29.5% when the strain-rate increased from the static value to $1x10^2$ /s.

- Second-order pushover analyses were carried out for frame A and frame B at different strain-rates to know the effect of the strain-rate value on the overall capacity of the structure, first, the dynamic increasing factors (DIF) of each material property was calculated as the result of the strain-rate values using the CEB-FIP-1990 code.

  The results obtained from the analyses show that the increase of the strain-rate value changes the material properties and increases the material strength therefore significantly increase in the strength of the whole structure. The unexpected instantaneous high pressure of the explosions causes strain-rates at the range of 10^2 - 10^4 which is less than the values recommended by the UFC-3-340-02.

- The global responses of three different loading patterns were compared for the two frames in two different TNT weight scenarios of 100 and 300 Kilograms using nonlinear dynamic analysis. The blast pressure at the roof had no remarkable effect on the lateral global response of the structures compared to the rear wall pressure therefore the exact progressive loading pattern showed a larger storey drift ratio than those of the other two loading patterns.

  The global response of the models in the exact, progressive and simplified progressive with considering the largest incident angles are very consistent as similar as the previous studies and the use of these simplifications in the analysis save a lot of time and effort in the calculation and modeling of the blast functions.

  Frame B appears to have storey drifts which are apparently more than that of frame A, so the concrete grade 30 showed strength more than the concrete grade 10.

- To detect the progressive resistance capacity of the frames, a nonlinear dynamic analysis was carried out for both frames using the alternative path method as per GSA guideline by SAP2000 software; Plastic hinges are also found out at the frames i.e. IO, LS, CP, etc. When the hinges go beyond the Collapse prevention state, hinges are considered to be collapsed. Plastic hinge rotations beyond CP state are 0.025 radians. So when the plastic hinge rotations exceed 0.025 radians for any member, it is considered as collapsed.

  The case of the two internal columns removal was the most critical for both frames. In the cases of the corner column and internal column removal frame A resisted the progressive collapse without any member failure while frame B experienced partial failure at all above spans supported by the removed column, But in the case of the two internal column removal both frames experience total collapse due to the long span, therefore the concrete grade 30 showed more resistance for the progressive collapse than the grade 10.

5.2 RECOMMENDATIONS

This study revealed the effect of the strain-rates on the strength of the structures, compared some blast load modeling techniques, and also investigated the resistance capacity of two structures one designed with low strength concrete and the other with relatively high strength concrete for Surface burst and progressive collapse hazards. Thus, the following recommendations are suggested:

- Study the local response of reinforced concrete structures to near-field and far-field ground explosions.
- Study the effect of windows, doors and neighboring structures on the response of structures to blast loads.
- Comparison of the resistance capacity of structures designed by the different progressive collapse design methods for large explosions.
- Study the global and local response of reinforced concrete structures on internal explosions.
- Comparison of the resistance capacity of high-rise buildings and low-rise buildings for blast loads and progressive collapse.

REFERENCES

[1] D. of Army, Navy, *Tm_5_1300_1990.Pdf*. 1990.

[2] T. Gamaniouk, *Parametric Analysis of Progressive Collapse in High-Rise Buildings*. 2014.

[3] W. Sun, Y. Jiang, and W. He, "An overview on the blast loading and blast effects on the RC structures," *Appl. Mech. Mater.*, vol. 94–96, pp. 77–80, 2011, doi: 10.4028/www.scientific.net/AMM.94-96.77.

[4] D. Nourzadeh, H. Jagmohan, and A. Braimah, "Global response of building structures to blast loading: case study of a 10-storey building," *1th Int. Conf. Shock Impact Loads Struct.*, no. July, pp. 1–10, 2015.

[5] H. Draganić and V. Sigmund, "Blast Loading on Structures," *Teh. Vjesn.*, vol. 19, no. 3, pp. 643–652, 2012.

[6] D. Nourzadeh, J. Humar, and A. Braimah, "Comparison of Response of Building Structures to Blast Loading and Seismic Excitations," *Procedia Eng.*, vol. 210, pp. 320–325, 2017, doi: 10.1016/j.proeng.2017.11.083.

[7] D. Stephen, D. Lam, J. Forth, J. Ye, and K. D. Tsavdaridis, "An evaluation of modelling approaches and column removal time on progressive collapse of building," *J. Constr. Steel Res.*, vol. 153, pp. 243–253, 2019, doi: 10.1016/j.jcsr.2018.07.019.

[8] V. Karlos and G. Solomos, "Calculation of Blast Loads for Application to Structural Components. Administrative Arrangement No JRC 32253-2011 with DG-HOMEActivity A5 - Blast Simulation Technology Development," in *Scientific and Technical Research Series*, 2013.

[9] S. U. S. Ekhar and L. R. A. M. A. P. R. R. Eddy, "Analysis of Reinforced Concrete Structure Under Blast Loading Condition By Using SAP2000," vol. 11, no. 02, pp. 81–99, 2019.

[10] B. S. V. P. P. G. H. Cet, "Analysis of Blast Loading Effect on Regular Steel Building," 2007.

[11] S. W. Park, Q. Xia, and M. Zhou, "Dynamic behavior of concrete at high strain rates and pressures: II. Numerical simulation," *Int. J. Impact Eng.*, vol. 25, no. 9, pp. 887–910, 2001, doi: 10.1016/S0734-743X(01)00021-5.

[12] R. C. Malvar LJ, "Review of strain rate effects for concrete in tension American Concrete Institud Mater J," *ACI Mater. J.*, vol. 95, no. 95, pp. 735–739, 1998.

[13] J. Walvaren, *Model Code 2010, final drafts*, vol. 1 & 2, no. 65 & 56. 2012.

[14] US DoD, *UFC 3-340-02. Structures to resist the effects of the accidental explosions*, no.

December. 2008.

[15] L. J. Malvar and J. E. Crawford, “Dynamic Increase Factors for Steel Reinforcing Bars,” *Proc. Twenty-Eighth DoD Explos. Saf. Semin.*, no. August 1998, pp. 1–18, 1998.

[16] B. Erkmen, “Comparison of blast analysis methods for modular steel structures,” *Tek. Dergi/Technical J. Turkish Chamb. Civ. Eng.*, vol. 29, no. 2, pp. 8253–8277, 2018, doi: 10.18400/tekderg.389954.

[17] T. Ngo, P. Mendis, A. Gupta, and J. Ramsay, “Blast loading and blast effects on structures - An overview,” *Electron. J. Struct. Eng.*, vol. 7, no. September 2016, pp. 76–91, 2007.

[18] A. Mckay and P. E. Consultants, “Non-Linear Dynamic Alternate Path Analysis for Progressive Collapse : Detailed Procedures Using UFC 4-023-03 (revised July 2009),” 2009.

[19] A. Z. Shams-al, “Progressive Collapse Analysis of Four Existing Reinforced Concrete Buildings Using Linear Procedure,” 2012.

[18] Brode, H. L. Numerical solution of spherical blast waves. // Journal of Applied Physics, American Institute of Physics, Ney York, 1955.

[19] Newmark, N.M.; Hansen, R.J. Design of Blast Resistant Structures, Shock and Vibration Handbook, McGraw-Hill, New York, USA. 1961.

[20] Mills, C. A. The design of concrete structure to resist explosions and weapon effects. // Proceedings of the 1st Int. Conference on concrete for hazard protections, Edinburgh, UK, pp. 61-73, 1987.

[21] UFC 4-023-03, Design of Buildings to Resist Progressive Collapse, Unified Facilities Criteria, United States Department of Defence, Washington, DC, 2009.

[22] Cappel, K. L. (1959). Structural design for dynamic loads: by Charles H. Norris, Robert J. Hansen, Myle J. Holley, Jr., John M. Biggs, Saul Namyet and John K. Minami. 453 pages, diagrams, 6× 9 in. New York, McGraw-Hill Book Co., Inc., 1959.

[23] ASCE. 2010. Design of Blast Resistant Buildings in Petrochemical Facilities, ASCE Task Committee on Blast Resistant Design, 2nd Edition. Reston, Virginia, USA.

[24] Biggs, John M., and John Biggs. Introduction to structural dynamics. McGraw-Hill College, 1964.

[25] GSA. 2003. Progressive Collapse Analysis and Design Guidelines for New Federal Offi ce Buildings and Major Modernization Projects. The US General Services Administration: Washington, DC.

[26] Computers and Structures Inc., SAP2000 Users Manual, Version Advanced 20.2.0, Structural Analysis Program, Berkeley, CA, USA, 2018.

[27] OVERPRESSURE, Blast parameters and blast time-history calculator. Version 1.0.0.0, Eric Jaques, 2013.

[28] C.B.Anju, M.C. Mathew, "Assessment of Progressive Collapse Resistance of a Symmetrical Reinforced Concrete Framed Structure" International Journal for Research in Applied Science & Engineering Technology, Volume 5 Issue V, May 2017, ISSN: 2321-9653.

https://upload.wikimedia.org/wikipedia/en/thumb/7/77/Alfred_P._Murrah_Federal_Building_before_destruction.jpg/240px-Alfred_P._Murrah_Federal_Building_before_destruction.jpg.

https://upload.wikimedia.org/wikipedia/en/thumb/7/77/Alfred_P._Murrah_Federal_Building_before_destruction.jpg/240px-Alfred_P._Murrah_Federal_Building_before_destruction.jpg.

https://i.pinimg.com/originals/c1/c3/1e/c1c31e5434d0c7c418c289dbfe98ba2b.jpg.

APPENDIX-A

❖ Comparison of my results to the results of the previous studies

a) Strain-rate effects on the structural members:-

P.Mendis (2007)[17], figured out the effect of the strain-rates on the strength of the column shown below, using LS-DYNA. The concrete grade was 40Mpa.

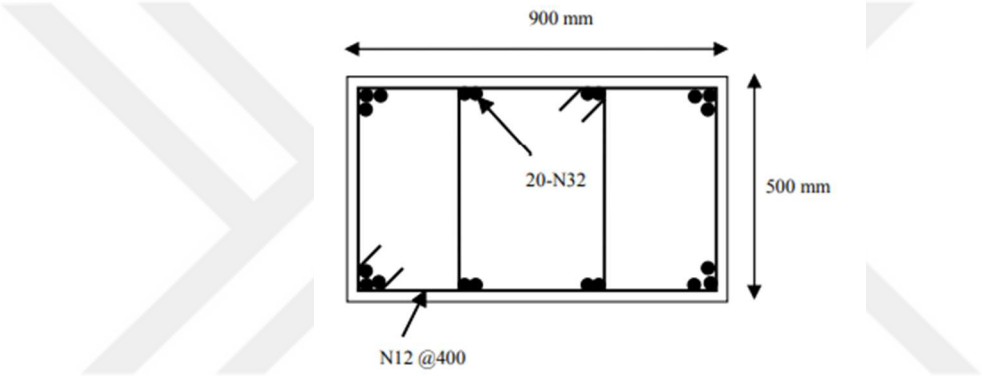

Figure 1: Column section detailing.

He modeled the moment-curvature relationship of the column under different strain-rates, and similar to my results in section **4.1** he found out that with the increase of the strain-rate value, the resistance capacity of the column increases.

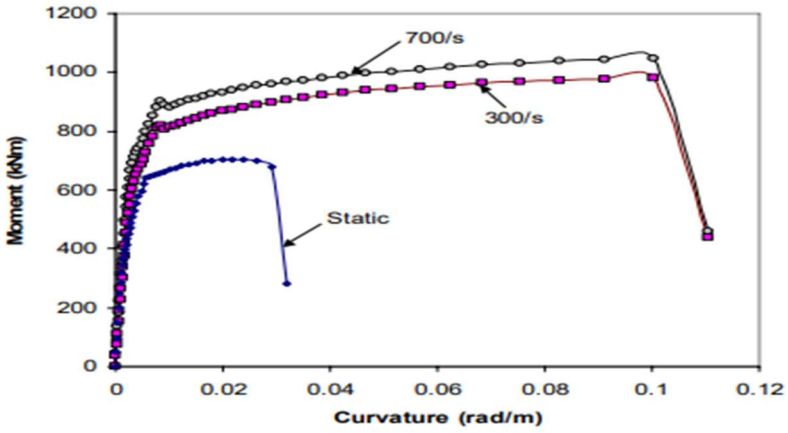

Figure 2: Moment-curvature of the column section under different strain-rates.

b) Blast analysis and comparison of the loading patterns:-

A.Braimah (2015)[4], investigated the global response of 10-storey building under ground burst using OPENSEES software, he also compared different loading patterns. Similar to my results in section **4.3.1**, he observed the lower and upper floors experience larger displacements compared to the mid floors, also the loading patterns give very close and acceptable results except the planar shockfront pattern which I did not consider in my study.

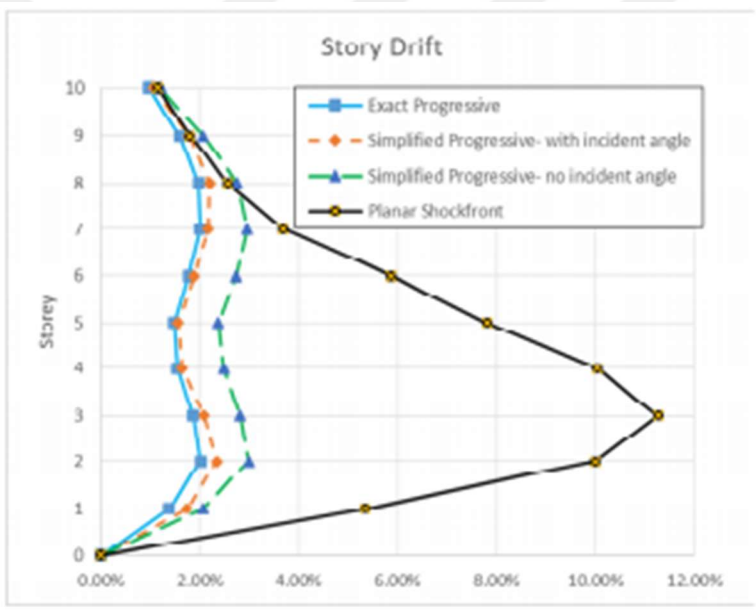

Figure 3: Maximum storey drift ratios for different types of loading patterns.

c) Progressive collapse analysis:-

M.C.George (2017)[28], examined the progressive collapse resistance capacity of 11 storey building in two cases; corner column failure and internal column failure in the first storey, and used nonlinear static analysis. Although our analysis methods are different but the results seem to be close, In the case of the corner column removal similar to my results in section **4.4.1.1** only the corner span was deformed and reached the plastic region.

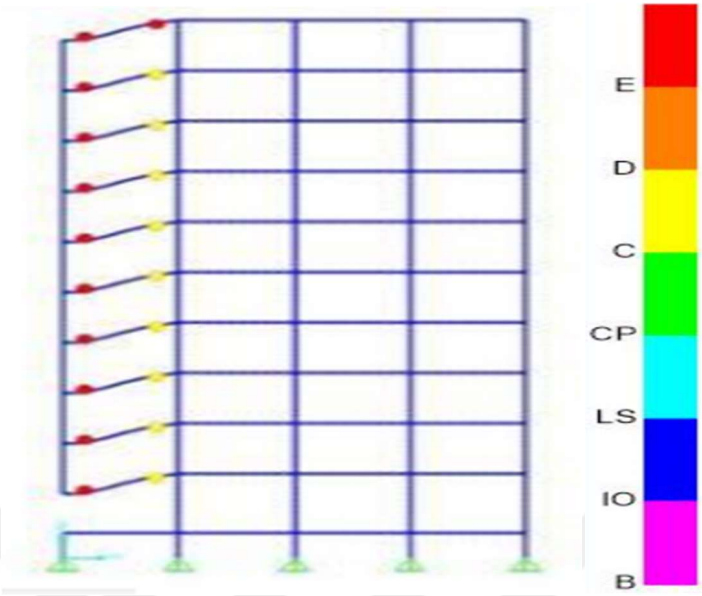

Figure 4: Corner column failure hinge formation.

Also in the case of the internal column removal similar to my results in section **4.4.1.2** only the two spans held by the removed column reached the plastic region.

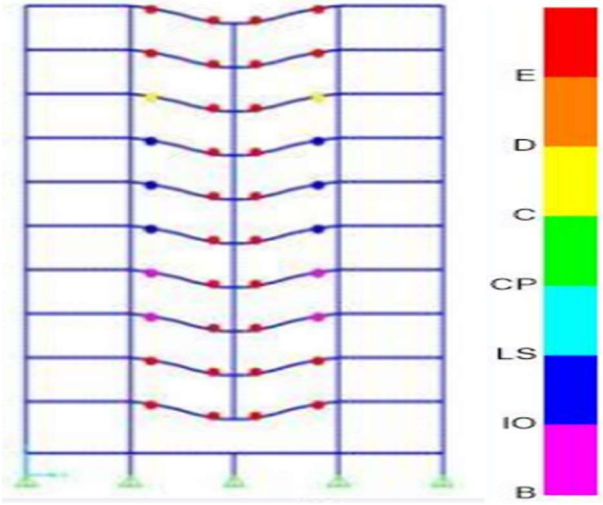

Figure 5: Internal column failure hinge formation.